Surface enhanced Raman scattering based assays for DNA detection

by

Danny van Lierop

May 2013

University of Strathclyde

Department of Pure and Applied Chemistry

Surface enhanced Raman scattering based assays for DNA detection

by

Danny van Lierop

2013

A thesis presented in fulfilment of the requirements for the degree of Doctor of Philosophy

2013

This thesis is the result of the author's original research. It has been composed by the author and has not been previously submitted for examination which has led to the award of a degree.

ACKNOWLEDGEMENTS

I would like to thank my supervisors Prof. Duncan Graham and Dr. Karen Faulds for giving me the opportunity, and their advice during my Ph.D research.

Big thanks to Dr. Paul Herron for providing the facilities to culture bacterial strains.

The undergraduate students that I supervised: Kenneth Lee for conducting experiments related to differences between double and single stranded DNA adsorption onto silver nanoparticles with different surface chemistries. Leigh Kirk for conducting experiments related to the Plexor DNA amplification reaction, evaluating the amplification of a DNA sequence originating to the *Staphylococcus aureus* gene *femA-Sa*.

A special thanks to a special person (Dr. Iain Larmour) who supported me in the lab with SEM analysis, the office, and the pub.

Big thanks to Lee Barrett, Hainan Xie, Richard N Cassar and the dirty old chatter box Sarah for brightening up my dark days, and Dr. Zeljka Krpetic for providing nanoparticles with a positive surface charge.

Further thanks to all my colleagues within the Centre of Molecular Nanometrology at the University of Strathclyde and especially my colleagues in the “Nostics” group.

I would like to acknowledge Renishaw Diagnostics Ltd., the Scottish funding council, and Strathclyde University Glasgow for funding.

Thanks to Maartje for being patient and supporting me all the way till the end of this thesis.

ABSTRACT

Surface enhanced Raman scattering (SERS) based molecular diagnostic assays for the detection of specific DNA sequences have been developed in recent years to compete with the more common fluorescence based approaches. Current SERS assays require either time consuming separation steps that increase assay cost and can also increase the risk of contamination, or are negative assays where the signal intensity decreases in the presence of target DNA. A new separation free SERS assay with an increase of signal intensity when target DNA is present using a specifically designed SERS primer has been developed in this thesis. The presence of specific bacterial DNA from *Staphylococcus epidermidis* was detected using Polymerase Chain Reaction (PCR) and SERS and indicates a new opportunity for exploration of SERS assays requiring minimal handling steps.

SERS primers have been used to directly detect specific PCR products utilizing the difference in adsorption between single stranded and double stranded DNA onto nanoparticle surfaces. Seven parameters important for improved positive SERS assays for real applications were investigated using a model system for optimization experiments. This was followed by a PCR assay to detect pathogen DNA, and the introduction of a novel assay which utilizes the 5'→3'exonuclease activity of *Taq* DNA polymerase to partly digest the SERS probe, generating dye labelled single stranded DNA increasing the SERS signals for detection of pathogen DNA. Applying the model system it was found that uni-molecular SERS primers perform better than bi-molecular SERS primers. However within the PCR assays it was found that uni- and bi-molecular SERS primers performed very similarly, the most reproducible results were obtained using the 5'→3'exonuclease digestion assay. The SERS based assays developed in this thesis offer new routes over conventional fluorescence based techniques.

SERS primers have been designed for multiplex pathogen detection. A selection of dyes for multiplex pathogen detection was made. Assay designs for the SERS primer digestion, and the SERS primer extension assay were made successfully, followed by cross reaction analysis of the oligonucleotides required for the multiplex detection. The results indicate that it is feasible to perform a multiplex detection using both types of assays. However it was decided to postpone the final multiplex detection part of the project and investigate assay systems that require less complex designs.

Additionally, to simplify the SERS primer assay novel cationic silver nanoparticles were synthesised and tested for discrimination between double stranded and single stranded DNA. These silver nanoparticles with a positive surface charge produced poor discrimination between double and single stranded DNA. However these cationic silver nanoparticles provide a simplified SERS substrate for DNA detection.

ABBREVIATIONS

A	Adenine
ABS	Absorbance
AgNPs	Silver nanoparticles
AuNPs	Gold nanoparticles
BGS	Background subtracted
BHQ	Black hole quencher
C	Cytosine
cDNA	Complementary DNA
Ct	Cycle threshold
Cy	Cyanine
DAPI	4',6-diamidino-2-phenylindole dihydrochloride
Dabcyl	4(dimethylaminoazo)benzene-4-carboxylic acid
DLS	Dynamic Light Scattering
DNA	Deoxyribonucleic Acid
DNases	Deoxyribonuclease
dsDNA	Double stranded DNA
EDC	*N*-(3-dimethylaminopropyl)-*N*'-ethylcarbodiimide hydrochloride
EDTA	Ethylenediaminetetraacetic Acid
FAM	5-(and 6)-Carboxyfluorescein
FDA	Food and Drug Administration
FRET	Förster Resonance Energy Transfer
Fw	Forward
FWHM	Full Width at Half Maximum
G	Guanine
gDNA	Genomic DNA
HDA	Helicase Dependent Amplification

HEG	Hexaethylene Glycol
HIV	Human Immunodeficiency Virus
HPA	Health Protection Agency
HPLC	High Performance Liquid Chromatography
Iso-dC	Iso-cytosine
Iso-dG	Iso-guanosine
LAMP	Loop Mediated Isothermal Amplification
LATE PCR	Linear After The Exponential PCR
LNA	Locked Nucleic Acid
MDx	Molecular diagnostics
mRNA	Messenger RNA
MRSA	Methicillin Resistant *Staphylococcus aureus*
NASBA	Nucleic Acid Sequence Based Amplification
NPs	Nanoparticles
PBS	Phosphate Buffered Saline
PCR	Polymerase Chain Reaction
PLS	Partial Least Square
PLL	Poly-*L*-lysine
RCA	Rolling Circle Amplification
rtPCR	Real Time Polymerase Chain Reaction
RNA	Ribonucleic acid
RNases	Ribonucleases
Rv	Reverse
SERRS	Surface Enhanced Resonance Raman Scattering
SERS	Surface Enhanced Raman Scattering
SNP	Single Nucleotide Polymorphism
ssDNA	Single stranded DNA
Sulfo-NHS	*N*-hydroxysulfosuccinimide
T	Thymine
Taq	*Thermus aquaticus*

T_m	Melting Temperature
TRIS	tris(hydroxymethyl)aminomethane
U	Uracil
UV	Ultraviolet

TABLE OF CONTENTS

1 INTRODUCTION

This chapter provides a general introduction to molecular diagnostic DNA detection. The process from clinical sample to diagnosis is discussed along with the detection of multiple targets at once, which are compatible with fully automated and integrated systems. The limitations of the common fluorescence based techniques will be briefly discussed, and an alternative technique, surface enhanced Raman scattering (SERS) for the detection of specific DNA sequences related to a disease will be introduced. A theoretical background section on surface enhanced Raman scattering will explain the technique and current SERS based DNA detection assays. Finally the aims and an outline of this thesis will be given.

1.1 Molecular Diagnostics

In the field of molecular diagnostics samples from patients are tested for the presence of a specific disease. To be able to diagnose if a sample contains a specific disease several different procedures are required, depending on the patient sample and the disease of interest. The following sections give a brief outline of the different procedures carried out in molecular diagnostic analysis, *i.e.* the detection of specific genes in a clinical sample which refer to a genetic disease and or viral / bacterial infection.

1.1.1 Clinical samples

There are many different types of clinical samples that can be obtained depending on the type of disease or infection to be identified. Examples include faeces for *Clostridium difficile*[1], blood for Human Immunodeficiency Virus (HIV)[2] and nose swabs for Methicillin Resistant *Staphylococcus aureus* (MRSA)[3] infections. For the detection of the presence of specific genes, it is necessary to isolate DNA and or ribonucleic acid (RNA) from the clinical sample. To achieve this, the cells containing the nucleic acid need to be opened, i.e. lysed, and the

nucleic acids purified from all other components that may inhibit downstream analysis. Amplification of the DNA is often required because the amount of target DNA in the clinical sample is too low to be directly detected. The most commonly used methods will be discussed in the following sections.

1.1.2 Cell lysis

Cell lysis is the process carried out to open cells. Lysis of cells is needed to access the DNA and can be carried out using various methods. Several different methods are available and their effectiveness depends on the type of cell they are applied to. Table 1.1 provides an overview of different lysis methods and examples that can be used.

Table 1.1 Overview of lysis methods

Method	Examples	Target example
Chemical	pH, Salt	Gram negatives
Mechanical stress	Heat, Shearing, Pressure	Spores
Enzymatic	Lysostaphin, Lysozyme	Gram positives

For chemical lysis of cells different reagents can be used, including high salt concentrations and detergents. These methods are relatively cheap however they are mainly suitable for mammalian and Gram negative bacterial cells.[4]

Enzymatic lysis methods use enzymes to degrade the cell wall thereby releasing the inner cell components. An example is the incubation of Gram positives with lysostaphin to break down the peptidoglycan double layer cell wall.[5, 6] Although these methods are more specific they are also more expensive and therefore only used for more difficult to lyse cells such as Gram positive bacteria. Enzymatic lysis is more difficult in clinical sample matrices (e.g. faeces) because of enzymatic reaction inhibiting components may be present in the sample.[7]

Physical lysis methods include heat, ultrasonic treatment, and bead milling, all of which disrupt the cells by shear stress. These methods are relatively cheap and are suitable for all types of samples depending on the frequency, power and time

the treatment is applied to the cells. Disadvantages of these methods are the cost of the equipment and the efficiency for clinical samples containing lower cell concentrations.[8]

Each type of target cell will react differently to the lysis method used. By considering the properties of the cell and choosing the optimal lysis method, specific lysis of the target cells can be obtained.

1.1.3 Nucleic acid extraction

During the process of nucleic acid extraction, nucleic acids are purified from other biomolecules such as proteins, and nucleic acid degrading enzymes; including deoxyribonucleases (DNases) and ribonucleases (RNases), which inhibit the subsequent PCR.

To achieve efficient extraction, different approaches are available. One of the most commonly used extraction methods in molecular diagnostics is the "Boom extraction" which is named after the inventor Rene Boom.[9] In this method the nucleic acid is bound to a silica surface in the presence of a high concentration of chaotropic salt such as guanidinium hydrochloride (for DNA) and guanidinium thiocyanate (for RNA). Hydrophobic interactions between the silica surface and the nucleic acid are responsible for the reversible binding. Proteins are washed out of the sample by washing the sample with lower salt concentrations and solvent (ethanol, isopropanol, and acetone). In the final step the nucleic acid is released from the membrane using water at elevated temperatures, typically around 70°C.[9, 10]

1.1.4 Nucleic acid amplification

After isolation of the DNA from the clinical sample, detection must then be carried out. To detect low concentrations of DNA i.e. low copy numbers of genes (1-1000 per mL), specific regions of genes can be amplified using several different techniques. Isothermal nucleic acid and signal amplification methods are available.[11, 12] A review of these methods was carried out by Gill *et al*. in 2008.[11]

A target amplification method which is not isothermal and requires thermal cycling is the Polymerase Chain Reaction (PCR).[13] This method is the most widely used method for DNA amplification.

1.1.5 Polymerase Chain Reaction

The polymerase chain reaction (PCR) was developed by Mullis in 1983[13] and was a major discovery that had a huge impact on DNA detection and on the work of molecular biologists, and eventually clinicians and doctors. Using the PCR, Mullis was able to synthesise an unlimited number of DNA copies from the original template DNA.

The PCR is achieved using the following major components; primers, DNA polymerase, deoxynucleoside triphosphates of the four different bases A,T,G,C, (dNTP), and template DNA.

The process starts with heating of the sample to ~95°C. At this temperature hydrogen bonds break and the template DNA which is double stranded becomes single stranded DNA. After ~1 minute the template DNA is in its single stranded form.

In the next step the sample is cooled to ~55°C for ~1 minute. At this temperature two short synthetic pieces of DNA called primers can hybridise to the 3' end of the template DNA. These primers are designed to be specific to the target piece of DNA.

When the primers are hybridised to the template DNA the sample is heated to ~72°C for ~1 minute. At this temperature an enzyme, a thermostable DNA polymerase isolated from the thermophilic bacterium *Thermus aquaticus* (*Taq*) can extend the primers using deoxynucleoside triphosphate molecules as building blocks. This results in two exact copies of the original template DNA.

PCR is an exponential process and cycling these steps several times theoretically results in two to the power N (where N is the number of cycles) of copies of the

original template DNA.[13-18] Figure 1.1 provides a schematic overview of the PCR reaction.

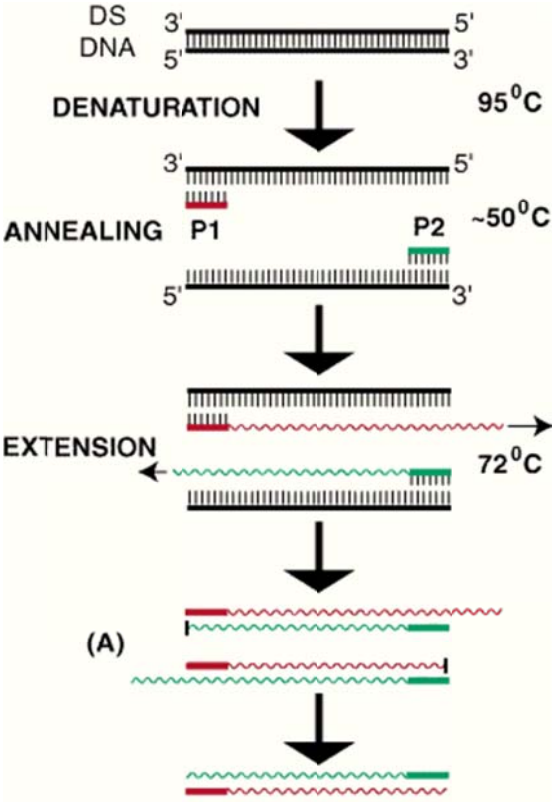

Figure 1.1 Schematic overview of the PCR. From top to bottom; the double stranded template DNA is heated to 95 °C and turns into two ssDNA stands. In the next step the sample is cooled to approximately 50 °C and specific primers bind to the single stranded template DNA. Then the sample is heated to 72 °C and a DNA polymerase extends the primers resulting in two exact copies of the original template DNA. By repeating these steps multiple times template DNA can be copied exponentially.[19]

1.1.6 Detection of nucleic acids

Through the years many techniques have been developed to detect target nucleic acid sequences selectively. A widely used technique is the labelling of nucleic acids using an intercalating dye such as ethidium bromide or SYBR® Green I in combination with gel electrophoresis which allows the separation of different lengths of nucleic acids and their detection by fluorescence.[20] An intercalating dye is a fluorescent molecule which emits limited fluorescence when free in solution and emits more fluorescence upon binding to DNA. An

example of an intercalating dye is SYBR® Green I which binds to the minor groove of dsDNA and emits more fluorescence upon binding to dsDNA.[20] SYBR® Green I can also be used in combination with fluorescence spectroscopy and PCR where the DNA amplification reaction can be monitored during the reaction by so called Real Time quantitative PCR[21] with the possibility to do an amplicon melt analysis.[22] A draw back of this method is that it can only be done for one target per reaction and higher fluorescence is observed for unspecific amplification. The combination of PCR and fluorescence spectroscopy has had a huge impact on DNA analysis.[21, 23-25]

1.1.7 Real time reaction monitoring using fluorescence and Förster resonance energy transfer

In fluorescence spectroscopy, a molecule is excited to a higher electronic state and when it returns to its ground state it releases a photon at longer wavelength (Figure 1.2). Therefore the wavelength of the excitation source is chosen to be close to the absorption maximum of the fluorescent molecule and emission is detected at a longer wavelength. The intensity of the fluorescence is proportional to the concentration of the fluorophore, making it a quantitative technique.

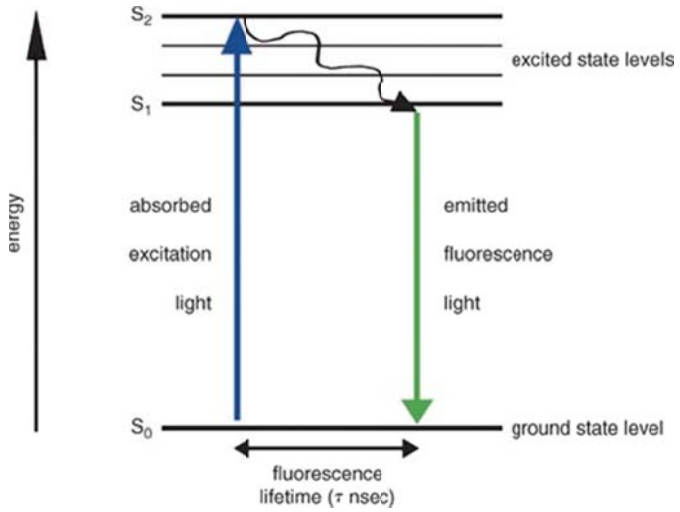

Figure 1.2 A fluorescence energy level diagram illustrating the release of a photon with a longer wavelength than the incident photon.[26]

A unique feature of fluorescence is that it can be quenched by another molecule, so called quenchers. These quenchers accept energy in the form of light from the fluorophore and release the energy in the form of light or heat. This is known as Förster resonance energy transfer (FRET).[27]

FRET involves a dipole interaction which allows an excited donor fluorophore to transfer its energy to an acceptor. Figure 1.3 shows how the incident photon energy excites the fluorophore into an excited level, this energy is then transferred to the acceptor. For FRET to occur the emission spectrum of the donor has to overlap with the absorbance spectrum of the acceptor.

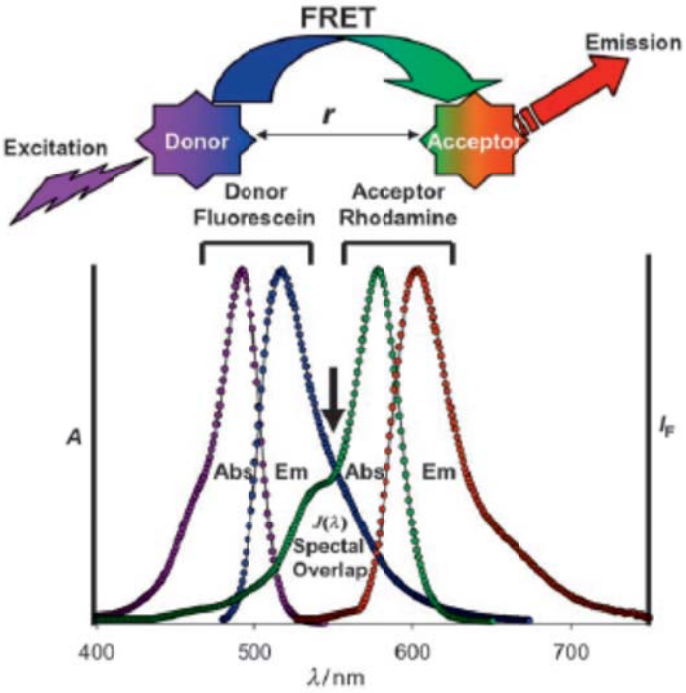

Figure 1.3 A schematic overview of the FRET process; upon excitation of the donor it transfers energy to the acceptor. The spectra show absorption and emission of fluorescein (donor) and Rhodamine (acceptor).[28]

The acceptor molecule can be a fluorophore or a non-fluorescent molecule, in the case of a fluorescent molecule the transferred energy is emitted as fluorescence at a longer wavelength. The distance between the donor and acceptor can be up to 10 nm.[29] This is a very useful technique in DNA detection

since DNA can be labelled on one site with a fluorophore and at another site with a quencher. The following sections describe how fluorophore and quencher labelled DNA molecules can be used for the detection of specific DNA sequences.

1.1.7.1 5'exonuclease assay

The 5'exonuclease assay, often called Taqman assay, is a combination between PCR and FRET. The Taqman assay uses the 5'→ 3'exonuclease activity of the Taq polymerase to release the fluorophore from the quencher. A DNA probe labelled at the 5' with a fluorophore and at the 3' with a quencher molecule binds to the target strand (Figure 1.4). The *Taq* polymerase extends along the primer and will digest the Taqman probe when it encounters it in the sequence due to its exonuclease activity, thus releasing the fluorophore from the quencher and resulting in fluorescence emission upon excitation.[30]

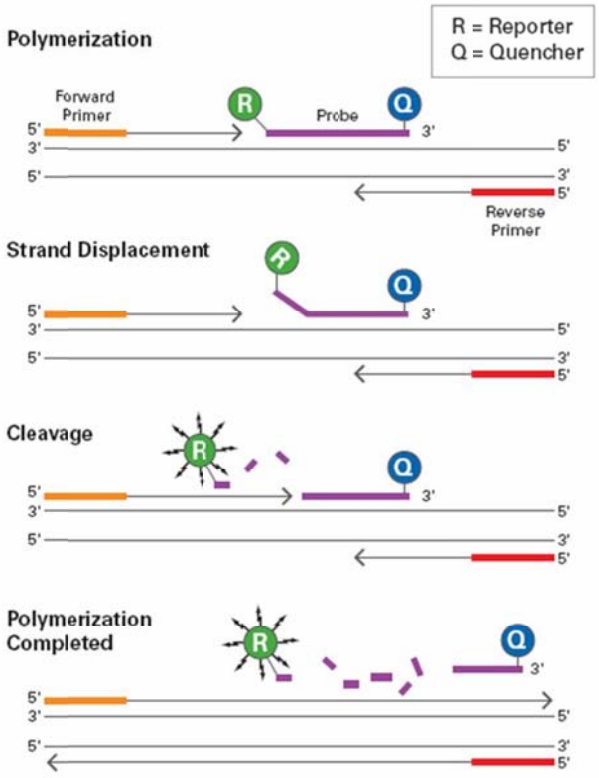

Figure 1.4 Taqman assay where DNA polymerase is displacing and digesting the probe using its 5'→3' exonuclease activity. When fluorophore and quencher are separated the fluorescence signal increases and this is proportional to the amount of target DNA amplified.

By using combinations of fluorophore and quencher sets, with different excitation wavelengths, multiple targets can be detected simultaneously during the PCR reaction.[31]

1.1.7.2 Molecular beacons

Another assay that uses the FRET mechanism involves the use of molecular beacons. Molecular beacons consist of a synthetic piece of ssDNA that is complementary to the target of interest. However in this case additional bases are added at each end of the complementary region to create a self complementary DNA stem, forming a hairpin loop (Figure 1.5). At one end of the stem a fluorophore is attached and on the other end a quencher molecule is attached. Figure 1.5 shows that when the stem is closed the fluorescence is quenched and when the beacon binds to its target the beacon opens and the fluorophore and quencher move further away from each other resulting in a fluorescent signal.[32, 33]

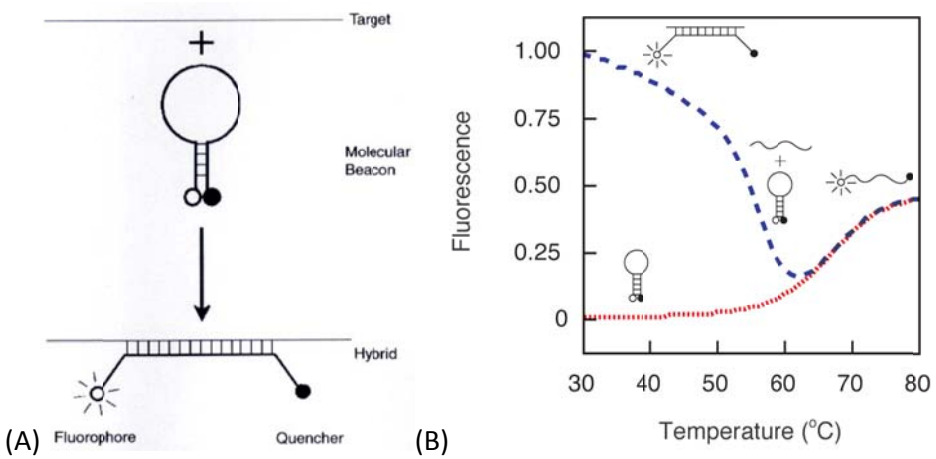

Figure 1.5 (A) Molecular beacon binding to its target and generating higher fluorescent signal.[32] (B) Molecular beacon and its fluorescence profile at different temperatures. Red line represents the molecular beacon without target DNA present, at lower temperatures the molecular beacon is closed and fluorescence is quenched. At higher temperatures the beacon is opened and fluorescence is emitted. The blue line represents the fluorescent signal in the presence of target DNA were at lower temperatures the fluorescence signal increases when the molecular beacon binds to its target. [37]

Similar to the Taqman probes, molecular beacons can also be used to detect multiple targets simultaneously during the PCR.[21, 33, 34] Molecular beacons are not digested and the signal is reset each cycle. Therefore melting analysis can be performed using molecular beacons to find a single nucleotide polymorphisms (SNP).[33] Molecular Beacons find use in many different applications such as PCR[32], nucleic acid sequence based amplification (NASBA)[35] and *in situ* mRNA labelling.[36]

1.1.7.3 Scorpion primers

Scorpion primers are self probing primers which are essentially a primer and a molecular beacon linked together with a hexaethylene glycol (HEG) linker, resulting in a uni-molecular probing system. The scorpion primer is used in combination with a normal primer. Figure 1.6 shows when target DNA is present the scorpion primer binds to the target and the DNA polymerase extends the 3' of the primer. Then during the annealing step of the PCR the molecular beacon part of the primer can bind to the extended part of the primer, increasing the distance between the fluorophore and quencher resulting in an increased fluorescent signal. Then during the extension step of the PCR the reverse primer displaces the molecular beacon and the HEG unit, or so called blocker, prevents the DNA polymerase from copying the stem and the beacon region.[38 39]

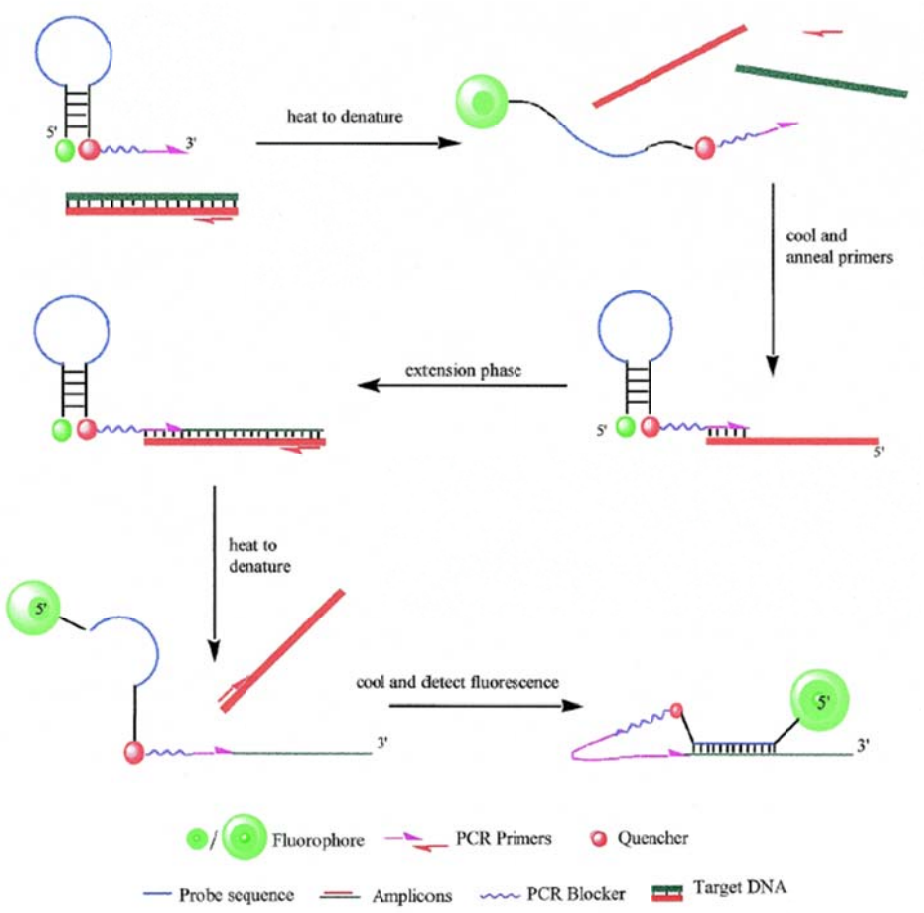

Figure 1.6 The mode of action of the scorpion primer. During the extension phase the primer is extended by the DNA polymerase and during the annealing phase the molecular beacon which is attached to the primer can bind to the extended primer.[39]

1.1.7.4 Plexor® assay

The Plexor® assay is a relatively new assay for quantitative detection of DNA amplification. In 1990 Piccirilli *et al.* demonstrated an extended genetic alphabet and synthesised six unnatural base pairs.[40] In 2004 Sherrill *et al.* incorporated one of these base pairs (iso-guanosine (iso-dG) and iso-cytosine (iso-dC) base pair) into a PCR product.[41] Johnson *et al.* demonstrated the Plexor® reaction itself,[42] and multiplex DNA detection.[43]

The Plexor® assay relies on a third unnatural base pair, iso-G and iso-C and incorporation of a fluorescence quencher molecule in close proximity to a fluorophore labelled primer. This event results in a decrease in fluorescence upon the presence of target DNA and diminishes over the number of cycles until the reaction has reached completion (Figure 1.7).

(A) (B)

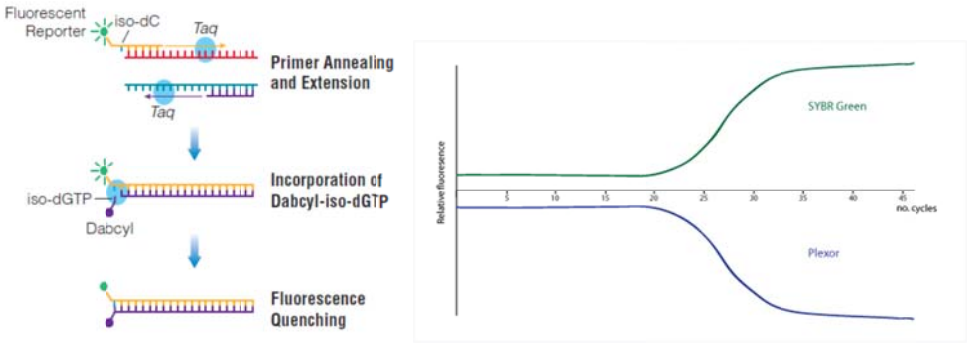

Figure 1.7 (A) A schematic representation of the Plexor® reaction. At the top in yellow the forward PCR primer containing a fluorophore and an iso-dC base and in purple the reverse PCR primer both being extended by the Taq DNA polymerase. In the middle the iso-dGTP base labelled with Dabcyl is incorporated at the iso-dC position in close proximity to the fluorophore within the forward primer. At the bottom the resulting fluorescence is quenched.[44] (B) Top fluorescence increase of a SYBR Green® PCR and bottom left a fluorescence reduction in a Plexor® reaction.[45]

1.1.7.5 Disease diagnosis

Finally disease diagnosis is carried out after the results from a DNA amplification reaction such as PCR are obtained, providing a qualitative yes or no answer to the presence or absence of a particular disease. Additionally when real time amplification reactions are used quantitative information about the disease can be provided, for disease state diagnosis for example in the case of HIV treatment, effectiveness of the treatment can be determined.

1.1.8 Fully integrated molecular diagnostic platform

Many companies are operating in the field of molecular diagnostics. In this section an interesting example is given of a company which made a fully integrated molecular diagnostic platform.

Cepheid is an American company that recently entered the molecular diagnostic market with their GeneXpert system (Figure 1.8). This system consists of a computer and a cartridge handler which can take cartridges for several diseases simultaneously, for example; Flu, *Clostridium difficile* and MRSA. Within the cartridge all the processes (lysis, extraction, amplification and multiplex detection) required for diagnosis of a specific disease are carried out without the need of additional handling steps, and a single test only requires about 45 to 90 min depending on the specific test to be carried out.[46]

Figure 1.8 A fully automated molecular diagnostic system developed by Cepheid. Left the system where multiple samples can be run with random access (not to scale). Right the cartridge in which the specific assay is carried out by the system.[46]

1.1.9 Multiplexed DNA detection

All previously described methods used a fluorescence detection approach. Although it is a robust, sensitive, well established and commonly used method there are some drawbacks. One of these drawbacks is the simultaneous detection of multiple analytes in solution. Therefore multiple excitation wavelengths and or filter sets are required to detect multiple targets. Current PCR machines offer detection of six fluorophores simultaneously.[47]

To overcome the multiplex detection limitations of fluorescence there are so called microarrays. These arrays consist of spots of specific DNA to a target on a solid surface which then corresponds to the genetic information. Once the

specifically amplified and fluorescently labelled DNA is hybridised to the solid surface it can be detected.[48, 49] The advantage of this method is that millions of short sequences can be tested at once which significantly increases the quality of the results. However the development of such arrays might be challenging and costly.[50]

An alternative which competes with the existing approaches is surface enhanced Raman scattering (SERS). Due to the 10 to 100 times narrower Raman bands of the labels compared to absorption and emission bands of fluorophores [51, 52] simultaneous detection of analytes could be increased.[53-55]

1.2 Surface enhanced Raman scattering

1.2.1 Raman scattering

Raman scattering was first demonstrated by Sir C.V. Raman in 1928.[56] When monochromatic light interacts with a molecule, the light can either be scattered or absorbed. Three different types of scattering are observed namely Rayleigh, Stokes and anti-Stokes Raman.

In Rayleigh scattering, the photons are scattered elastically at the same frequency as the incident photon and therefore the scattered wavelength is the same as the incident photons.

Approximately one in every 10^6 photons are scattered inelastically, i.e. Raman scattered and this is caused by the incident photon interacting with the molecule of interest. Energy transferred to or from the molecule changes the frequency of the scattered light. This can occur in two ways, the photon can transfer energy to the molecule (Stokes) or the molecule can transfer energy to the photon (anti-Stokes). Figure 1.9 illustrates the three types of scattering. During Rayleigh scattering, the molecule is excited to a virtual energy state of equal energy to the exciting wavelength, and then relaxes to the same vibrational energy level it was in initially. In Stokes Raman scattering the molecules are in their lowest vibrational energy level of the ground electronic state (m), when excited to the virtual state and relaxes to an excited vibrational state in the ground electronic state (n). Anti-Stokes scattering is when the molecules are in an excited vibrational energy level (n), and relax back to a lower vibrational state (m). At room temperature the majority of the molecules are in the lowest vibrational energy state of the electronic ground state and thus most Raman scattering is Stokes Scattering.

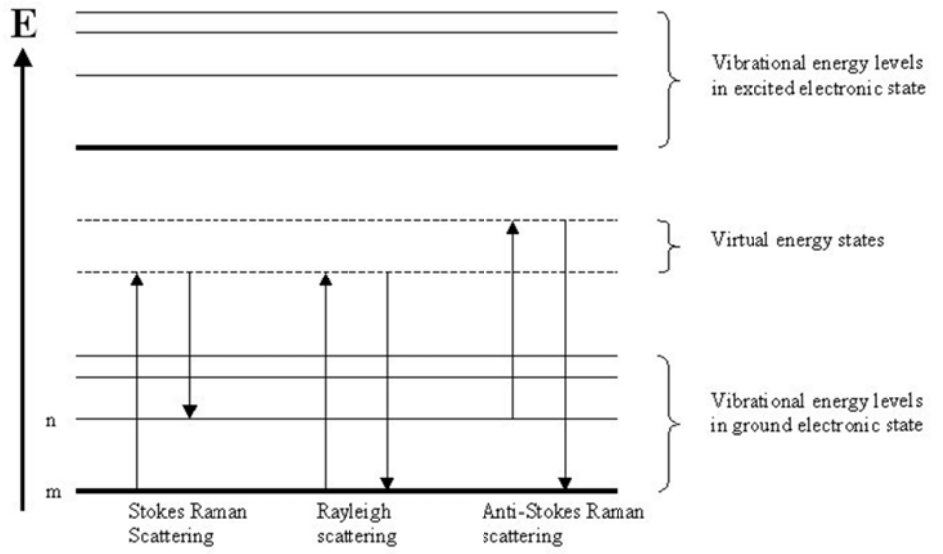

Figure 1.9 Energy transitions associated with Stokes scattering, Rayleigh scattering & anti-Stokes scattering.

Raman scattering is not destructive to the molecules being analysed and little sample preparation is required. Raman can provide electronic and vibrational information unique to the analyte. Raman scattering can also be carried out in solution, with water being a good solvent to use because it is a poor Raman scatterer.[56]

1.2.2 Resonance Raman scattering

In resonance Raman scattering the excitation source (laser) is tuned or chosen to be close to the absorbance wavelength of the molecule. This means that the frequency of the laser will correspond with an electronic transition within the molecule, therefore the Raman signals will be enhanced (see Figure 1.10). Increased signal intensity significantly improves the sensitivity.[57] The advantage of resonance Raman scattering is an enhancement of ~10^3 in peak over normal Raman intensity thereby enabling the analysis of more dilute samples. A disadvantage of using RRS to measure fluorophores is the emission of fluorescence, thereby obscuring the Raman peaks. Therefore non fluorescent labels such as benzotriazole dyes are preferred.[58]

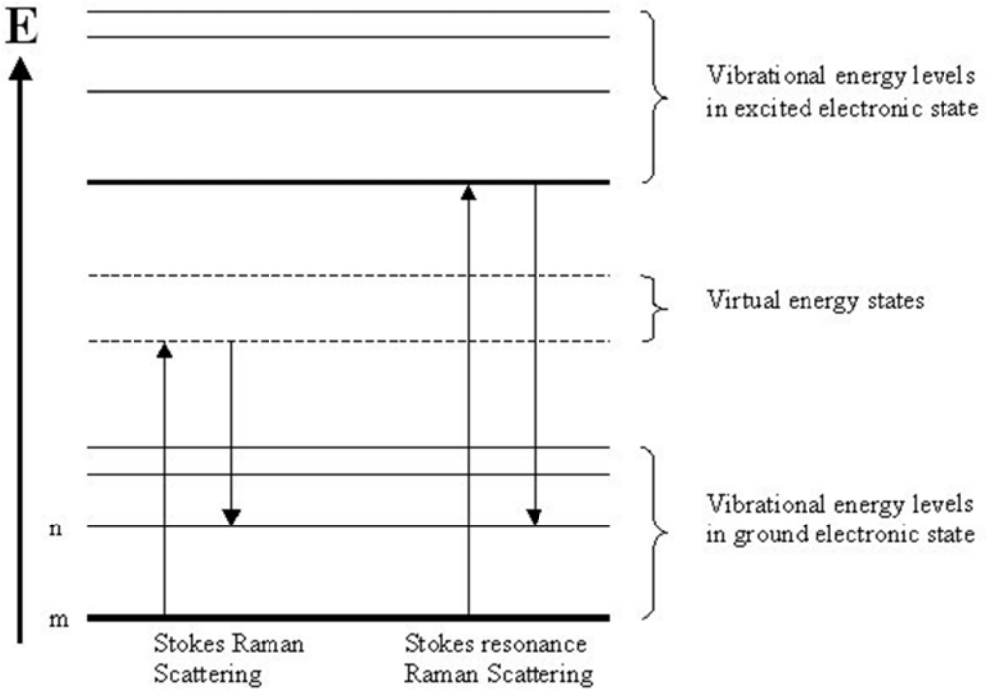

Figure 1.10 Energy levels associated with resonance Raman scattering.

1.2.3 Surface enhanced Raman scattering

Surface Enhanced Raman Scattering (SERS) was first published by Fleischmann *et al*. in 1974.[59] While studying the adsorption of pyridine on a silver electrode using Raman scattering it was found that there was a far greater intensity using a roughened electrode than using a smooth electrode surface. The initial explanation was thought to be that the increase in surface area led to more adsorption of pyridine on the surface and thereby giving higher intensities. However this was later attributed to a surface enhancement effect from the metal surface. Jeanmaire and Van Duyne[60] and Albrecht and Creighton[61] showed an enhancement of 10^6 when pyridine was adsorbed on a roughened metal surface compared to pyridine in solution. SERS has been shown using different metals namely silver, gold, and copper.[62, 63] Many roughened metal surfaces have been used for surface enhancement techniques such as metal island films[64] and colloidal suspensions.[65] The advantages of SERS over Raman and resonance Raman scattering are that analytes can be studied at lower concentrations using

less laser power resulting in less chance of photo bleaching of the sample. The analyte has to be in close contact and preferably in a perpendicular orientation to the surface to produce the most intense signals.[66]

1.2.4 Surface enhanced resonance Raman scattering

In 1983, Stacy and Van Duyne published the first paper on surface enhanced resonance Raman scattering (SERRS).[67] This is a combination of the two earlier described techniques, resonance Raman and surface enhanced Raman scattering, taking advantage of both techniques. The sensitivity can be increased by a factor of 10^{14} over normal Raman.[68] It is believed that the principles behind the enhancement effect are the same in SERRS as in SERS. However it has been revealed that the contribution proposed in the charge transfer theory is significantly smaller with the laser in-resonance (SERRS), than out of resonance (SERS).[69] For SERRS to occur the sample must contain a visible chromophore. In order to obtain enhancement, the excitation must be close to an electronic transition of the chromophore. This enhancement is maximised when the surface plasmon of the metal also matches this frequency.

1.3 Nanoparticles as Raman enhancers

Suspensions of metal nanoparticles are often used as the roughened metal surface for SERS.[70-72] The dimensions of nanoparticles are smaller than 100 nm. Commonly used metals in SERS analysis are gold, silver and copper due to the surface plasmon of these metals lying in the visible region of the electromagnetic spectrum.[62] This corresponds with the common laser excitation wavelengths. Silver nanoparticles are often synthesised via a method developed by Lee and Meisel which involves the citrate reduction of silver nitrate to form silver nanoparticles.[70] Ethylenediamine tetraacetic acid (EDTA),[73] hydroxylamine[74] and sodium borohydride[75] can also be used as reducing and capping agents to form silver nanoparticles with an overall negative charge.[76] The surface charge prevents the nanoparticles from clustering or aggregating in solution. When salts or polyamines are added, nanoparticles aggregate and a roughened metal surface is created which is ideal for SERS. The aggregating agent can have two roles, allowing the analyte to be adsorbed onto the metal surface as well as promoting aggregation of the nanoparticles.[77] Aggregation is required to create nanoparticle dimers and trimmers which are SERS "hot spots" providing a high electromagnetic field and greater Raman peaks.[78-80]

Mirkin *et al.* developed gold nanoparticles functionalised with ssDNA,[81] and SERS active dye.[82] With the later particles, nucleic acid targets were detected. Via a hybridisation assay on a solid glass substrate pre-functionalised with capture ssDNA, the target induced hybridisation events were detected via SERS and also a flatbed scanner.[82] Graham *et al.* created a SERS based ON / OFF switch by DNA target induced aggregation of silver nanoparticles pre-functionalised with ssDNA and a SERS active dye.[83] By coupling nanoparticles via DNA hybridisation, controlled interparticle junctions were created, and the interparticle distance effect in SERS could be studied experimentally.[84] This study proves experimentally that the SERS signal was strongest when the interparticle distances were shortest, which is in agreement with theoretical calculations.[85]

1.4 DNA detection using SERS

Direct detection of DNA via the bases can be performed intrinsically,[86] however for successful detection of multiple diseases, multiple Raman reporters, and an assay system are required to link the Raman reporter signal to a specific disease. Over the past fifteen years multiple SERS based DNA detection assays have been developed. [82, 83, 87-96] Unfortunately there are drawbacks with these assays. The first example of SERS based DNA detection was carried out by Dou *et al.* in this method DNA was detected using 4',6-diamidino-2-phenylindole (DAPI) staining and SERS readout. However this assay resulted in a low DAPI SERS response when double stranded DNA (dsDNA) was present, and no genetic information was obtained due to the unspecific intercalation of DAPI.[87] Cao *et al.* developed a bio barcode assay with a SERS read out where multiplexing was shown, however the assay required washing steps which increase the number of labour intensive handling steps and the risk of sample contamination.[82] Li *et al.* reported stronger adsorption of single stranded DNA (ssDNA) than dsDNA onto a gold nanoparticle surface due to electrostatic interactions.[88] The difference in adsorption capabilities between ssDNA and dsDNA onto a gold or silver nanoparticle surface has been used to develop colorimetric, fluorescence and SERS based DNA detection approaches.[88-91] However, colorimetric detection is limited in terms of detecting multiple analytes in solution due to the non-specific nature of the output signal. MacAskill *et al.* developed a SERS based multiplexed detection of PCR products using this mechanism.[91] However, this assay resulted in a reduced signal in the presence of the target molecule, making the judgment of the assay performance more difficult due to the lack of signal when target DNA was present. Wabuyele *et al.* developed a molecular beacon modified with a thiol group on one end to a nanoparticle surface and on the other end a Raman reporter dye (molecular sentinels) resulting in a reduced SERS response and an increased fluorescence response in the presence of target DNA,[92] and in 2009 a multiplex detection utilizing the molecular sentinels was demonstrated.[97] Faulds *et al.* improved this assay by attaching a benzotriazole azo dye instead of the

thiol group to the molecular beacon where the benzotriazole group functioned as a surface attachment group and the azo dye as a SERS reporter and as an internal control mechanism,[93] again this assay had a reduced signal response in the presence of target. A method demonstrated by Graham *et al.* which showed an increase in SERS response, involved streptavidin coated magnetic bead separation to detect biotin labelled PCR products which contained a pre-hybridized SERS active dye labelled DNA sequence.[98] Assays involving magnetic bead based separation steps increase the risk of sample contamination and are more labour intensive and therefore Monaghan *et al.* performed the bead assay in a microfluidic chip.[94] An advancement was carried out by Graham *et al.* who developed a DNA detection assay which utilized the coupling of DNA modified nanoparticles via target DNA resulting in an increased SERS response of the Raman reporter dye attached to the nanoparticle surface.[83] Herein a ssDNA concentration of 1.25 nM was detected. Later Harpster *et al.* labelled target DNA with two pieces of complementary DNA, one labelled with a Raman reporter dye and the other labelled with a thiol group for nanoparticle surface attachment.[95] However detection of only 8.5 µM target DNA was carried out. Zhang *et al.* have demonstrated coupling between magnetic nanoparticles and gold nanoparticles containing a Raman reporter via target DNA derived from West Nile virus with detection of concentrations down to 10 pM.[96] In this assay, sample volumes of 1.5 mL were magnetically concentrated into a small volume, which significantly increased the local concentration of target DNA and Raman reporter labelled gold nanoparticles above the native concentrations in the original solution.

A method with an increase in SERS signal intensity in the presence of the target and without separation or washing steps is the preferred method.

This thesis will investigate alternative routes to make SERS based DNA detection assays which will preferably be closed tube, require a minimal amount of handling steps, and capable of multiplex detections.

1.5 Outline of this thesis

The aim of this project is to investigate the possibility of using surface enhanced Raman scattering to detect DNA targets in a separation free assay. Further the long term goal is to produce this in a closed tube assay format. A closed tube assay is a reaction that does not require opening of the tubes to add or remove reagents, thereby lowering the possibility of sample contamination.

In Chapter 2 the focus lies on the investigation of a molecule which can discriminate whether target DNA is present or absent using SERRS, in a concept similar to molecular beacons that use fluorescence spectroscopy. This will result in a separation free SERS assay. Initially the proof-of-concept will be tested using synthetic DNA and later the SERS primer will be incorporated into the PCR reaction detecting the presence or absence of specific DNA originating from *Staphylococcus epidermidis*. In Chapter 3 possible variations on the assay described in Chapter 2 will be investigated. In Chapter 4 the possibilities to use the newly developed assays to detect multiple DNA gene targets simultaneously will be investigated. Finally in Chapter 5 the use of positively charged silver nanoparticles for discrimination between single and double stranded DNA will be investigated to simplify the SERS assays.

The ultimate goal would be PCR less quantitative SERS based multiplex detection assay, which means that low concentrations (i.e. copy numbers) of DNA targets need to be detected directly without the need of DNA target or signal amplification.

2 SERS PRIMERS FOR PATHOGEN DETECTION BY SERS

2.1 Introduction

For the successful detection of pathogenic DNA an assay method is required to detect and identify specific DNA sequences. As previously discussed in the introduction current SERS assays for the detection of unlabelled target DNA have some drawbacks, either they require separation steps using magnetic beads [94] or are so called "negative assays" where the signal decreases when the target is present.[88, 89, 91-93, 99] Separation steps are labour intensive, expensive and increase the risk of sample contamination. Negative assays have the disadvantage that it can be difficult to judge if a reduction in signal is due to poor assay performance or the target being present, and an internal performance control target also lowers, or even disappears, during the assay. This could potentially be solved by having two internal controls, one to check the reagents are functioning, which will give a high signal, and the other to check that the assay is functioning correctly, which will give a low signal. However this would make the assay overly complex. Therefore it is more advantageous to design an assay which increases signal upon the presence of target DNA.

In this chapter a new proof-of-concept assay for the detection of gene specific DNA targets from biological samples will be investigated. The assay generates an increased SERS response upon hybridization of target DNA without the need for additional separation steps (Figure 2.1) and is fully compatible with PCR.

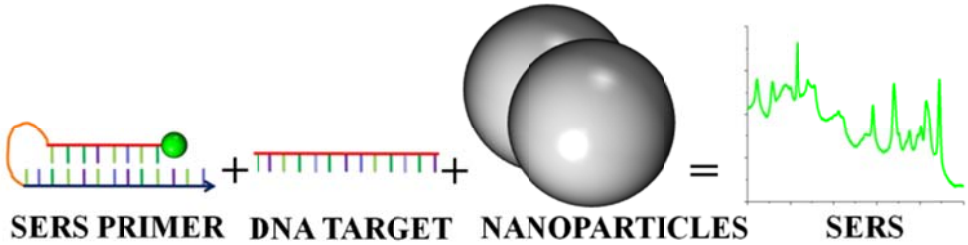

Figure 2.1 Mixing a SERS primer with target DNA and nanoparticles results in a strong SERS signal

SERS primers consist of double stranded DNA labelled with a SERS active molecule, in this case a fluorescent dye. When SERS primers interact with target DNA, the dye labelled part of the SERS primer becomes single stranded DNA (ssDNA) and interacts with the nanoparticle surface, resulting in an increase in the SERS response. The difference in adsorption between ssDNA and double stranded DNA (dsDNA) onto a nanoparticle surface has been used to develop colorimetric, fluorescence and SERS based DNA detection approaches.[88-91] Colorimetric detection is limited in terms of detecting multiple analytes in solution. The fluorescence quenching and the SERS approaches with reduced signal in the presence of the target molecule, make the judgment of the assay performance more difficult. Therefore a SERS primer method with an increase in SERS signal intensity in the presence of the target is the preferred method. In this positive assay approach, SERS primers are incorporated into PCR products, exposing the fluorophore labelled ssDNA and allowing adsorption onto the surface of the nanoparticles resulting in an increased SERS response, thereby detecting the specific gene of a pathogen. This method has potential for the detection of multiple genes in solution by SERS when different fluorophores and DNA sequences are used.

2.2 Experimental

In this section experimental procedures used in Chapter 2 are described.

2.2.1 Assay design

The *femA* gene of *Staphylococcus epidermidis* (*femA-SE*) was targeted, the *femA* gene has been previously used for bacterial identification of *Staphylococcus epidermidis* and *Staphylococcus aureus*.[23] The sequence of the whole genome including the *femA* gene of *Staphylococcus epidermidis* National Culture Type Collection (NCTC) strain NCTC 13360 was obtained from the National Centre of Biotechnology Information (NCBI) website.[100] The *femA-SE* assay design was carried out using the Primer3Plus online server.[101] Parameters within this software were set to 50 mM monovalent salt, 1.5 mM divalent salt, and 250 nM of DNA. For the table of thermodynamic parameters the setting "Santalucia 1998" was used.[102] For salt correction the formula set by "Owczarzy *et al.* 2004" was used.[103] Internal folding of the sequence region selected by Primer3Plus was analysed using the DINAMelt server.[104] Parameters were set to 58°C, 50 mM monovalent salt, 1.5 mM divalent salt, and 250 nM of DNA. Basic Local Alignment (BLAST) was carried out using the BLAST tools from the NCBI website.[105]

2.2.2 Preparation of Reagents

All reagents were obtained from Sigma Aldrich (United Kingdom) unless stated otherwise.

2.2.2.1 Phosphate Buffered Saline

Phosphate Buffered Saline (PBS) was prepared in a 500 mL glass bottle (Schott Duran) by dissolving 1 PBS tablet (Oxoid) in 100 mL of distilled water. The solution was then autoclaved for 15 min at 121°C. After cooling, the solution was transferred into two sterile 50 mL Falcon tubes (BD) in a Laminar Air Flow (LAF) cabinet and stored at -20°C in a freezer. Table 2.1 shows the exact concentrations of the salts in the PBS buffer and the pH was 7.3 ±0.2.

Table 2.1 Overview of the salt concentrations in the PBS

Name	Formula	Concentrations (mM)
Sodium Chloride	$NaCl_2$	140
Potassium Chloride	K	5.11
diSodium Hydrogen Phosphate	Na_2HPO_4	8.1
Potassium diHydrogen Phosphate	KH_2PO_4	1.47

2.2.2.2 Spermine tetrahydrochloride

Spermine tetrahydrochloride (Sigma Aldrich) stocks were prepared by weighing 34.8 mg of spermine into a 1.5 mL Eppendorf tube and storing at -20°C. When required one tube containing 34.8 mg spermine tetra hydrochloride was taken from the freezer and 1 mL of diethylpyrocarbonate (DEPC) treated water was added to make a 0.1 M solution of spermine tetra hydrochloride. This solution was then diluted 10 times by pipetting 100 µL of the 0.1 M solution into a 1.5 mL Eppendorf tube containing 900 µL of DEPC treated water.

2.2.3 UV-Vis spectroscopy DNA melts

Ultraviolet and visible light (UV-Vis) spectroscopy was carried out to monitor the thermodynamic and kinetic properties of the SERS primer, and in the presence of its complementary target sequence as well as in the presence of a nonsense sequence.

UV-Vis spectroscopy was carried out on a Varian Cary 300 BIO spectrophotometer with Peltier thermal control cycling from 10 °C to 90 °C and back with 1 °C increments per minute while the UV absorbance was measured at 260 nm every minute.

Samples were prepared in six labelled 1.5 mL Eppendorf tubes. Table 2.2 shows the exact amounts and concentrations used in the UV hybridisation experiment. Briefly, 50 µL of SERS primer (10 µM), 50 µL of diethylpyrocarbonate (DEPC) treated water (Bioline, London, United Kingdom), target or non-target DNA (10 µM), and 400 µL of 1 × PBS obtained from Oxoid (Hampshire, United Kingdom).

Table 2.2 Sample setup for DNA hybridisation experiments, SP represents the SERS primer, C represents the complementary sequence of the SERS primer, Rv represents the reverse primer sequence.

Sample	Component 1	Component 2	PBS (µL)	Expectation
1	50 µL 10 µM SP	50 µL Water	400	Self Complementary Hybridisation
2	50 µL 10 µM SP	50 µL 10 µM C	400	Complementary Target Hybridisation
3	50 µL 10 µM SP	50 µL 10 µM Rv	400	No Hybridisation
4	50 µL Water	50 µL 10 µM C	400	No Signal Change
5	50 µL Water	50 µL 10 µM Rv	400	No Signal Change
6	50 µL Water	50 µL Water	400	No Signal Change

After all the positions in the UV spectrometer were filled with blanks consisting of 100 µL of water and 400 µL of PBS, the samples were pipetted into 500 µL microcuvettes. After this the samples were placed into the different slots of the UV spectrometer. The program was set to cycle from 10°C to 90°C and back to 10°C with 1°C increments per minute and the UV absorbance at 260 nm measured every minute. This cycle was repeated four times, data analysis was carried out ignoring the first cycle. The average of the following three cycles was used for data analysis after baseline correction at 20°C, the absorbance at 260 nm was then plotted against the temperature.

2.2.4 Synthesis of silver EDTA nanoparticles

Prior to synthesis of the nanoparticles all glassware was cleaned using aqua regia (HCl, HNO_3 – 3:1 v/v) for two hours in a fume hood. The glassware was then filled with distilled water and rinsed at least five times until the pH of the rinsings was neutral. Previous washings were collected and neutralised with sodium carbonate before being poured down the sink with excess water.

Two litres of distilled water was heated towards boiling using a hotplate while being constantly stirred, EDTA (94.7 mg) was added directly and prior to boiling sodium hydroxide (0.35 mg) was added. Upon reaching 100 °C silver nitrate (88 mg / 10 mL) was added dropwise, and the solution was boiled for a further 30 min. The colloid was then allowed to cool to room temperature and stored in plastic bottles at 4 °C.

Alternative batch 2 silver EDTA nanoparticles were synthesized using the previously reported method.[91] The basic native pH of the colloid (pH 11) was adjusted by the addition of TRIZMA® hydrochloride (0.5 mL of 200 mM pH 7.0) and Tween20 (0.5 mL of 0.2% v/v) to 9 mL of the as prepared colloid. This reduced the pH to 7, to prevent dsDNA denaturation.

2.2.5 Nanoparticle Characterisation

The synthesised nanoparticles were characterised using the following techniques.

2.2.5.1 Hydrodynamic radius

The hydrodynamic radius of the nanoparticles was determined using a Malvern HPPS particle sizer. A sample of ~1.5 mL was pipetted into a plastic cuvette and before each measurement a standard of 40 nm polystyrene beads was analysed.

2.2.5.2 ζ (Zeta) Potential

ζ (Zeta) potential measurements were carried out using a Malvern 2000 Zetasizer, using the default method protocol. A minimum sample volume of 3 mL was injected. Before each measurement a standard solution of -63.8 mV was measured.

2.2.5.3 UV-Vis spectroscopy of silver nanoparticles

Silver nanoparticle samples were analysed using a Varian Cary 300 Bio UV-Vis spectrophotometer. Silver nanoparticle samples were five times diluted in water and transferred into 500 µL glass cuvettes.

The concentration of the colloid was calculated using the Beer-Lambert law as detailed in Equation 2.1.

$$A = \varepsilon l c$$

Equation 2.1 Beer Lambert law.

Where; A = absorbance at λ_{max}

ε = extinction coefficient in $dm^3\ mol^{-1}\ cm^{-1}$

l = path length in cm

c = concentration of sample in mol dm^{-3}

The silver nanoparticle concentrations were calculated using an extinction coefficient (ε) of Ag 40 nm = 2.87 x 10^{10} M^{-1} cm^{-1}, and for 80nm = 1.04 x 10^{11} M^{-1} cm^{-1} from Yguerabide's papers [106, 107] and a path length of 1 cm.

2.2.6 pH measurements

pH measurements of the buffers were carried out using a Jenway 3510 pH meter, before the measurements the pH meter was calibrated using pH 4 phthalate, pH 7 phosphate, and pH 10 borate buffers. pH measurements of nanoparticle solutions using pH paper with a resolution of 0.2.

2.2.7 SERS primer limit of detection experiments

After UV-Vis analysis three replicates of each sample were used for the SERS limit of detection experiment. A volume of 2.5 µL of DNA sample (100 nM – 5 nM) was mixed with 125 µL of 1 ×PBS, 10 µL of 0.01 M spermine tetrahydrochloride and 137.5 µL of freshly buffered silver EDTA colloid (135 pM) in a microtiter plate. Each sample was analyzed one minute after preparation using a Raman Microscope (Renishaw inVia equipped with a 514.5 nm laser excitation with ~ 10 mW unfocussed laser power, coupled to a 20× / N.A. 0.40 long working distance objective). SERS spectra were analysed using Matlab 2008b, spectra were imported using the free GSTools toolbox from Gussem *et al*.[108] Fluorescence

background subtraction was carried out according to Lieber *et al*.[109] The peak intensity of the 1632 cm^{-1} peak was used for subsequent analysis and the intensities were plotted against the concentration of DNA.

2.2.8 SERS primer and varied target concentration experiments

For experiments where the target concentration was varied, SERS analysis was carried out using 2.5 µL of 100 nM SERS primer and 2.5 µL of its complementary sequence as target in 110 µL of PBS buffered at pH 7.3 ±0.2 as a positive control and a 20 base pair long nonsense DNA sequence as a negative control. The samples were pre-hybridized for 10 min at 95°C and 10 min at 20°C using a Stratagene MX4000 thermocycler. The target concentrations were varied over a range of concentrations from 0.1 to 5 nM final concentration after the addition of 10 µL of 0.01 M spermine tetrahydrochloride and 125 µL of silver EDTA nanoparticles. Samples were mixed in microcuvettes and analysed within one minute using a Raman Probe (Renishaw system coupled to a 514.5 nm Melles Griot laser with ~ 6 mW laser power using a 20× / N.A. 0.35 long working distance objective). Typical integration times were between 1 and 10 s and 3 accumulations. The fluorescent dye attached to the 5'-terminus of the SERS primer was 5-(and 6)-carboxyfluorescein (5,6-FAM) which has a λ_{max} of 490 nm. Data analysis was carried out using the strong peak in the spectrum at 1632 cm^{-1} which represents the xanthene ring C-C stretch.[110, 111] Matlab 2008b and a fluorescence background subtraction method published by Lieber *et al*. were used for data analysis.[109]

The repeats of this experiment used exactly the same volumes and concentrations except for the silver nanoparticle suspension which was 22 pM and 80 nm in size.

2.2.9 Culturing, lysis and genomic DNA extraction of *Staphylococcus epidermidis*

Bacterial strains of *Staphylococcus epidermidis* (NCTC 13360) and *Staphylococcus aureus* (NCTC 8325) were obtained from the national health protection agency

culture collections (HPACC Salisbury, UK) and cultured in sterile Tryptone Soy Broth (Oxoid). Tryptone Soy Broth (TSB) medium was prepared by weighing 15 g of TSB (Oxoid) into a 500 mL glass bottle and dissolved in 500 mL of distilled water and autoclaved for 30 min at 121°C. 20 g of Tryptone Soy Agar (TSA) (obtained from Oxoid) was weighed into a 500 mL glass bottle and filled up with 500 mL of distilled water and autoclaved for 30 min at 121°C.

The glass tube containing lyophilized cells was opened in a LAF cabinet and 500 µL of TSB was added. The cells were then incubated overnight at 37°C. Using an inoculation loop, cells were streaked onto a TSA plate and after overnight incubation at 37°C a single colony was picked from the plate and transferred into a 50 mL Greiner tube (BD) containing 5 mL of TSB and incubated again overnight at 37°C.

The cells were centrifuged at 16,110 × g for 10 min at 4°C, the supernatant was then removed and 1 mL of Lysostaphin was added. The suspension was incubated for 30 min at 37°C to lyse the cells. DNA was extracted according to the manufacturer's protocol from the lysate using a QIAamp DNA minikit (Qiagen, Crawley, UK).

The quality of the genomic DNA was measured using a UV spectrometer (Eppendorf Biophotometer), the absorbance (ABS) at 230 nm, 260 nm and 280 nm was noted and the ratios 260/230nm and 260/280 were calculated.

2.2.10 Polymerase Chain Reactions containing SYBR® Green

All reagents were aliquoted into single use sample volumes and either stored in the fridge at 4°C or the freezer at -20°C. PCR reactions were setup in an analytical batch format, preparing a master mix containing all the reagents needed except for primers, probes, and dyes. For each reaction a total volume of 25 µL was used, containing 0.5 µL of DNA polymerase Phusion® Hot Start II 2U/µL (Finnzymes), 5 µL of 5x Phusion® HF buffer (Finnzymes), 0.5 µL of deoxynucleoside triphosphates (dNTP) 10 mM each (New England Biolabs) and

for the reactions containing SybrGreen® I (Invitrogen) 1 µL of a 12.5x work solution was added, otherwise SybrGreen® I was replaced by an extra 1 µL of water. 1 µL of 2.5 µM forward and 1 µL of 2.5 µM reverse primer were also added. Volumes were made up to a total volume of 15 µL using water and finally 10 µL of template DNA at different concentrations was added.

Table 2.3 PCR reaction sample setup.

Reagents NEB	Stock concentration	Volume (µL)	Final concentration
Buffer HF	5x + 7.5 mM $MgCl_2$	5	1x + 1.5 mM $MgCl_2$
Polymerase Phusion NEB	2U/µL	0.5	1 U (0.04U/µL)
dNTP's NEB	10 mM each	0.5	200 µM each
SYBR® Green I	12.5x	0/1	0.5x
Fw Primer	2.5 µM	1	100 nM
Rv Primer	2.5 µM	1	100 nM
Water	X	7/6	X
Template	9, 0.9,0.09,0.009,0 ng/µL	10	90, 9, 0.9, 0.09, 0 ng
Total	X	25	X

Thermal cycling and fluorescence detection was carried out using a Stratagene MX4000 Real Time PCR machine and fluorescence detection was carried out using a 492 nm excitation filter and a 515 nm emission filter during the annealing phase. The cycling protocol was: 10 s at 98°C, thereafter 30 repeats of 10 s at 98°C, 30 s at 58°C, and 30 s at 72°C. Data analysis was carried out using the MX4000 standalone analysis software.

2.2.11 Capillary gel electrophoresis

Capillary gel electrophoresis was carried out using an Agilent Bioanalyzer and DNA1000 kit including microfluidic chips and reagents (Agilent Technologies, UK). All procedures were carried out following the manufacturer's protocol. Briefly, a DNA1000 chip was loaded with gel. Running buffer including the upper and lower markers was added to the sample wells and the sample was added, well mixed and transferred to the Bioanalyzer, and the run was started.

2.2.12 Polymerase Chain Reactions for SERS analysis

PCR reactions were setup in a total volume of 25 µL for each reaction. Each reaction contained 0.5 µL of 2 U μL^{-1} DNA polymerase Phusion® Hot Start II (New England Biolabs, UK), 5 µL of 5x Phusion® HF buffer (New England Biolabs, UK), 0.5 µL of deoxynucleoside triphosphates (dNTP's) 10 mM each (New England Biolabs, UK). 2 µL of 2.5 µM forward and 2 µL of 2.5 µM reverse primer. Volumes were made up to a total volume of 15 µL using DEPC treated water and finally 10 µL of 0.09 ng μL^{-1} genomic template DNA was added. Thermal cycling was carried out using a Stratagene MX4000 Real Time PCR machine. The cycling protocol was: 30 s at 98°C, thereafter 30 repeats of 10 s at 98°C, 60 s at 62°C, and 60 s at 72°C and a final extension at 72°C for 1 minute. After cycling the sample was cooled to 20°C.

2.2.13 SERS analysis of PCR samples

PCR samples were analysed in the SERS assay as follows, 1 µL of the PCR sample was added to 499 µL of PBS buffer. 115 µL of the sample was mixed with 10 µL of 0.01 M spermine tetrahydrochloride and 125 µL of five times concentrated silver EDTA nanoparticles buffered in 10 mM TRIZMA hydrochloride and 0.01% v/v Tween20. SERS analysis was carried out as discussed above.

2.3 Results and discussion

In order to make a positive SERS assay, a SERS primer was designed which contained a dye labelled segment which was rendered single stranded upon hybridization to a target sequence (Figure 2.2). This single stranded region will have a higher affinity for the metal surface than double stranded DNA, resulting in an increase in the SERS signal. The SERS primer can be used to detect target DNA directly, or used as a primer in combination with PCR.

(A) (B)

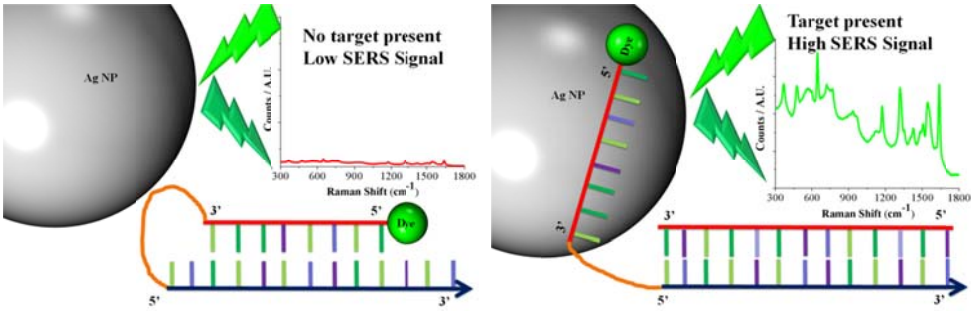

Figure 2.2 Schematic representation of the SERS probe. Ag NP represents a silver nanoparticle. (A) In the case of a negative sample (when target DNA is absent), the SERS primer is closed and predominantly dsDNA. This means it does not adsorb onto the negatively charged nanoparticle resulting in a low SERS response. (B) In the case of a positive sample, the complementary target DNA displaces the partly self complementary region of the SERS primer which is destabilized using mismatches, this results in a dye labelled ssDNA region which is then free to adsorb onto the negatively charged nanoparticle surface resulting in a high SERS response.

2.3.1 Assay design

The f*emA-SE* gene of *Staphylococcus epidermidis* was chosen as a model system for this work. The sequence of the f*emA-SE* gene (gene bank accession number U23713)[23, 112] was obtained from the National Center for Biotechnology Information (NCBI).[100] Primer3 online software was used to generate specific primers.[102, 103, 113] The primers and amplicon region were selected by the Primer3 software allowing analysis for internal folding, and for hetro- and homo-dimer formation at 58°C using online software mFold, UNAFold and DINAmelt available

from the Rensselaer Polytechnic Institute.[102, 104, 114, 115] Finally the specificity of the primers was checked against other bacteria using NCBI BLAST.[105]

The designed primer sequences are shown in Table 2.4. These sequences are specific to the gene *femA-SE* of *Staphylococcus epidermidis* and are designed to generate a minimal amount of internal foldings. The T_m values are an indication of the temperature at which half the oligonucleotide strands in a sample are bound to their complements.

Table 2.4 Overview of selected oligonucleotide sequences.

Name	Sequence 5' → 3'	T_m (°C)[113]
Forward Primer	TACTACGCTGGTGGAACTTCAAATCGTTATCG	61
Reverse Primer	GAACCGCATAGCTCCCTGC	59.2

The region of genomic DNA selected by the Primer3 software was checked for internal sequence folding at 58°C containing 50 mM monovalent salt and 1 mM divalent salt and sequence type linear using the DINAmelt Two state folding online software.[104]

The positions of the primers within the *femA-SE* gene are indicated in yellow, whilst the regions most likely to fold are shown in red in Figure 2.3. Therefore the red areas were to be avoided as primer binding regions.

TGAGAAACGTCCAGAGAATAAAAAAGCACATAACAAAAAGGAAAATTTAGAACAACAACTCGATGCAAATCAGCAAAAAATT
AATGAAGCTAAAAACTTAAAACAAGAACATGGCAATGAATTACCCATCTCTGCTGGCTTCTTTATAATTAATCCGTTTGAAG
TAGTTTACTACGCTGGTGGAACTTCAAATCGTTATCGCCATTTTGCAGGGAGCTATGCGGTTCAATGGAAGATGATTAACTA
TGCAATTGAACATGGTATTAATCGGTATAATTTC

Figure 2.3 The base numbers 1191 to 1470 of the *femA-SE* gene. The region with an increased risk of internal folding of the template DNA is shown in red. In yellow are the positions of the selected primers.

Although the results are obtained from computational models, these models can provide good insights into the performance of an assay. The software used to create these models was developed using experimental data in order to predict accurately the performance of the assay being investigated.[102, 104, 105, 113-119]

2.3.2 Design of the SERS primer

Before the SERS primer was finalised a standard PCR assay was designed using Primer3 PCR sequence design software.[113] The forward primer designed in the assay design section 2.3.1 will be modified into the SERS primer.

The forward (Fw) primer selected in the previous section was modified into the SERS primer by creating a self complementary probe sequence with a melting temperature (T_m) 10 to 15°C lower than that of the primer sequence.

The SERS primer was split up into four different sections, allowing the design of different sections each with its function (see Figure 2.4).

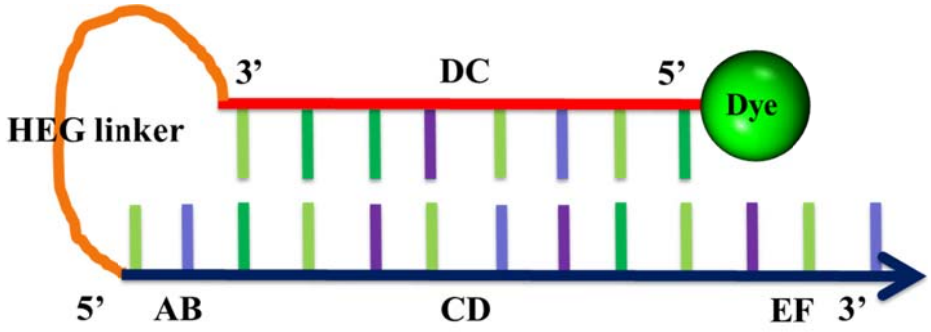

Figure 2.4 Simplified schematic of the SERS primer showing the design areas. Section AB and EF are overhang regions, section CD and DC are the self complementary regions.

The following rules were applied to the design of the SERS primer.

1. T_m of the SERS primer priming sequence region (ABCDEF) must be greater than the SERS primer self complementary region (CD) by approximately 15°C. This is because the SERS primer priming region has to bind to the target sequence before the SERS primer becomes double stranded.
2. The length of the HEG linker is ~2.6 nm thus AB must < 7bp (2.6 nm). This ensures the SERS primer self complementary region can easily find its complement primer sequence (region CD).
3. Region CD's T_m should be > 25°C to ensure the SERS primer is double stranded while analysed at room temperature in the SERS assay.

4. SERS primer priming sequence (region ABCDEF) should be > 15 bases to create priming specificity.

The designed oligonucleotides are shown in Table 2.5. The forward (Fw) primer selected in the previous section was modified with a self complementary probe sequence with a melting temperature (T_m) that was approximately 15°C lower than that of the primer sequence by using four mismatches in the self complementary sequence.

Table 2.5 Oligonucleotide sequences designed for this study. Red bases represent mismatches in the self complementary part of the SERS primer to reduce the T_m of the hairpin structure.

Name	Sequence 5'→3'	T_m (°C)	Hairpin T_m (°C)
SERS primer	FAM-GAAGTTACATCAGAA-HEG- TACTACGCTGGTGGAACTTCAAATCGTTATCG	61.0	46.6
SERS primer complement	CGATAACGATTTGAAGTTCCACCAGCGTAGTA	61.0	N/A
Reverse primer	GAACCGCATAGCTCCCTGC	58.6	N/A

The proof-of-concept was carried out using synthetic oligonucleotides and SERS.

2.3.3 SERS primer hybridisation

UV-Vis spectroscopy was used to monitor the hybridization profile of the SERS primer in the presence of complementary target DNA and non-target DNA (e.g. Reverse primer). Single stranded DNA absorbs more light at 260 nm then dsDNA, and double stranded DNA becomes single stranded upon heating. The temperature where half of the DNA is in single stranded form is called the T_m. The absorbance at 260 nm was thus monitored against temperature and this shows the formation of single stranded DNA (Figure 2.5).

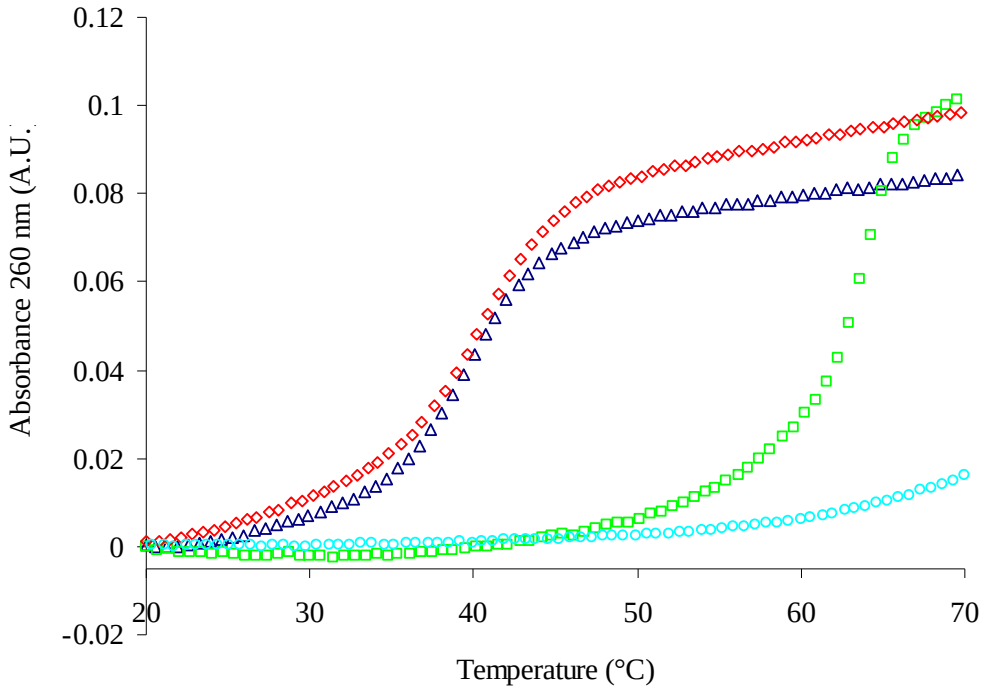

Figure 2.5 UV-Vis DNA melt analysis. Blue triangles represent the SERS primer, the T_m value of the self complementary region was found to be 40°C. Green squares represent the SERS primer and target DNA, the T_m of the complementary target DNA is 62°C. Red diamonds are the SERS primer and non-target DNA, the T_m of the self complementary region is 40°C. Cyan circles are the water control.

The SERS primer (blue triangles) denatures and becomes ssDNA when heated above 50°C, and when cooled in the presence of target DNA (green squares) forms a duplex before the partly self-complementary region of the SERS primer can hybridize back to itself. This results in a duplex between the target and the SERS primer with a region of single stranded dye labelled DNA attached. In the case of non-target DNA (red diamonds) the SERS primer did not form a duplex with the added ssDNA and forms a duplex with its partly self complementary sequence. The water control (cyan circles) showed little increase in absorbance upon heating.

The UV-Vis data showed that the target DNA hybridized to the SERS primer with a Tm of 62°C before the self complementary region of the SERS primer hybridized back to itself with a Tm of 40°C. In the presence of non-target DNA

the SERS primer closed itself at the same temperature (Tm 40°C) as without target DNA proving that the SERS primer is specific to its complementary target.

The calculated and experimental Tm's of the hybridisation between the SERS primer and the target DNA closely match with only 1°C difference. The calculated Tm for the closure / hairpin formation of the SERS primer was 6°C higher than the experimentally observed Tm of 40°C. This is not problematic because the clear differences in Tm's (22°C) between target and no target DNA present in the sample ensure that the target can bind to the SERS primer before the hairpin structure of the SERS primer was closed.

2.3.4 Nanoparticle characterisation

Two batches of silver EDTA nanoparticles were synthesised and characterised, using the methods described in section 2.2.4. The second batch was prepared when the first batch was running low. Differences observed between the batches are discussed in the following sections.

2.3.4.1 Basicity of the nanoparticle solutions

The pH of the nanoparticle solutions was measured and it was found that batch one had a pH of 6 and batch two had a pH >11. Since DNA can become single stranded at higher pH values, the second batch had to be buffered using a final concentration of 10 mM TRIS resulting in a pH value of 7. A surfactant, Tween20 at 0.01% v/v was added to reduce the speed and size of aggregates formed upon spermine addition, before SERS analysis. These conditions were used in the study by Macaskill *et al.*[91] A possible reason for the difference in pH between the first and the second batch of silver EDTA nanoparticles is aging of the nanoparticle solution.

2.3.4.2 Hydrodynamic radius

DLS measurements were carried out and the results show that the average hydrodynamic diameter of the nanoparticles in the first batch of silver nanoparticles was 56 ± 4.1 nm. The commercial standard of 40 nm ± 1.8 nm

polystyrene beads was slightly underestimated at 39.2 ± 2.1 nm but the average was within the range to be an acceptable measurement. The second batch of nanoparticles was measured both before and after addition of water, buffer and surfactant. These measurements were carried out to check that the buffer did not aggregate the colloid. Pure nanoparticles had an average size of 85 ± 1.6 nm, after adding 10% v/v distilled water the average size was 87 ± 2.1 nm, replacing the water with 10% v/v TRIS 10 mM final concentration resulted in a size of 87 ± 1.8 nm, and finally when adding 10% v/v TRIS and Tween20 0.01% v/v the average size of the nanoparticles was 90 ± 1.0 nm. An increase in hydrodynamic radius was found but no significant aggregation of the nanoparticles was observed. A possible reason for the difference in size between the two batches could be a slight variation in the amount of silver nitrate, EDTA, or sodium hydroxide added during the nanoparticle synthesis. The slight increase in hydrodynamic radius after addition of TRIS might be due to adsorption of TRIS onto the nanoparticle surface via the primary amine, the larger increase in hydrodynamic radius after addition of tween20 might be because tween20 is a long molecule increasing the water shell around the particles therefore increasing the overall hydrodynamic radius.

2.3.4.3 ζ (Zeta) Potential

The ζ potential of silver EDTA nanoparticles was measured in batch one and it was found that the overall negative surface charge was -52.5 ± 7.8 mV. For the pH 7 TRIS buffered nanoparticle batch 2, an overall negative surface charge of -51.4 ± 0.7 mV was measured. These batches can be considered stable, since the ζ potential is lower than -30 mV.

2.3.4.4 UV-Visible spectroscopy

UV-Visible spectroscopy was carried out to measure the absorption maxima of the silver EDTA nanoparticle solution, and thereby the quality of the nanoparticle suspension. Absorbance maxima and the width of the peak relate to the size and monodispersity of the colloidal solution. The data in Figure 2.6 shows the UV-

Visible absorbance spectrum of silver EDTA nanoparticle batch 1. A peak was observed at 415 nm. A full width at half maximum (FWHM) of 70 nm was measured indicating a monodispersed colloidal suspension of silver nanoparticles.

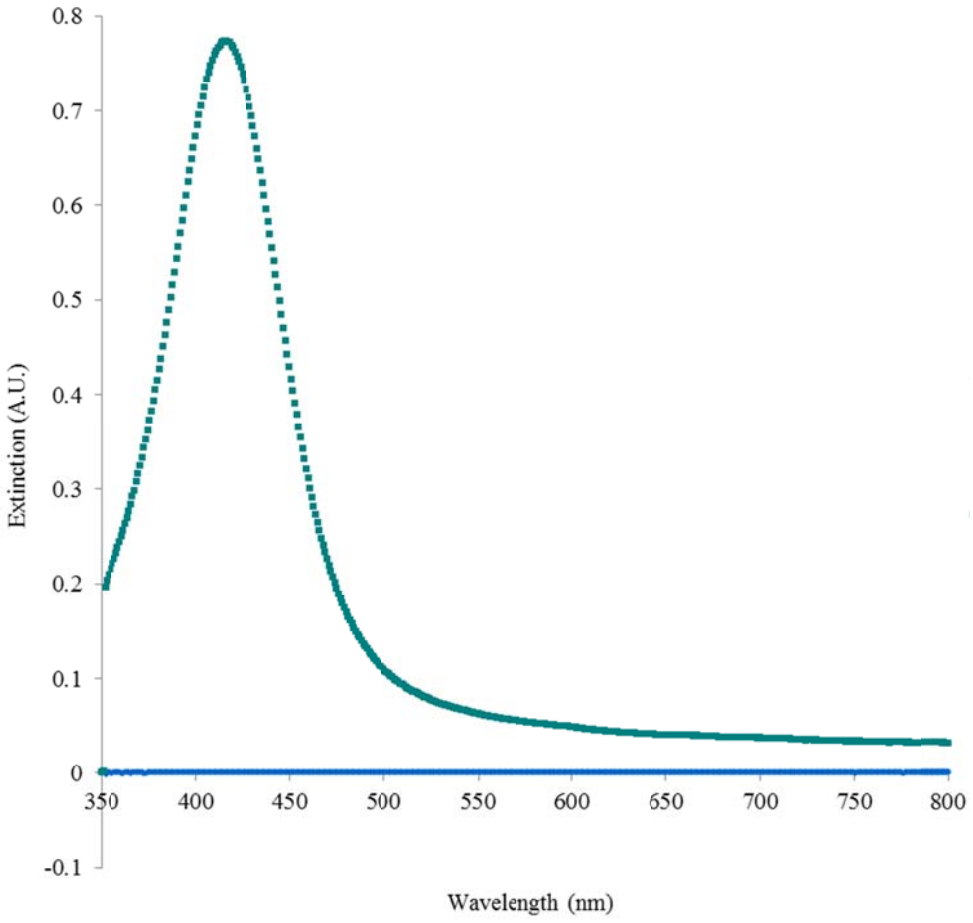

Figure 2.6 Absorbance spectrum of batch one silver EDTA nanoparticles (green), and water (blue). λ_{max} of the Ag-EDTA nanoparticles was observed at 415 nm.

From the absorption spectrum, the nanoparticle batch one concentration was calculated to be 135 pM using Beers law and the extinction coefficient (ε) of 40 nm Ag of 2.87 x 10^{10} M^{-1} cm^{-1} from Yguerabide's paper [106, 107] and a path length of 1 cm. Nanoparticle batch one had a concentration of 135 pM.

The second batch of silver EDTA nanoparticles was analysed to see if the nanoparticles were stable in a 10 mM TRIS buffer solution. A peak was observed at 420 nm with full width at half maximum (FWHM) of 85 nm. The λ_{max} of the buffered colloid was 421 nm and the FWHM was 85 nm indicating no significant changes or aggregation effects due to buffering the colloid (Figure 2.7).[120]

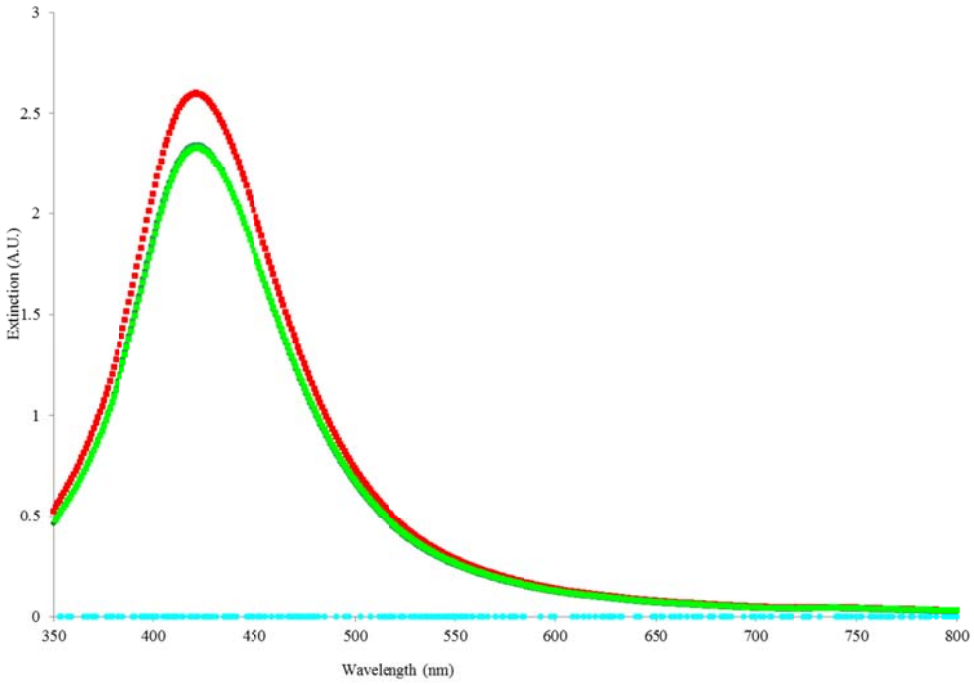

Figure 2.7 UV-Vis spectra obtained from batch two silver EDTA nanoparticles (red), 90% silver EDTA nanoparticles diluted in water (dark green), 90% silver EDTA nanoparticles buffered in TRIZMA® (10 mM) (green), 90% silver EDTA nanoparticles in TRIZMA® (10 mM) and Tween 20 (0.01%) (light green), and water control (cyan).

From these results it can be seen that the colloid did not aggregate. A decrease in the peak height was observed due to dilution of the colloid. The size of the buffered silver EDTA nanoparticles was determined with dynamic light scattering using a Malvern HPPS particle sizer. The hydrodynamic diameter of the particles was measured as 90 ± 1 nm. Therefore the extinction coefficient of 80 nm diameter Ag of 1.04 x 10^{11} M^{-1} cm^{-1} was used to calculate the concentration which was 22 ± 1 pM.

2.3.5 SERS primer dilution series

A dilution series of the SERS primer and target with a ratio of 1:1 was conducted in order to find the limit of detection. A positive signal was observed from just 90.9 pM of SERS primer and target. It is clear that below this level, discrimination between target and non-target by eye is not obvious (Figure 2.8).

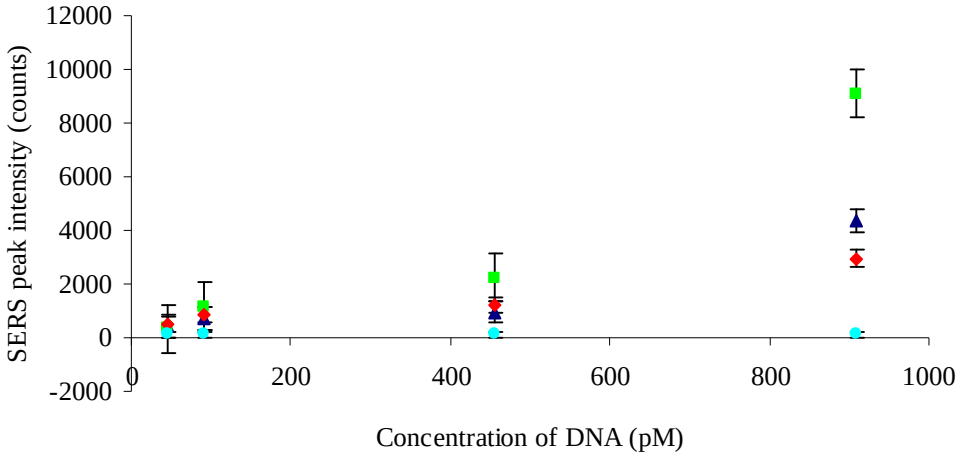

Figure 2.8 A dilution series of the SERS primer was obtained using the peak intensity at 1632 cm^{-1}. SERS primer (blue triangles), SERS primer and perfect match (green squares), SERS primer and non-target DNA (red diamonds), blank (cyan circles). A 514.5 nm laser excitation and 10s integration time and 3 accumulations were used during SERS analysis. Error bars represent the standard deviation of three individual samples.

Figure 2.9 shows the SERS response for this positive assay. When no target or nonsense DNA is present a low SERS signal intensity was observed (blue triangles, red diamonds), and when the SERS primer hybridized to its target sequence an increase in SERS signal intensity was observed (green squares). The blank control (cyan circles) showed no SERS signal as expected. Spermine tetrahydrochloride was used to aggregate the silver EDTA nanoparticles and enhance the SERS response of the FAM labelled DNA. Without using spermine tetrahydrochloride no SERS response was observed from the FAM labelled DNA.

(A) (B)

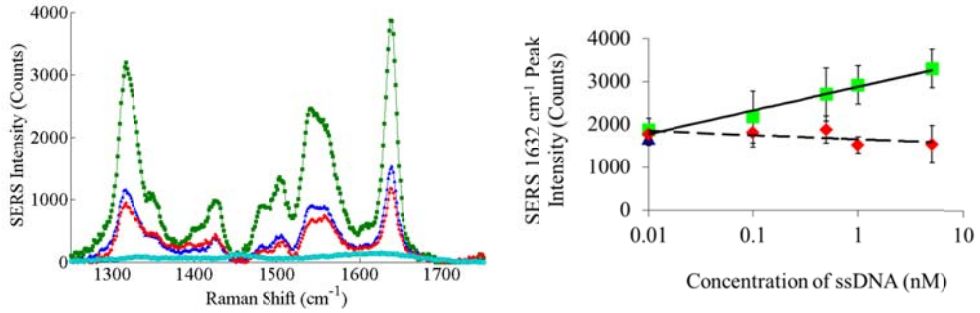

Figure 2.9 (A) SERS spectra of 1 nM SERS primer (blue triangles), SERS primer and 1 nM perfect match (green squares), SERS primer and 1 nM non-target DNA (red diamonds), blank (cyan circles). Exposure time was 1 second using 3 accumulations. (B) SERS intensities of SERS primer with a concentration of 1 nM and different concentrations of target and non-target DNA. For the three repeats of the samples the peak at 1632 cm^{-1} was monitored following 3 accumulations of 1 second exposure. SERS primer 1 nM no DNA was added (blue triangle), SERS primer 1 nM and different concentrations of complementary target DNA (green squares), SERS primer 1 nM and different concentrations single stranded non-target DNA (red diamonds). Each point represents the mean of 3 replicates and error bars represent the standard deviation. The detection limit of target DNA was 1 nM, using 1 nM of SERS primer (3 times standard deviation of the control).

The ratio of SERS primer to target needed to afford a clear discrimination between target and non-target DNA was therefore investigated by keeping the SERS primer concentration constant at 1 nM and varying the concentration of target and non-target DNA over a range of 0.01-5 nM (Figure 2.9B). The ratio between SERS primer and target was found to be important in the discrimination between a positive and a negative sample. Reliable discrimination between target and non-target DNA becomes problematic below a 1:1 ratio. This is reported in more detail in the following chapter.

The DNA concentration range and monolayer coverage effect was further investigated using the second batch of nanoparticles. In Figure 2.10 it can be seen that the dynamic range is from 500 pM to 1000 pM, the monolayer coverage effect starts to play a significant role at 2500 pM and the SERS peak intensity decreases further when higher concentrations of DNA are used. For the

first batch of nanoparticles the monolayer coverage effect starts to play a role between 5000 and 10000 pM.

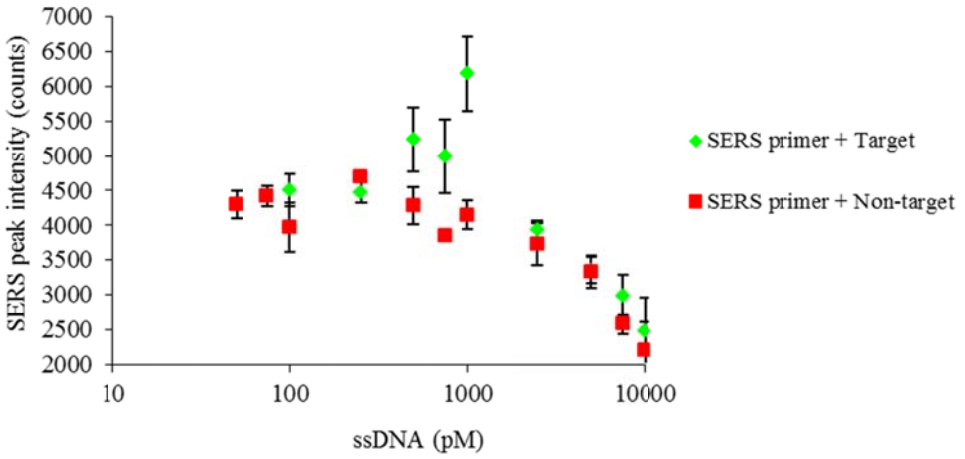

Figure 2.10 SERS peak intensities at 1634 cm^{-1}, SERS primer concentration was kept constant, concentration of complement and nonsense DNA were varied over a range of 100-1000 pM.

The second batch of nanoparticles were larger and at a lower concentration than the first batch, batch one was 135 pM and 50 nm compared to batch two which was 22 pM and 87 nm. Batch two nanoparticles had less than half the surface area compared to batch one. This perhaps explains why the monolayer coverage effect was reached at lower DNA concentration using the second batch. In conclusion the upper limit of the DNA concentration range is dictated by the available surface area on the nanoparticles. However, when there is a need for an extended dynamic range the nanoparticles can be concentrated to increase the available metal surface area. This will be further explained in the following chapter.

2.3.6 Culturing, lysis, and DNA extraction of bacterial cultures

Genomic DNA from the bacterium *S. epidermidis* was used as template DNA for the PCR reaction. *S. epidermidis* was cultured in growth medium to confluent levels before cells were lysed using lysostaphin. Genomic DNA was then extracted using “Boom” DNA extraction. Table 2.6 shows the amount and quality of the genomic DNA (gDNA) isolated. DNA absorbs light at 260 nm and twenty

five ng/µL gDNA provides an absorption value of 0.5.[121] The gDNA concentration was calculated to be 90.2 ng/µL. The absorption ratio 260/280 (proteins absorb light at 280 nm) provides information on the amount of proteins carried over into the sample, with a good quality value for gDNA being is 1.7-1.9.[122] The 260/230 ratio informs on the amount of guanidine hydrochloride left in the sample and a good value for this is ~1.7-2.2.[121, 122] Our analysis observed a value of 1.28 for the 260/280 ratio which indicates there was slight protein contamination. A value of 1.11 for the 260/230 ratio also indicated a guanidine hydrochloride carry over.[122] The quality of this DNA was a little poor since the values obtained were below the values set for high quality. However the gDNA can still be used in the PCR reaction because the protein, salt and ethanol contaminants will be diluted in water before the PCR.

Table 2.6 Yield and quality of the isolated genomic DNA. Negative sample is a DNA extraction without using bacterial cells. The yield and purity are detailed for samples containing *S. epidermidis* and *S. aureus* cells.

	Concentration (ng/µL)	260/280 (Proteins)	260/230 (GuHCl)
Negative control	7.6	1.26	0.96
S. epidermidis	90.2	1.28	1.11
S. aureus	33.0	1.87	1.83

2.3.7 Polymerase Chain Reaction with the SERS primer

It is likely that the SERS primer cannot be used on PCR product because the self complementary part of the SERS primer can bind to the DNA strand synthesised by the forward primer. This would result in the SERS primer self complementary region being double stranded resulting in the failure of the assay (Figure 2.11). Therefore it was decided to directly introduce the SERS primer into a PCR reaction.

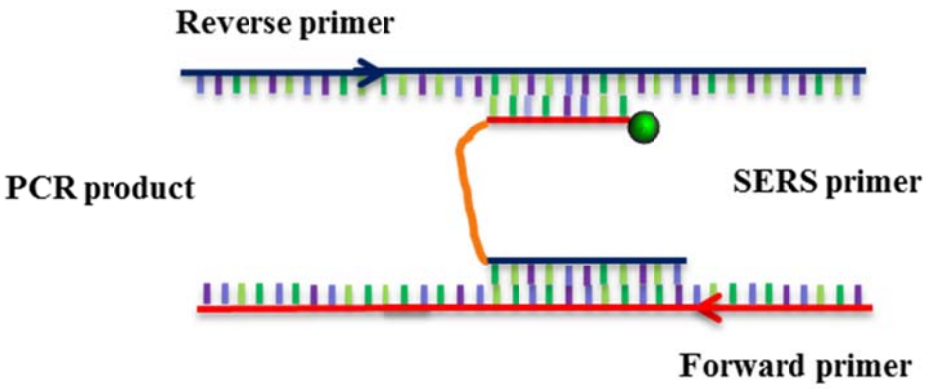

Figure 2.11 Mode of action of SERS primer on PCR product.

It was important to select a DNA polymerase (Phusion® Hot Start II) without 5'→3' exonuclease activity to keep the self complementary part of the SERS primer intact during and after the PCR (see Figure 2.12). Since the self complementary unit of the SERS primer can hybridise to the antisense strand of the template DNA during the PCR reaction, the self complementary region of the SERS primer would be digested by the 5'→3' exonuclease activity of a 5'→3' exonuclease active DNA polymerase enzyme. This problem could be avoided using a 5'→3' exonuclease deficient DNA polymerase.

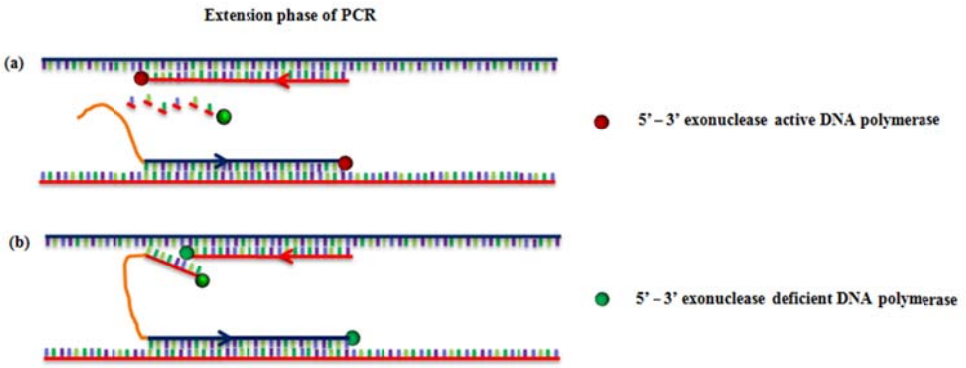

Figure 2.12 Difference between DNA polymerase with 5'→3' exonuclease activity (a), and a DNA polymerase without 5'→3' exonuclease activity (b). In situation (a) the exonuclease activity digests the self complementary part of the SERS primer. In situation (b) the 5'→3'exonuclease deficient DNA polymerase displaces rather than digests the self complementary part of the SERS primer.

Before incorporating the SERS primer into the PCR reaction, target DNA was required. It was decided to use genomic DNA isolated from *Staphylococcus epidermidis.*

After isolating the gDNA the selected target region of the *femA-SE* gene was amplified using PCR and incorporate the SERS primer. This was achieved using quantitative PCR (qPCR) with SYBR® Green I. During the PCR reaction, the DNA is amplified and when SYBR® Green I is incorporated it will emit an increased fluorescent signal. Figure 2.13 shows that the isolated gDNA was amplified due to the increase in SYBR® Green I signal. A difference in Cycle threshold (Ct), value smaller then 3.4 between 90 ng & 9 ng of gDNA shows that inhibitors in the gDNA were diluted. Since the PCR process is an exponential process and a ten fold dilution should theoretically result in a Ct value difference of 3.4 e.g. $2^x = 10$ therefore x = 3.4. The quantities 9, 0.9, 0.09 ng of gDNA show good PCR efficiency because the Ct difference per 10 fold dilution was ~3.4. No fluorescence was observed in the negative control, therefore no contamination was observed.

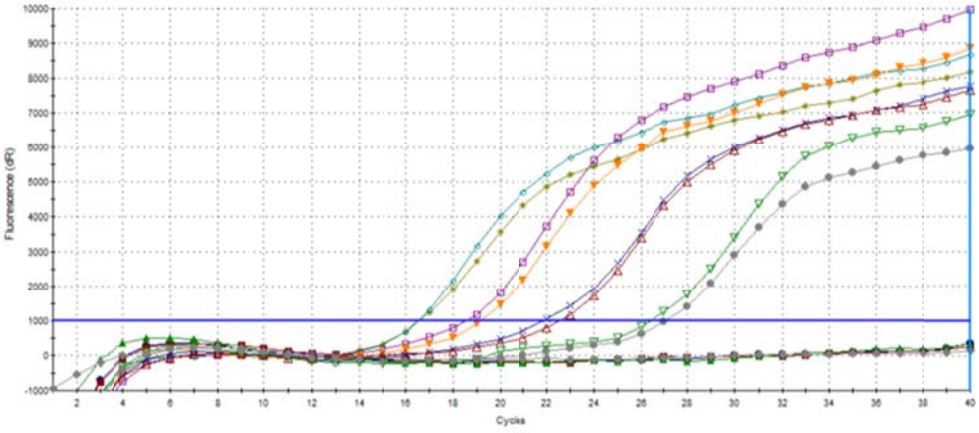

Figure 2.13 From left to right duplicates of 90, 9, 0.9, 0.09, and 0 ng gDNA amplification curves. The blue line represents the cycle threshold (Ct) line which was set to 1000 fluorescence units.

A SYBR® Green I melt i.e. a dissociation curve was measured to identify the melt profile of the product or products made. Figure 2.14 shows the first derivative of

the fluorescence signal on the y axis against temperature on the x axis. From these results it can be seen that the PCR product i.e. amplicon, melted at 82°C, and no additional curves were observed which indicates specific amplification of the desired product.

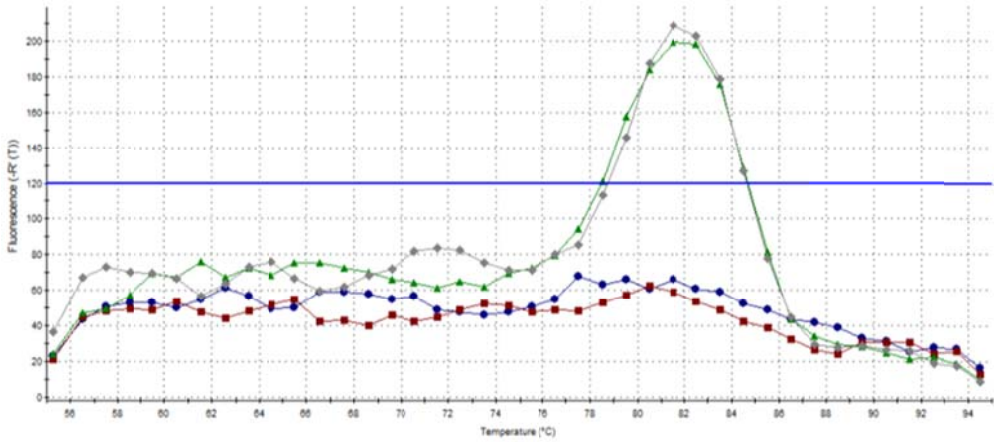

Figure 2.14 SYBR® Green I dissociation curve, of two negative (blue and Red) and two positive (Green and Grey) samples. The blue line represents the threshold line.

To confirm these results, capillary gel electrophoresis was carried out using the samples without SYBR® Green I. In capillary gel electrophoresis of DNA, different sizes of dsDNA are separated. By using a gel matrix, a potential difference, and the overall negative charge of the DNA, it is possible to make the dsDNA move towards the positive electrode. Smaller molecules move faster than larger molecules, thereby different PCR products can be separated from each other. Using a separate lane with a DNA mixture of known sizes (i.e. a ladder) it is possible to analyse if the correct size products were made during the PCR. Figure 2.15 shows the electrophoresis result. From bottom to top the green line represents the 15 bases long lower DNA marker, the following line is the so called primer dimer formation, a phenomenon which is not very well understood.[118] It is likely due to dimer formation between SERS primer and the reverse primer since computational modelling showed heterodimer formation between the SERS primer and the reverse primer, however mis-priming, internal folding as well as homodimer formation could be possible reasons for the

formation of the so called primer dimers. The third line from the bottom (50 – 100 bp) is the 91 bases long PCR product (Dye + 15 bases SERS primer self complement + HEG unit + 32 bases SERS primer priming region + 7 amplified bases + 19 bases reverse primer = dye + 15 bases ssDNA + HEG + 58 bases dsDNA ≈ 91 bases), the 2nd band is shorter than 50 base pairs and from lane 9 and 10 it can be concluded that is the double stranded SERS primer, and as no other bands are shown. From these results we can conclude that the correct PCR product was amplified.

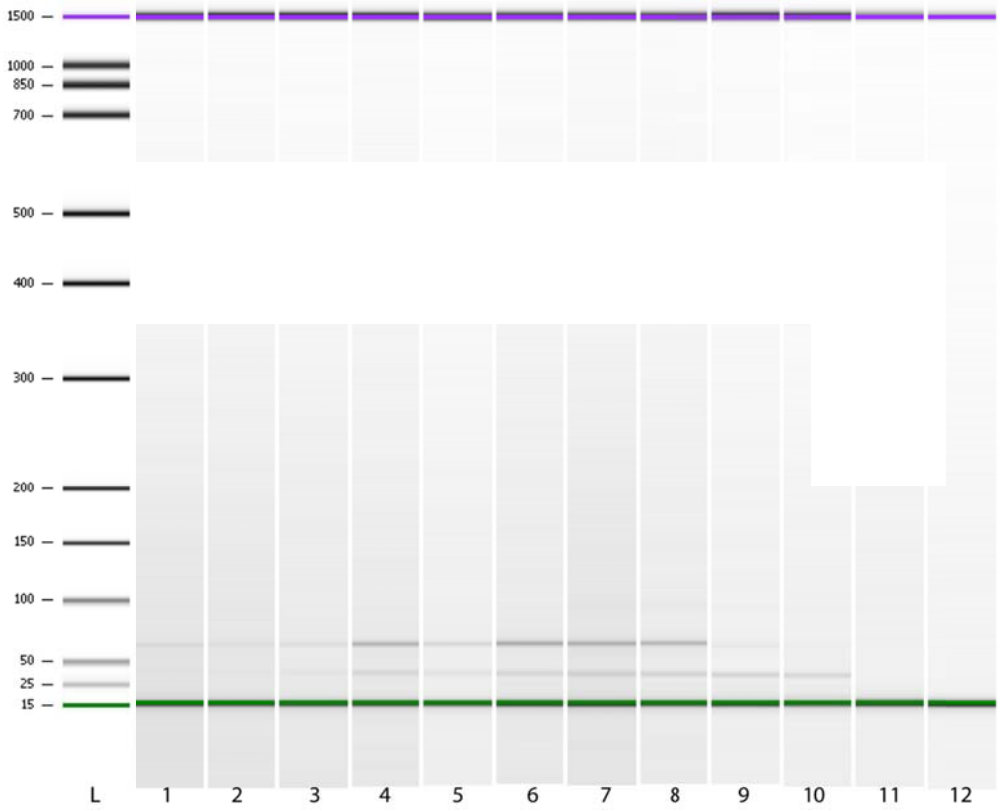

Figure 2.15 Bioanalyzer gel electrophoresis results; 1 & 2: 90ng, 3 & 4: 9ng, 5 & 6: 0.9ng, 7 & 8: 0.09ng, 9 & 10: 0ng, 11 & 12: water.

Quantitative capillary electrophoresis showed specific amplification of the *femA-SE* gene of *Staphylococcus epidermidis* with a yield of 57.5% (product output (nM) / primer input (nM)*100%) (Figure 2.16 and Table 2.7).

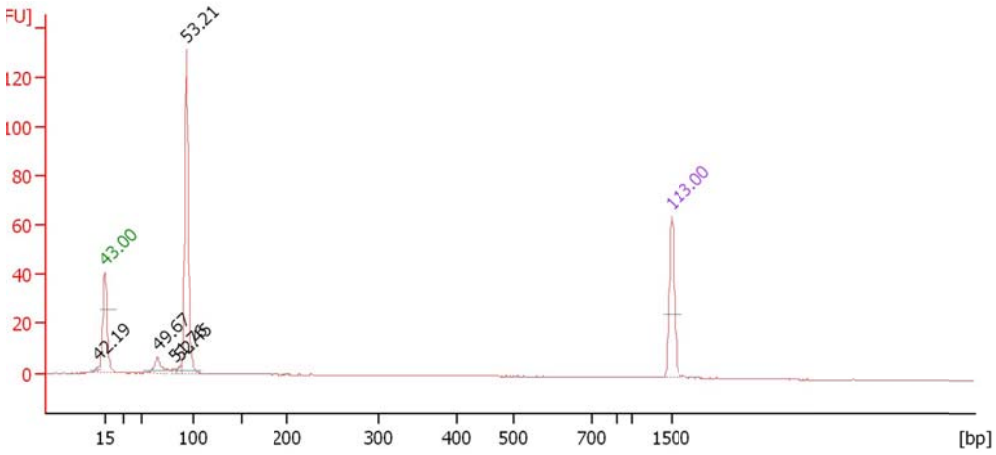

Figure 2.16 Bioanalyzer electrophorogram of the PCR *Staphylococcus epidermidis* positive sample. The most intense peak proves the amplification of the *femA-SE* gene specific region of *Staphylococcus epidermidis*. The numbers above the peaks represent the retention time in s.

Table 2.7 Quantitative data obtained from the Bioanalyzer of the PCR *Staphylococcus epidermidis* positive sample.

Peak	Size (bp)	Concentration (ng μL^{-1})	Molarity (nM)	Observations
1	15	4.20	424.2	Lower marker
2	65	0.72	16.6	
3	82	0.14	2.7	
4	87	0.15	2.6	
5	93	7.09	115.4	
6	1500	2.10	2.1	Upper Marker

Amplification of DNA was not observed when using 1 ng *Staphylococcus aureus* DNA (Figure 2.17, and Table 2.8) or in the No Template Control (NTC) (Figure 2.18, and Table 2.9.

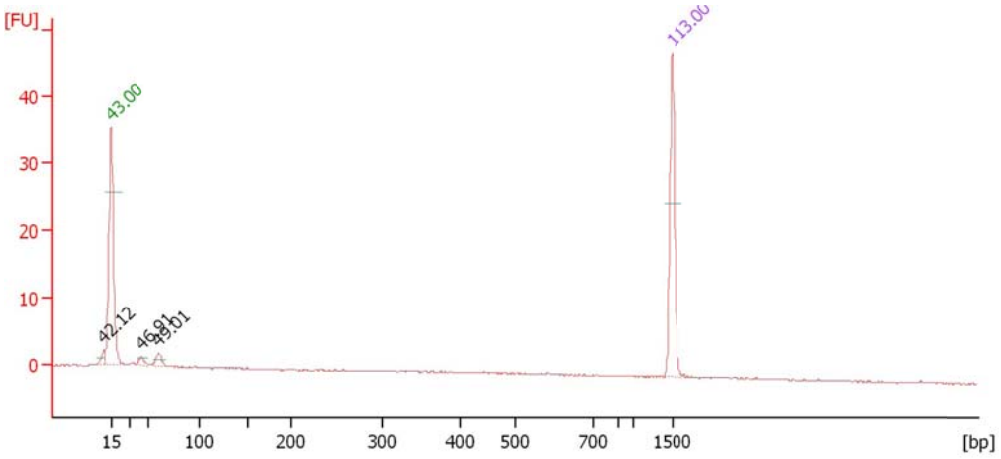

Figure 2.17 Bioanalyzer electrophorogram of the PCR *Staphylococcus aureus* negative sample. No amplification of the *femA-SE* gene observed. The numbers above the peaks represent the retention time in s.

Table 2.8 Quantitative data obtained from the Bioanalyzer of the PCR *Staphylococcus aureus* negative sample

Peak	Size (bp)	Concentration (ng μL^{-1})	Molarity (nM)	Observations
1	15	4.20	424.2	Lower marker
2	42	0.19	6.7	
3	60	0.25	6.2	
4	1500	2.10	2.1	Upper Marker

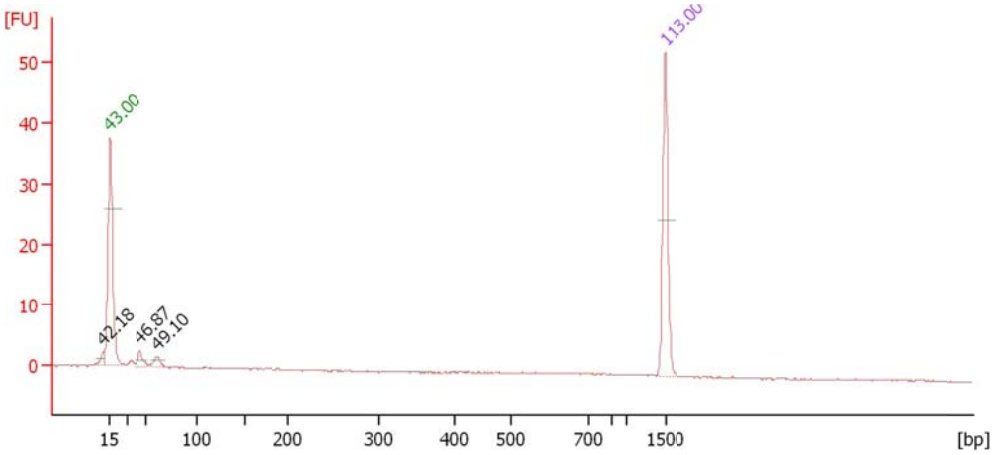

Figure 2.18 Bioanalyzer electrophorogram of the PCR no template control (NTC) sample. No amplification of the *femA-SE* gene observed. The numbers above the peaks represent the retention time in s.

Table 2.9 Quantitative data obtained from the Bioanalyzer of the PCR *Staphylococcus aureus* negative sample.

Peak	Size (bp)	Concentration (ng μL^{-1})	Molarity (nM)	Observations
1	15	4.20	424.2	Lower marker
2	42	0.32	11.7	
3	61	0.24	5.9	
4	1500	2.10	2.1	Upper Marker

2.3.8 SERS primer PCR SERS

To show the full compatibility of the SERS primer with biological samples, 1 ng of genomic DNA from *Staphylococcus epidermidis* was amplified using the SERS primer in PCR. The schematic mechanism is shown in Figure 2.19.

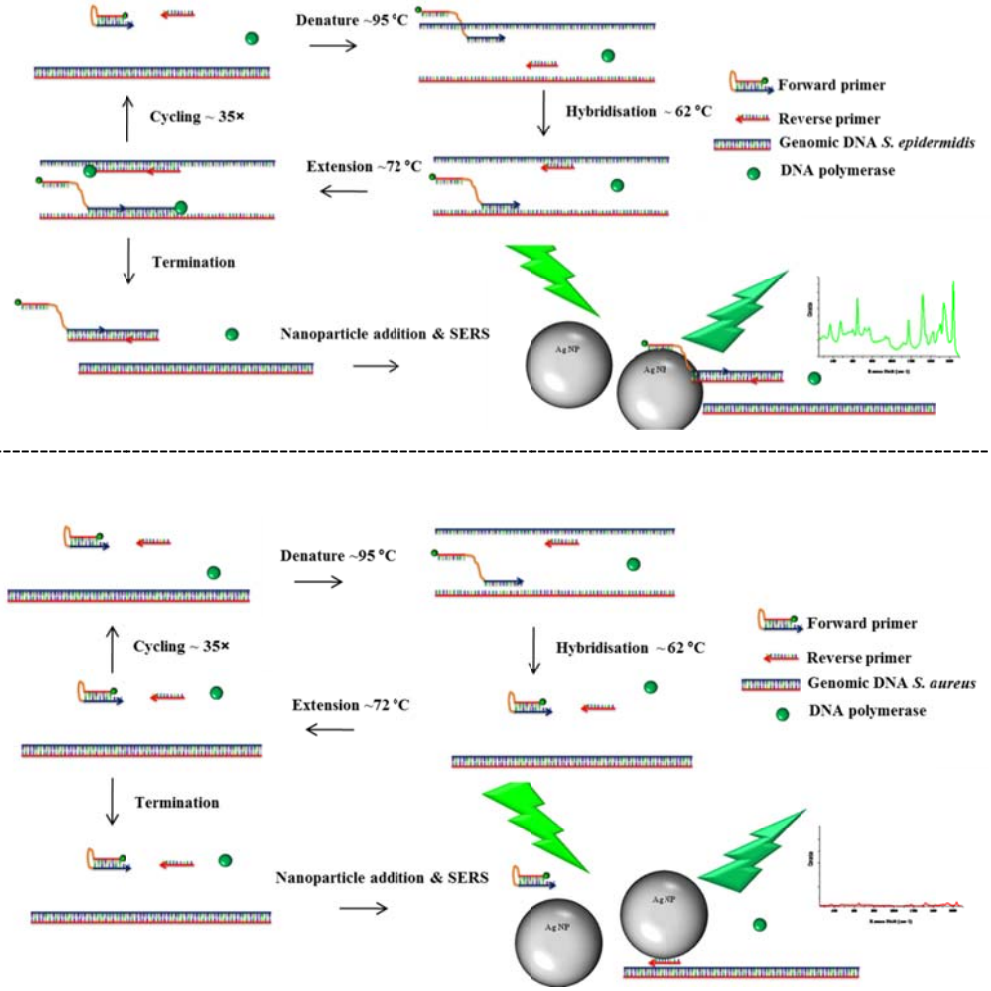

Figure 2.19 Schematic representation of PCR reaction and SERS analysis. (Top) In case of a positive sample, during the first step of the PCR at 95 °C the DNA is melted, then the reaction is cooled down towards the hybridization temperature of the SERS primer (forward) and the reverse primer. After heating the sample to the ideal temperature for the 5' → 3' exonuclease deficient DNA polymerase, the polymerase extends the two primers resulting in two exact copies where the SERS primer is incorporated in one of the two strands. After multiple cycles these products hybridize to each other and a double stranded piece of DNA with a single stranded region attached can then provide higher SERS intensities. (Bottom) In the case of a negative sample no amplification occurs and the SERS primer is double stranded resulting in a low SERS response.

Nanoparticles were added after the PCR reaction to avoid unwanted artefacts such as adsorption of PCR components onto the nanoparticles during the PCR, and aggregation of the nanoparticles by salts present in the PCR.

When the SERS assay is applied to PCR products, it is important that the yield of the PCR reaction is above 50 % in order to discriminate between target and non-target DNA. Furthermore the single stranded Reverse primer, dNTP's, and other components in the PCR reaction could compete for adsorption onto the silver nanoparticle surface thereby hindering the adsorption of the SERS primer. To overcome this problem five times concentrated colloid was used to increase the available surface area. Figure 2.20 shows the spectra obtained from the samples that underwent the PCR cycling process. The most intense SERS response was observed from the positive sample (green squares), lower intensities were observed for the negative samples (blue triangles, red diamonds).

(A) (B)

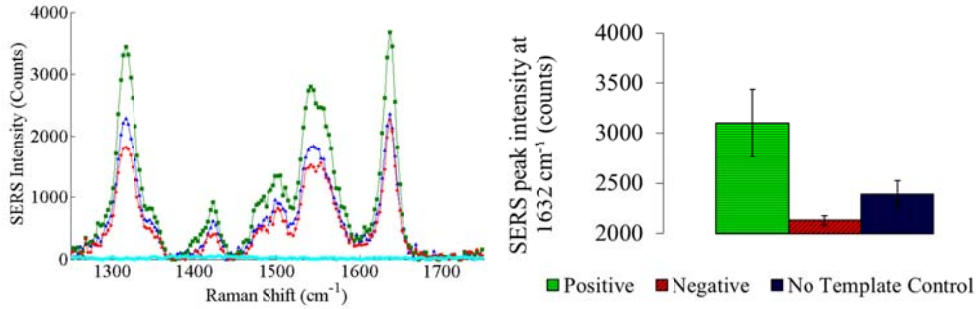

Figure 2.20 SERS of PCR products, no template control PCR (blue triangles), positive PCR sample (green squares), negative PCR sample (red diamonds), and blank (cyan circles). B) Average SERS signal peak intensity at 1632 cm^{-1} and standard deviation for three positive (*Staphylococcus epidermidis*) PCR samples (green horizontal shading), three negative (*Staphylococcus aureus*) PCR samples (red diagonal shading), and three no template control (NTC) PCR samples (blue vertical shading).

This system is a unique approach that allows the first direct detection of DNA sequences and PCR product using SERS in a positive assay. The extension of this methodology with the previously shown multiplexing capabilities of SERS will make this assay a useful tool for high degree multiplexing of DNA sequences.

2.4 Conclusion

Proof-of-concept of a new positive SERS assay that can discriminate between target and no target DNA in a homogenous sample without additional separation steps has been developed. Starting from a bacterial culture, DNA was isolated, a specially designed primer was incorporated into the PCR products and the presence or lack of target was identified within two hours. The high multiplexing capabilities of SERS make this a very promising approach for future DNA analysis. This method has the potential for single molecule detection of nucleic acid targets in a positive manner when SERS is combined with PCR and this is the first step towards a highly competitive SERS based molecular diagnostic assay.

3 THE MODE OF ACTION OF SERS PRIMERS AND SERS PROBES

3.1 Introduction

In Chapter 2, SERS primers were incorporated into polymerase chain reaction (PCR) products to detect pathogen deoxyribonucleic acid (DNA) directly using a surface enhanced Raman scattering (SERS) based detection approach.[123] SERS primers consist of double stranded DNA labelled with a SERS active molecule. When SERS primers interact with target DNA, a dye labelled part of the SERS primer becomes single stranded DNA (ssDNA) and interacts with a nanoparticle surface, resulting in an increase in the SERS response.

In Chapter 3 the proof-of-concept assay presented in Chapter 2 will be further optimised, and the performance of SERS primers in a uni- and bi-molecular manner using a synthetic model system, and in combination with PCR assays for separation free detection of pathogen DNA by SERS will be investigated. Additionally a new SERS primer assay will be presented, in the new assay the SERS primer will be used as an internal probe in the PCR reaction and the 5' → 3' exonuclease activity of the *Taq* DNA polymerase can partly digest the SERS primer and generate a dye labelled single stranded DNA, resulting in an increase in SERS response.

A quick reminder of the first SERS primer assay approach (Figure 3.1), SERS primers are incorporated into PCR products, exposing the fluorophore labelled

ssDNA, allowing adsorption onto the nanoparticles surface resulting in an increased SERS response, thereby detecting the specific gene of a pathogen.

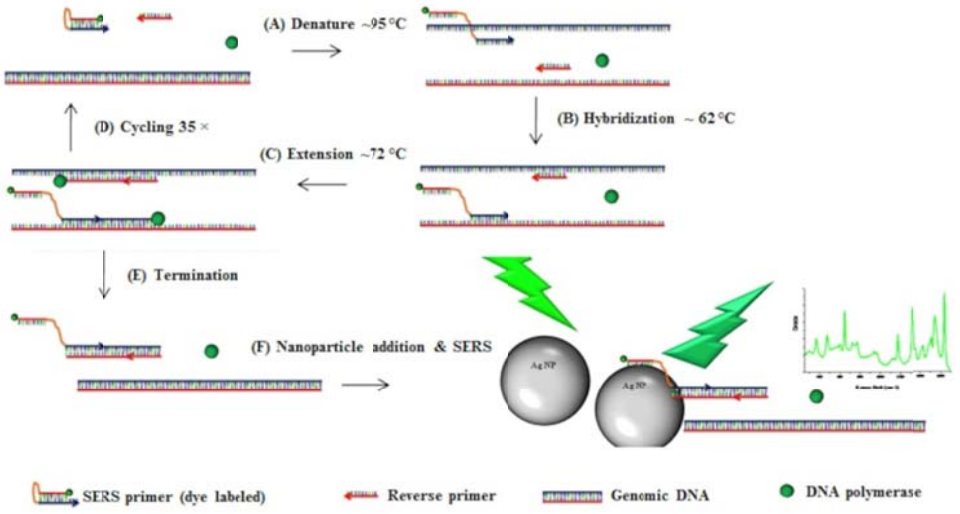

Figure 3.1 Schematic representation of a PCR reaction incorporating the SERS primer. (A) Denaturation of the DNA using heat, generating single stranded SERS primer and target DNA. (B) Hybridization by cooling the sample, specific hybridization of the SERS primer and reverse primer occurs. (C) Extension phase, DNA polymerase extends the 3' prime ends of the primers. Repeating step (A) till (C) generates multiple copies of the product (D). (E) After the reaction a double stranded PCR product is generated with a single stranded dye labelled end, (F) and after addition of nanoparticles SERS can be obtained from the single stranded piece of DNA. In case of a negative sample the SERS primer remains double stranded resulting in low SERS of the dye.

The performance of the SERS primers in the positive assay was investigated in several different ways. A model system for optimization experiments was applied, followed by application to a PCR assay to detect pathogen specific DNA. A schematic representation of the synthetic model system (Figure 3.2) shows the variation in the structure of the SERS primers used in this study. These models were applied to investigate SERS primer performance using uni- and bi-molecular SERS primer with and without overhangs, and the mirrored orientation of the uni-molecular SERS primer.

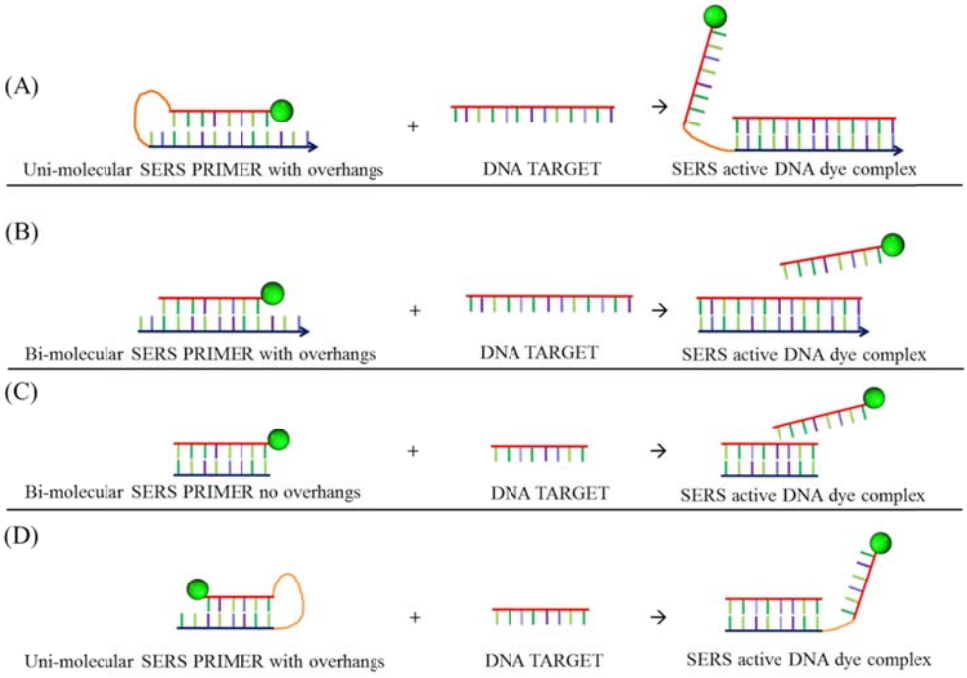

Figure 3.2 Schematic representation of the synthetic model assay formats investigated. (A) Uni-molecular SERS primer where the dye labelled region of the SERS primers is attached via a HEG linker to the 5' terminal end of the primer region of the SERS primer with overhangs. Stepwise the uni-molecular SERS primer, addition of target DNA, binding of the target to the uni-molecular SERS primer opens the uni-molecular SERS primer, which then becomes a SERS active DNA dye complex, and after addition of nanoparticles creates an increase in SERS signal. (B) A bi-molecular SERS primer where the dye labelled region was not attached to the primer region of the SERS primer with overhangs. Stepwise the bi-molecular SERS primer binding to the target producing dye labelled more SERS active single stranded DNA. (C) The bi-molecular SERS primer where the primer region is without overhangs. (D) The uni-molecular SERS probe with mirrored orientation, where the dye labelled region is linked to the 3' terminal end of the priming region via a HEG linker.

The following seven factors with respect to the assay performance were considered.

- Type of nanoparticles: Three types of nanoparticles with different surface chemistry were considered to test the importance of the nanoparticle surface coating layer.

- Nanoparticle and analyte concentration effects: To ensure a fully quantitative assay, the dose response with respect to the nanoparticle and analyte concentrations on the SERS response was assessed.
- SERS primer design: The correct folding of a SERS primer will be affected majorly by the sequence composition. The hairpin folding of SERS primers was modelled using computational software and the effect of this folding on the assay was investigated with a synthetic model.
- SERS primer to target molecule ratio: The effect of the SERS primer to target ratio was investigated to determine if more targets could increase the SERS signal intensity by opening more SERS primer which could then significantly improve the performance of the assay.
- Uni-molecular and bi-molecular SERS primers: The use of a bi-molecular over a uni-molecular system reduces the cost of the SERS primer, which makes the commercialization and implementation of these probes more attractive. Uni-molecular and bi-molecular Scorpion primers in combination with fluorescence detection have been reported[38] and intensively studied by Thellwell *et al.* who concluded that uni-molecular probes result in a more sensitive method.[39] However for SERS detection there still appears the question of whether ssDNA attached to dsDNA hinders the adsorption and thereby the achievable SERS intensity. This also leads to an investigation of the closure of the SERS primer to minimize background signal, and maximum displacement of the fluorophore labelled self-complementary sequence by the target to ensure maximum signal generation in a synthetic SERS model.
- Terminal overhangs on the SERS primer: The first SERS primer developed[123] had terminal overhangs which were in contradiction with the theory of DNA adsorption, therefore SERS primers without these overhangs were investigated.
- Orientation of the SERS primer: In order to use SERS primers in 5' → 3' exonuclease digestion assays a mirrored SERS primer was developed

which had the 5' terminus free for digestion by *Taq* DNA polymerase. This was then used as an intermolecular probe, and introduced in a new assay which utilizes the 5'→3' exonuclease activity of *Taq* DNA polymerase to partly digest the SERS probe and release the dye labelled ssDNA which was then detected by SERS. This method might have several advantages; one of them is the generation of more target than SERS probe by using a higher concentration of primers to SERS probes. When using the SERS probes an extra level of specificity was created, therefore universal primers can be used to minimize the number of oligonucleotide sequences needed to detect multiple targets. The latter method was not investigated in this study but will be considered for further work.

3.2 Experimental

3.2.1 Materials

All materials were obtained from Sigma Aldrich unless stated otherwise.

3.2.2 DNA oligonucleotide design

The *femA* gene was previously used for bacterial identification of *Staphylococcus epidermidis* and *Staphylococcus aureus*.[23] The whole genome sequence of *Staphylococcus epidermidis* National Culture Type Collection (NCTC) strain NCTC 13360 and *Staphylococcus aureus* (NCTC 8325) were obtained from the National Centre of Biotechnology Information (NCBI) website.[124] The oligonucleotide sequence design was carried out using the Primer3Plus online server.[101] Parameters within this software were set to 50 mM monovalent salt, 1.5 mM divalent salt, and 250 nM of DNA. For the table of thermodynamic parameters the setting "Santalucia 1998" was used.[102] For salt correction the formula set by "Owczarzy *et al.* 2004" was used.[103] Internal folding of the sequence region selected by Primer3Plus was analyzed using the DINAMelt webserver[104] and the oligoanalyzer webserver from Integrated DNA Technologies (IDT)[125]. Parameters were set to 58°C, 50 mM monovalent salt, 1.5 mM divalent salt, and 250 nM of DNA. Basic Local Alignment (BLAST) was carried out using the BLAST tools from the NCBI website.[126] The performance of the SERS primers strongly depends on the DNA sequence design. Therefore to ensure correct folding of the SERS primer, computational design and folding software (such as Primer 3 plus, IDT oligoanalyzer, mFold and DINAmelt) were the preferred tools to investigate the folding of the hairpin loop and binding to the target. Alternative hairpin structures in the SERS primers were reduced to zero for the most successful SERS primers. Oligonucleotide sequences shown in Table 3.1 were HPLC purified and obtained from ATD Bio (Southampton).

Table 3.1 Overview of the oligonucleotide sequences, uni- and bi-molecular SERS primers with target and non-target sequences. FAM - 5-carboxyfluorescein, PHO - phosphate PCR extension blocker, HEG - internal hexaethylene glycol spacer unit, the red colored bases represent mismatches, and the purple bases represent base overhangs.

Name	Sequence 5'→ 3'
Uni-molecular SERS primer I	FAM-GAAGTTACATCAGAA-HEG-TACTACGCTGGTGGAACTTCAAATCGTTATCG
Bi-molecular SERS primer I	FAM-GAAGTTCCACCAGCG-PHO TACTACGCTGGTGGAACTTCAAATCGTTATCG
Target I	CGATAACGATTTGAAGTTCCACCAGCGTAGTA
Non-target & reverse primer I	GAACCGCATAGCTCCCTGC
Uni-molecular SERS primer II	GCATGCCATACAGTCATTTCACGCA-HEG-TACTTGAAATGTCTGTAT-FAM
Bi-molecular SERS primer II	FAM-TGCTTGAAATGTCTGTATGGGATGC-PHO GCATGCCATACAGTCATTTCACGCA-PHO
Target II	TGCGTGAAATGACTGTATGGCATGC
Non-target 1 & reverse primer II	AGTAAGTAAGCAAGCTGCAATGACC
Non-target 2 & forward primer II	AACAGCTAAAGAGTTTGGTGCCTTT

3.2.3 UV-Vis spectroscopy

UV-Vis spectroscopy was carried out on a Varian Cary 300 BIO spectrophotometer with Peltier thermal control cycling from 10°C to 90°C and back with 1°C increments per minute and the UV absorbance measured at 260 nm every minute. Samples were prepared using 50 µL of SERS primer (10 µM), 50 µL of diethylpyrocarbonate (DEPC) treated water (Bioline, London, United Kingdom), or target or non-target DNA (10 µM), and 250 µL of 1 × phosphate buffered saline (PBS) obtained from Oxoid (Hampshire, United Kingdom), and finally the volume was made up to 500 µL with DEPC water.

3.2.4 Bacterial culturing

Bacterial strains of *Staphylococcus epidermidis* (NCTC 13360) and *Staphylococcus aureus* (NCTC 8325) were obtained from the national health protection agency

culture collections (HPACC Salisbury, UK) and cultured for 24 h in 10 mL sterile Tryptone Soy Broth (Oxoid). The cells were centrifuged at 16,110 × g for 10 min at 4°C, the supernatant was then removed and 1 mL of Lysostaphin was added to the remaining pellet. The suspension was incubated for 30 min at 37°C to lyse the cells. DNA was extracted according to the manufacturer's protocol from the lysate using a QIAamp DNA minikit (Qiagen, Crawley, UK).

3.2.5 Polymerase chain reactions

PCR reactions were set up in a total volume of 25 µL for each reaction. Each reaction contained 0.5 µL of 2 U μL^{-1} 5'→3' exonuclease deficient DNA polymerase Phusion® Hot Start II (New England Biolabs, UK), and for the 5'→3'exonuclease digestion assay 0.5 µL of 2 U μL^{-1} DyNAZyme™ II Hot Start DNA polymerase (New England Biolabs, UK), 5 µL of 5x Phusion® HF buffer (New England Biolabs, UK), 0.5 µL of deoxynucleoside triphosphates (dNTP's) 10 mM each (New England Biolabs, UK). 2 µL of 2.5 µM forward and 2 µL of 2.5 µM reverse primer, and for the exonuclease assay 1 µL of 2.5 µM premixed probes. Volumes were made up to a total volume of 15 µL using DEPC treated water and finally 10 µL of 0.01 ng μL^{-1} genomic template DNA was added. Thermal cycling was carried out using a Stratagene MX3005P thermo cycler. The cycling protocol was: 30 s at 98°C, thereafter 30 repeats of 10 s at 98°C, 60 s at 62°C, and 60 s at 72°C and a final extension at 72°C for 1 minute. After cycling, the sample was cooled to 20°C.

3.2.6 Gel electrophoresis

Capillary electrophoresis of the PCR products was carried out using an Agilent Bioanalyzer and the DNA1000 reagent kit and handling procedures were carried out according to the manufacturers protocol.

3.2.7 Nanoparticles

Silver ethylenediaminetetraacetic acid (EDTA) nanoparticles were synthesized using a method previously reported by Fabrikanos *et al.*[73] Citrate reduced silver nanoparticles were prepared via a method reported by Lee & Meisel.[70] Sodium

borohydride reduced silver nanoparticles were prepared via the method reported by Creighton *et al.*[75] The sodium borohydride reduced silver nanoparticles were used on the same day as it is well known that these particles are unstable over time. The pH of the nanoparticle suspensions was adjusted to pH 7 by the addition of TRIZMA® hydrochloride (0.5 mL of 200 mM pH 7.0) and Tween20 (0.5 mL of 0.2%) to 9 mL of the nanoparticle suspension the nanoparticle suspensions were used within 4 h after addition of the buffers. The λ_{max} of the nanoparticles was determined using UV-Vis spectroscopy. The size of the metal core was determined by scanning electron microscopy (SEM) on a Sirion 200 Schottky field emission electron microscope (FEI) operating at an accelerating voltage of 5 kV. Samples did not require additional metallic coating before imaging. Image analysis was carried out using Image J version V1.43y, 250 nanoparticles were measured for each nanoparticles suspension and the average value ± the standard deviation reported. The nanoparticle concentration was determined using UV-Vis spectroscopy and the following extinction coefficient values for silver nanoparticles: $\varepsilon_{40\,nm} = 2.87 \times 10^{10}\ M^{-1}\ cm^{-1}$, $\varepsilon_{30\,nm} = 1.85 \times 10^{10}\ M^{-1}\ cm^{-1}$, and $\varepsilon_{20\,nm} = 4.16 \times 10^{9}\ M^{-1}\ cm^{-1}$.[106] For the comparison experiments different types of nanoparticles were adjusted to similar concentrations by adjusting the optical density taking into consideration the size difference of the nanoparticles.

The hydrodynamic radius and the ζ (Zeta) potential of the nanoparticles were determined with dynamic light scattering using a Malvern Zetasizer Nanoseries Nano-ZS.

3.2.8 Surface enhanced Raman scattering

For the model system experiments where the target concentration was varied, SERS analysis was carried out using 2.5 µL of 100 nM SERS primer and 2.5 µL of its complementary sequence (10 – 1000 nM) in 110 µL of PBS buffered at pH 7.3 ± 0.2 as a positive sample and a 20-25 base pairs long non-target DNA sequences as negative sample, pre-hybridized for 10 min at 95°C and 10 min at 20°C using a

thermocycler (Agilent MX3005P). The target concentrations were varied from 0.1 to 10 nM final concentration after the addition of 10 µL of 0.01 M spermine tetrahydrochloride and 125 µL of concentrated silver EDTA nanoparticles (approximately 250 pM).

PCR samples were analysed in the SERS assay as follows, 1 µL of the PCR sample was added to 499 µL of PBS buffer. 115 µL of this sample was then mixed with 10 µL of 0.01 M spermine hydrochloride and 125 µL of concentrated silver EDTA nanoparticles (approximately 500 pM) buffered to pH 7 in 10 mM TRIZMA® hydrochloride and 0.01% Tween20.

All samples were prepared in at least triplicate in PMMA micro-cuvettes and analysed within 1 min using an Avalon probe system Ramanstation R3 equipped with an optical fibre probe with a 532 nm diode laser excitation a laser power of approximately 24 mW at the sample. Typical exposure time was 3 s (1 s integration and 3 accumulations). Data analysis was carried out using the xanthene ring C-C stretching peak[110, 111] of the fluorescent dye carboxyfluorescein (FAM) at 1632 cm^{-1} minus the 1660 cm^{-1} position in the spectrum. The threshold line was plotted and used to find the detection limits, which was calculated using the mean plus three times the standard deviation of the control samples.

3.3 Results and discussion

3.3.1 Type of silver nanoparticles

In order to test the robustness of the ssDNA vs dsDNA assay and the importance of the surface stabilizing layer three types of nanoparticle were tested in the assay i.e. EDTA, citrate and sodium borohydride reduced silver nanoparticles. Nanoparticle characterization data is shown in Table 3.2 and Figure 3.3.

Table 3.2 Nanoparticle characterization data λ_{max} (nm) and FWHM (nm) are determined by UV-Vis spectroscopy, the metal core size diameter (nm) by scanning electron microscopy (SEM), the hydrodynamic radius was determined by dynamic light scattering (DLS), and the ζ potential by the laser Doppler Anemometer technique. Error is ± one standard deviation of three individual samples. For experimental details see the Materials and methods section.

Name	λ_{max} (nm)	FWHM (nm)	Metal core diameter size (nm)	Hydrodynamic radius (nm)	ζ potential (mV)
Ag-EDTA	409	61	33.2 ± 4.9	20.7 ± 0.3	-33.4 ± 4.8
Ag-Citrate	409	75	39.6 ± 6.5	31.0 ± 0.3	-52.6 ± 6.3
Ag-BH_4	393	47	13.0 ± 2.7	7.6 ± 1.4	-7.8 ± 1.2

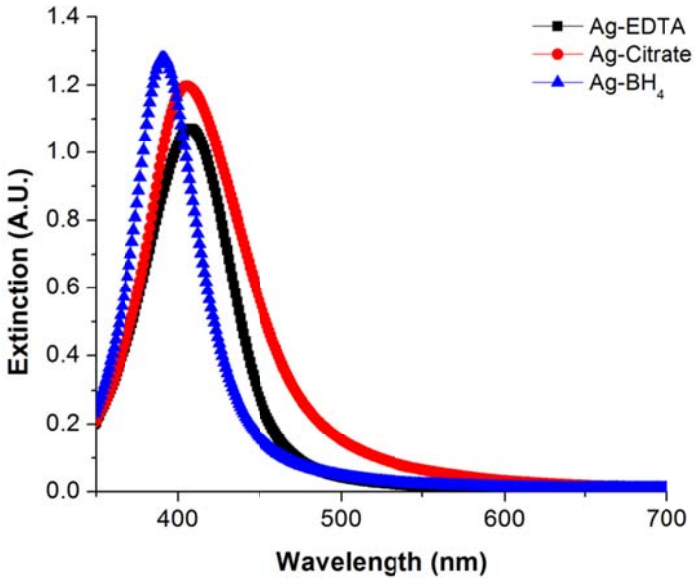

Figure 3.3 UV-Vis spectra of silver nanoparticles.

Data in Figure 3.4 and Table 3.3 shows that EDTA and citrate reduced silver nanoparticles performed in a similar fashion with respect to detecting ss and dsDNA. A similar ratio of ssDNA / dsDNA of 2.1 and 2.4 was observed although slightly more intense signals (approximately 5313 versus 5328 counts) were observed when citrate reduced silver nanoparticles were used. These slight differences were possibly due to the ease of citrate displacement and slightly larger particle diameter (approximately 33 versus 40 nm). Sodium borohydride reduced silver nanoparticles performed less well in terms of discrimination between double and single stranded DNA with a ssDNA / dsDNA ratio of ~1.4, and the SERS peak intensity was less intense (~500 counts) when compared to the EDTA and citrate nanoparticles, this is possibly due to the different surface chemistry and / or the smaller size (13 nm) of the nanoparticles.[85, 127] From these experiments it can be concluded that from the types of nanoparticles used silver citrate nanoparticles and silver EDTA nanoparticles were most successful for this assay with a slight preference for EDTA silver nanoparticles due to the ease of nanoparticle preparation and strong SERS peak intensity.

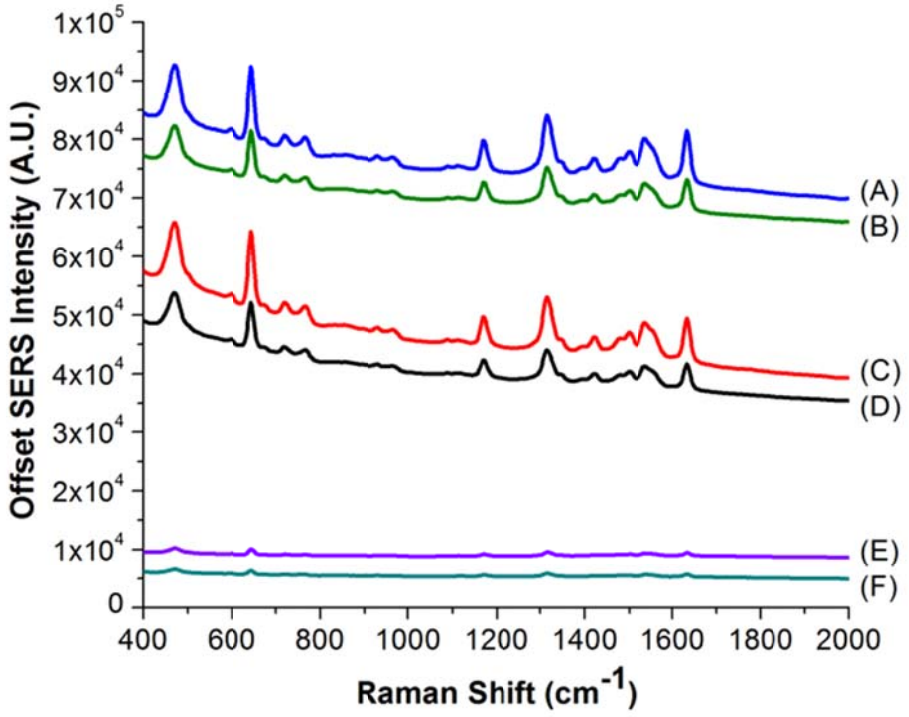

Figure 3.4 Offset SERS intensity from FAM labelled single stranded and double stranded DNA and silver nanoparticles with different surface chemistry using 532 nm laser excitation and three accumulations of one second. (A) Ag-Citrate with ssDNA, (B) Ag-Citrate with dsDNA, (C) Ag-EDTA with ssDNA, (D) Ag-EDTA with dsDNA, (E) Ag-BH_4 with ssDNA, (F) Ag-BH_4 with dsDNA.

Table 3.3 Overview of SERS peak intensities (mean counts ± standard deviation) obtained from single stranded and double stranded DNA using three different types of silver nanoparticles.

	Ag-EDTA	Ag-Citrate	Ag-BH_4
ssDNA	5313 ± 157	5328 ± 465	507 ± 24
dsDNA	2584 ± 199	2255 ± 100	371 ± 11
ssDNA / dsDNA	2.1	2.3	1.4

3.3.2 Nanoparticle and analyte concentration effects

The SERS peak intensity and the analyte concentration range over which a quantitative response is shown depends on the silver nanoparticle

concentration. This affects the number of particles in the laser beam, the interrogation depth of the laser into the sample which results in variation of the sample volume in the beam, and the total surface area available on the nanoparticles.[52, 128] When too low a nanoparticle concentration is used, less surface area is available for the analytes to adsorb onto resulting in a limited dynamic range of the system. When too high a nanoparticle concentration is used, there is enough surface area available for the analytes to adsorb onto but the interrogation depth of the laser beam is limited by the density of the nanoparticles resulting in less volume of the sample being analysed and therefore a reduced SERS intensity. For quantitative assays it is important that there is enough surface area available for the analytes to adsorb onto the nanoparticle surface to extend the analyte concentration range with a quantitative response from the system. For biological applications it is important that there is sufficient sensitivity to detect the analytes of interest.

(A) (B)

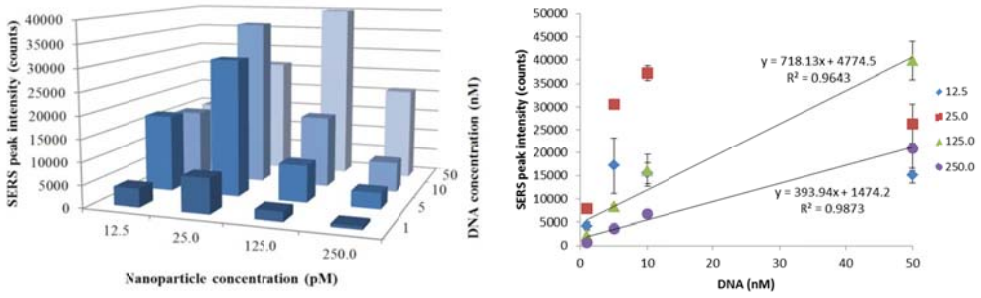

Figure 3.5 (A) The SERS peak intensity (Z-axis) using Ag-EDTA nanoparticles and 532 nm laser excitation and three accumulations of one second as a function of the nanoparticle concentration (X axis) and the DNA concentration (Y axis). (B) The SERS peak intensity (Y-axis) as a function of the DNA concentration (X axis). Linear regression fit on SERS peak intensity versus DNA concentration for the 125 and 250 pM silver EDTA nanoparticles. Error bars represent ± one standard deviation of three individual samples.

When the concentration of nanoparticles was 12.5 pM the maximum SERS peak intensity was approximately 17500 counts and when the nanoparticle concentration was increased to 25 pM the SERS peak intensity of the analyte was increased to approximately 30000 counts for 5 nM FAM labelled ssDNA (Figure

3.5). However the quantitative response range that was obtained was limited to less than 1 to 5 nM using nanoparticle concentrations below 25 pM (Figure 3.5). When the nanoparticle concentration was increased to 125 pM less intense signals were obtained and for 5 nM DNA a signal reduction of approximately 75% was observed when compared to 25 pM nanoparticles, due to the limited interrogation depth of the laser into the sample caused by the nanoparticle density. Nevertheless the analyte concentration range with a somewhat linear and quantitative response was extended from 1 – 5 nM to 1 - 50 nM with a linear fit R^2 value of 0.96. When the nanoparticle concentration was further increased to 250 pM a signal reduction of approximately 88% was obtained when compared to 25 pM nanoparticles. The analyte concentration range with a more linear and quantitative response of the system was 1 to 50 nM of FAM labelled ssDNA and the R^2 value within the linear regression fit improved to 0.98 (Figure 3.5 B). For these concentration graphs more data points (5 or more) are preferred. However the increased linearity in the dose response enables improved quantitative measurements of dye labelled ssDNA in the concentration range of 1 to 50 nM which was suitable to the model system concentration studies reported here which had a maximum concentration of 11 nM DNA. In the further model assay studies a final nanoparticle concentration of 125 pM was used to take advantage of the extended analyte concentration range with a linear response with this concentration of nanoparticles.

3.3.3 SERS primer design

Clearly for the most successful SERS primers the affinity for the target has to be higher than for the hairpin formation. This was optimized for target binding by incorporation of mismatches and a reduced number of bases in the hairpin folding region of the SERS primer. Mismatches and base reductions were chosen such that it minimized the number of alternative hairpin structures. UV-Vis spectroscopy was used to investigate the hybridization profiles of the hairpins in combination with target and non-target DNA and provided good insights into the performance of the SERS primers, in a uni- and bi-molecular fashion. Data shown

in Figure 3.6 shows the preferred binding of the SERS primer to the target. When no or non-target DNA was present the closure of the self-complementary region onto the SERS primer was observed. These experiments were the first steps towards successful SERS primers.

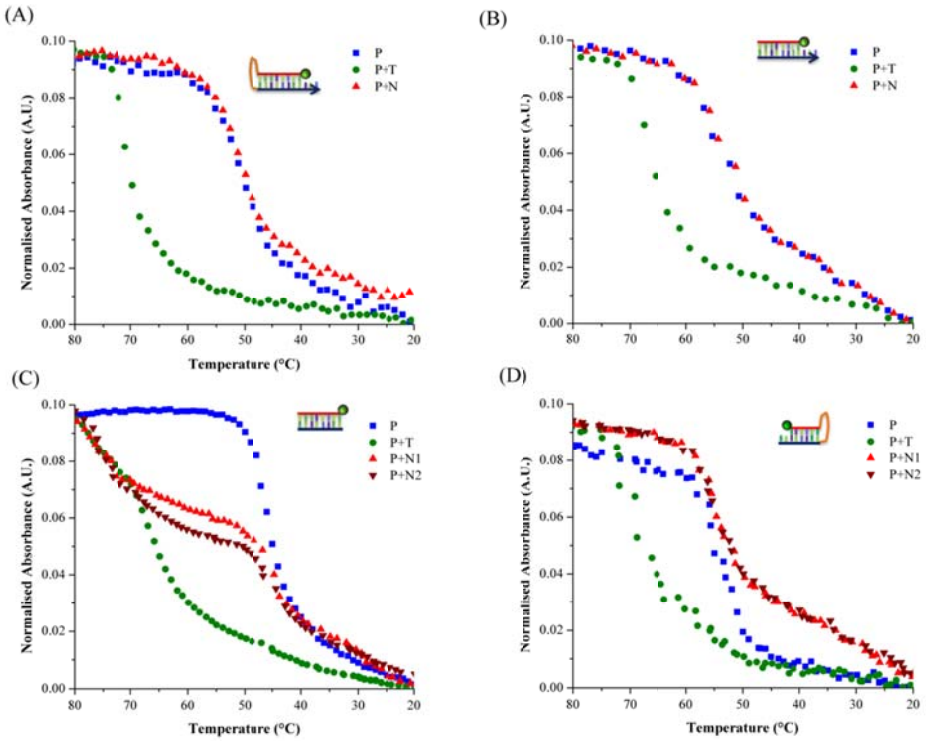

Figure 3.6 Hybridization curves of the SERS primers (P) and probes (P) to their target (T) and non-target (N) DNA sequences. (A) Uni-molecular SERS primer. (B) Bi-molecular SERS primer. (C) Bi-molecular SERS probe (D) Uni-molecular SERS probe.

3.3.4 SERS primer to target molecule ratio

The hairpin folding of the SERS primer is a uni-molecular event and therefore kinetically more favourable, whereas the binding of the target DNA to the SERS primer is a bi-molecular event in competition with the SERS primer hairpin folding. Therefore the hypothesis was that when the target to SERS primer ratio was increased a higher discrimination between target DNA and control samples would be obtained due to an increased occurrence of opened SERS primers. The importance of SERS primer to target ratio was investigated following a synthetic

experimental model approach (Figure 3.2). In this model the SERS primers were exposed to increasing concentrations (0.1 to 10 nM) of either target or non-target DNA. After hybridization, the addition of spermine and nanoparticles was followed by SERS analysis of the 1632 cm^{-1} peak intensity of the FAM dye.

Following this model system it was possible to carefully study the behaviour of the SERS primer in the SERS assay when more target and non-target DNA was added. Addition of more target DNA resulted in an increase in SERS peak intensity whereas the addition of more non-target DNA did not result in an increase in the SERS peak intensity. Although it was possible to detect target concentrations 0.5 times lower than the SERS primer concentration, the best contrast between positive and negative samples was obtained when the target to SERS primer ratio was greater than one, and preferably five to ten times higher than the SERS primer concentration. (Figure 3.7A) These results are in agreement with the theoretical hypothesis that a higher target concentration was needed to open more SERS primers due to the competitive and bi-molecular nature of the events.

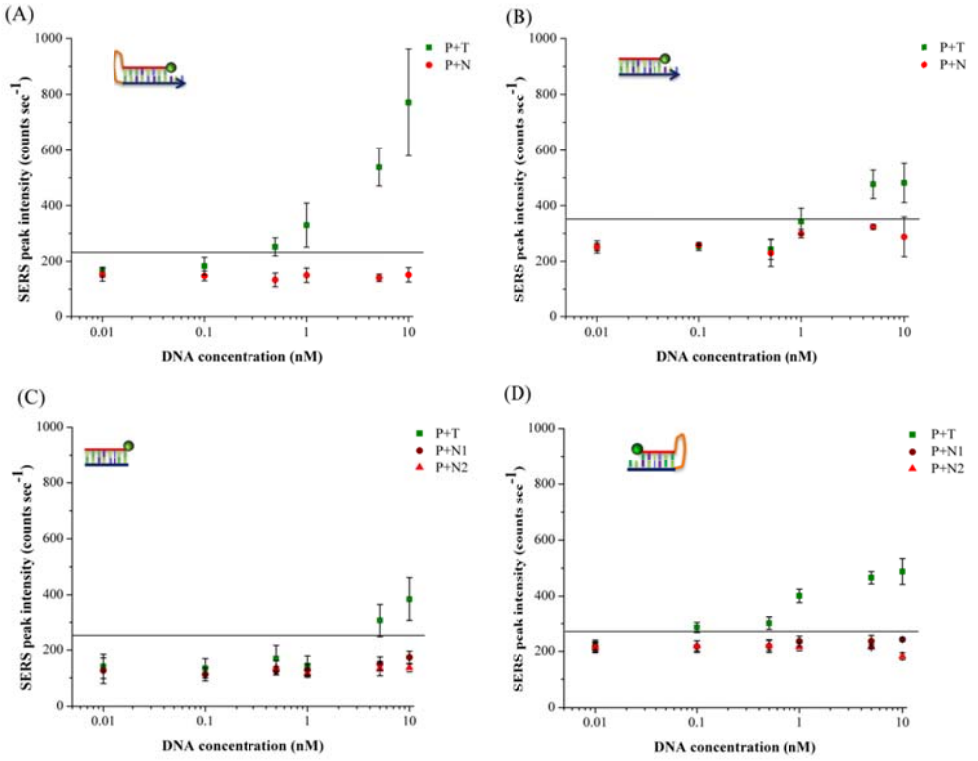

Figure 3.7 Response of the SERS primers (P) with increasing concentration of target (T) and non- target (N, N1 and N2) DNA. The horizontal line in each graph represents the threshold values set as the mean plus three times the standard deviation of the negative control sample. Threshold values were 215 (A), 346 (B), 264 (C), and 270 (D) respectively. (A) A uni-molecular SERS primer. (B) Performance of the bi-molecular SERS primer (P) with 3' terminus overhang. (C) Performance of the bi-molecular SERS probe (P) without overhangs. (D) Performance of the uni-molecular SERS probe (P) with different dye orientation. In the case of the SERS primers (A & B) one non-target sequence (N) was used because in the following PCR experiments this sequence was used as the reverse primer. In case of the SERS probes experiments (C & D) two non-target sequences were used because in the following PCR experiments these SERS probes were used in combination with reverse (N1) and forward (N2) primers. A 532 nm laser excitation and three accumulations of one second were used. Error bars represent ± one standard deviation of three individual samples.

3.3.5 Uni-molecular and bi-molecular SERS primers

Uni-molecular SERS primers are more likely to fully form double stranded DNA structures than bi-molecular events. Bi-molecular SERS primers are commercially more attractive due to the significant reduction in cost. Therefore the use of bi-molecular SERS primers was investigated in a synthetic SERS model assay. Uni-molecular probes had a slightly higher reproducibility and a highly reduced rate

of false positives and false negatives resulting in lower detection limits (Figure 3.7 A vs B & C vs D). The reduced performance with bi-molecular SERS primers might be due to cross reaction between the oligonucleotide sequences at 20°C.

As a result uni-molecular SERS primers were chosen as the preferred SERS primers over bi-molecular SERS primers due to their lower detection limits and higher reproducibility in the synthetic model assay. Bi-molecular SERS primers might still be useful in PCR-based detection assays because other assay parameters such as the free availability of the dye labelled ssDNA sequence might also play an important role but at this stage the performance of the uni-molecular SERS primer is the leading factor.

3.3.6 Terminal overhangs of the SERS primer

The influence of the overhangs in the SERS primer was investigated in a bi-molecular manner (Figure 3.7 B vs C). There was no significant effect observed from the 17 (5+12) base overhang on the SERS assay performance with respect to sensitivity only a slightly lower background signal was observed. However when the SERS primer without a 3' overhang was designed (FAM-AAAGGAACAAAACACTATAACTGTT-HEG-AACAGCTAAAGAGTTTGGTGCCTTT) good DNA hybridisation results were obtained (Figure 3.8A) but the SERS response of the assay turned into a negative assay format with a reduction in SERS signal intensity when the target DNA concentration was increased (Figure 3.8B). More intense SERS signals were obtained for the positive samples compared to the corresponding negative samples, this is possibly due to competition between the SERS primer and the single stranded non target DNA for the nanoparticle surface.

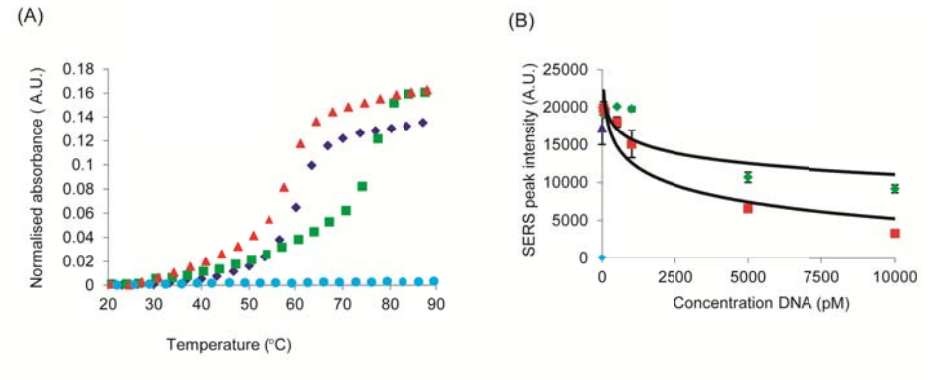

Figure 3.8 DNA hybridisation of the SERS primer where the 3' overhang was removed monitored by UV-Visible spectroscopy (A) The cyan circles represent the water control samples, blue diamonds represent the SERS primer control samples, green squares represent the SERS primer and target-DNA samples, and the red triangles represent non-target DNA control samples. On the right hand side the SERS assay performance of the SERS primer without 3' overhang (B). The cyan diamond represents the water control samples, blue triangles represent the SERS primer control samples, red squares represent the SERS primer including non-target DNA samples, green squares represent the SERS primer with target-DNA samples.

When the folding of the SERS primer was modelled it turned out that there was a possibility to form an alternative structure (Figure 3.9) resulting in a 20 base long single stranded region.

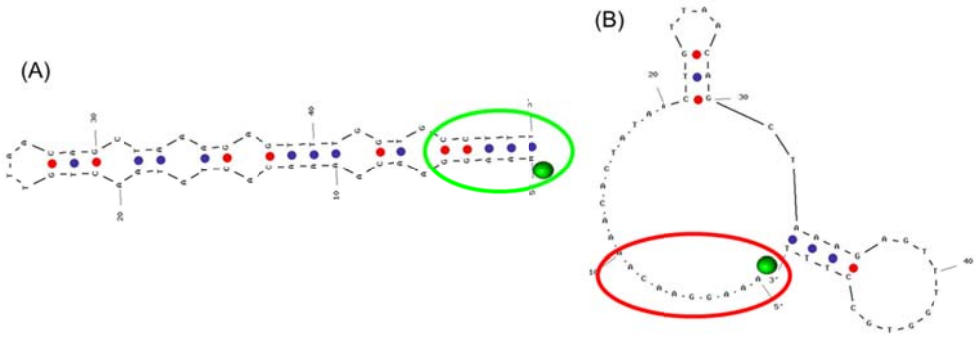

Figure 3.9 Two different structures of the SERS primer without overhang. (A) Folding of the SERS primer where the dye is attached to the dsDNA region. (B) Folding of the SERS primer where the dye is attached to the ssDNA region.

This event might be a possible reason for the inverse performance of the SERS primer in the assay. Because when there is no target DNA present the SERS primer consists of a single stranded piece of DNA with two small internal loops

(Figure 3.9B) and when the target is introduced the single stranded DNA is attached to a double stranded piece of DNA.

3.3.7 Orientation of the SERS primer

In order to use the SERS primer as an internal probe that can be digested by the 5'→3' exonuclease activity of the DNA polymerase the position of the fluorescent molecule and the HEG linker was changed to leave the 5' terminus of the probing sequence free for digestion (Figure 3.10).

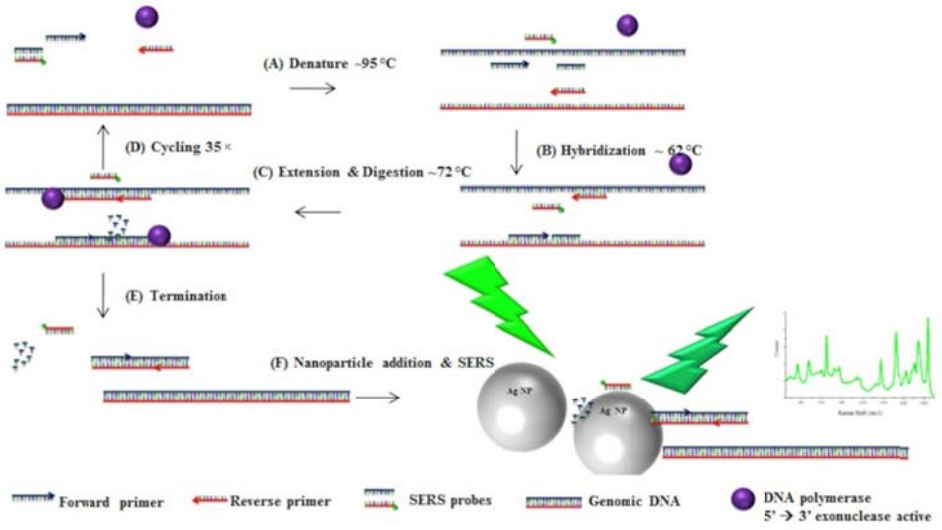

Figure 3.10 Schematic representation of a PCR reaction incorporating the SERS primer as an internal probe to be partly digested by the polymerase. (A) Denaturation of the DNA using heat, generating single stranded SERS primer and target DNA. (B) Hybridization by cooling the sample, specific hybridization of the primers and the SERS probe occurs. (C) Extension phase, DNA polymerase extends the 3' prime ends of the primers and digests the target binding sequence of the SERS probe generating dye labelled single stranded DNA which results in an increased SERS signal. Repeating steps (A) to (C) multiple copies of product can be generated (D). (E) After the reaction a double stranded PCR product is generated and short single stranded dye labelled sequences, (F) and after addition of nanoparticles SERS can be obtained from the single stranded piece of DNA. In case of a negative sample the SERS probe remains double stranded resulting in low SERS of the dye.

Firstly a SERS probe sequence was designed which contained a 3' terminus FAM fluorophore and an internal HEG linker molecule. Then the performance of this SERS probe with mirrored orientation was investigated in the synthetic model,

and the results in Figure 3.7D showed that this SERS probe performs with similar sensitivity as the uni-molecular SERS primer shown in Figure 3.7A.

These results confirm that the fluorophore can be either positioned at the 3' terminal end of the SERS primer as well as at the 5' terminal end of the SERS probe with no significant changes in the performance of the SERS primers or probes.

3.3.8 SERS primer digestion assay design

The f*emA-SA* gene of *Staphylococcus aureus* was chosen as a model system for this work. The sequence of the *femA-SA* gene (gene bank accession number X17688)[23, 129] was obtained from the National Center for Biotechnology Information (NCBI).[100] Primer3 online software was used to generate specific primers.[102, 103, 113] The primers and amplicon region were selected by the Primer3 software allowing analysis for internal folding, and for hetro and homo dimer formation at 58°C using online software mFold, UNAFold and DINAmelt available from the Rensselaer Polytechnic Institute.[102, 104, 114, 115] Finally the specificity of the primers was checked against other bacteria using NCBI BLAST.[105]

The designed primer sequences are shown in Table 3.4. These sequences are not specific to the gene *femA-SA* of *Staphylococcus aureus* and are designed to generate a minimal amount of internal folding events. The T_m values are an indication of the temperature at which half the oligonucleotide strands in a sample are bound to their complements.

Table 3.4 Overview of oligonucleotide sequences selected.

Name	Sequence 5' → 3'	T_m (°C)[113]
Forward primer	AACAGCTAAAGAGTTTGGTGCCTTT	64.3
Reverse primer	AGTAAGTAAGCAAGCTGCAATGACC	64.1
Internal probe	GCATGCCATACAGTCATTTCACGCA	66.5

The region of genomic DNA selected by the Primer3 software was checked for internal sequence folding at 58 °C containing 50 mM monovalent salt and 1 mM

divalent salt and sequence type linear using the DINAmelt Two state folding online software.[104]

The positions of the primers within the *femA-SA* gene are indicated in yellow, whilst the regions most likely to fold are shown in red in Figure 3.11. The red areas were to be avoided as primer binding regions.

ATAAAAGTATACGCAATTAAAGCGTTTATGTTTTAGTTTTAACATTAACTATTGTATACTTATTTAGATTAGATTTATTATT
TTTGACATTTGCAGAGGGGAAATAGAAAAACTGCAAATACGGAAATGAAATTAATTAACGAGAGACAAATAGGAGTAATGAT
AATGAAGTTTACAAATTTAACAGCTAAAGAGTTTGGTGCCTTTACAGATAGCATGCCATACAGTCATTTCACGCAAACTGTT
GGCCACTATGAGTTAAAGCTTGCTGAAGGTTATGAAACACATTTAGTGGGAATAAAAAACAATAATAACGAGGTCATTGCAG
CTTGCTTACTTACTGCTGTACCTGTTATGAAAGTGTTCAAGTATTTTTATTCAAATCGCGGTCCAGTGATTGATTATGAAAA
TCAAGAACTCGTACACTTTTTCTTTAATGAATTATCAAAATATGTTAAAAAACATCGTTGTCTATACCTACATATCGATC

Figure 3.11 The base numbers 450 to 940 of the *femA-SA* gene. In red is shown the region with an increased risk of internal folding of the template DNA. In yellow the positions of the selected primers.

Although the results are obtained from computational models, these models can provide good insights into the performance of an assay. The software used to create these models was developed using experimental data in order to predict accurately the performance of the assay being investigated.[102, 104, 105, 113-119]

3.3.9 SERS primers and probes in the PCR-based SERS assay

The previous parameters have all been investigated with synthetic models, in this section the results were transferred to the identification of bacterial cultures by coupling PCR-based DNA amplification with SERS detection. Firstly the performance of the uni- and bi-molecular SERS primers coupled with PCR was investigated. After PCR with the SERS primers and probes the DNA amplification, the length, and the concentration of the PCR products in the PCR reactions was determined by capillary electrophoresis (Agilent BioAnalyzer).

In the SERS primer assay the expected PCR product length was 58 bp. As discussed previous chapter, in the case of the uni-molecular SERS primers there was a difference of approximately 35 bp in PCR product length (93 bp) and the expected 58 bp (Figure 3.12 A). In the bi-molecular SERS primer assay the expected 58 bp product was obtained (Figure 3.12 B). This indicates that the size

difference in the uni-molecular SERS primer assay originates from the HEG linker, the ssDNA and / or the dye attached to the PCR product influencing the electrophoretic properties of the PCR product (Figure 3.12 A vs B).

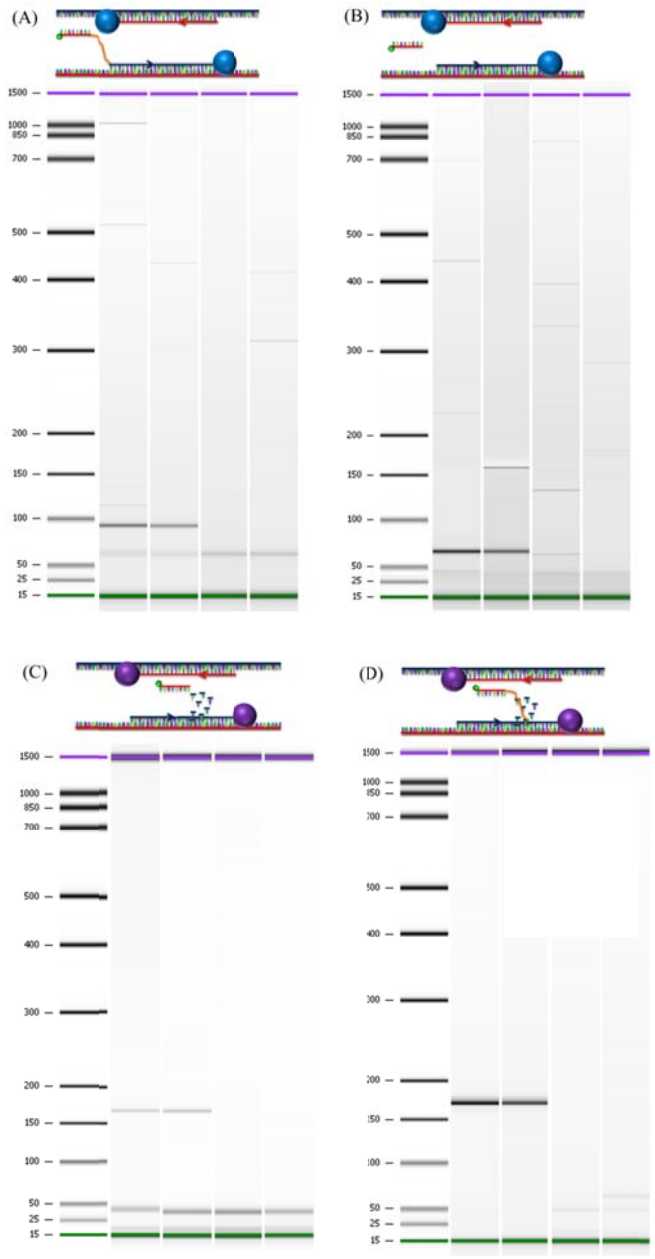

Figure 3.12 Gel electrophoresis result of target DNA amplification by PCR; lane 1 the DNA ladder, lane 2 & 3 positive samples, lane 4 & 5 negative control samples. (A) Uni-molecular SERS primer. (B) Bi-molecular SERS primer. (C) Bi-molecular SERS probe (D) Uni-molecular SERS probe.

In the 5' → 3' exonuclease digestion PCR assay (Figure 3.12 C & D) the expected length of the PCR products was 160 bp, and the obtained length was 170 bp in both cases. That there is no difference in length between uni-molecular and the bi-molecular digestion assay can be explained by the fact that the SERS probes in this case were partly digested and not part of the PCR product (Figure 3.12 C & D inset schematic). However the difference in expected and obtained length cannot be explained other than by instrumental error. The PCR yield was typically above 50% for both the SERS primers and SERS probes assay. In all reactions the negative control samples were negative for the expected PCR product length. Shorter DNA was observed in most cases but not considered to be problematic.

3.3.10 SERS primer PCR assay spermine hydrochloride concentration optimisation

The concentration of spermine hydrochloride was optimized with respect to direct analysis (within 1 min) and discrimination between positive and negative samples. The optimal final concentration of spermine was found to be 400 µM (Figure 3.13A). When spermine hydrochloride was added with a final concentration of 4 µM, discrimination between double stranded and single stranded DNA could be obtained after 480 s (Figure 3.13B).

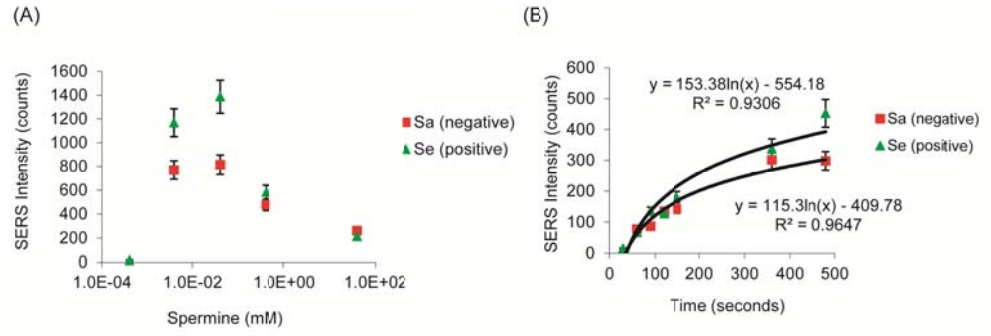

Figure 3.13 SERS primer and PCR & SERS assay optimization of spermine concentration (A). SERS peak intensities of SERS primer PCR products using a final spermine concentration of 4 µM over a time period of 480 s (B).

From the results in Figure 3.14A & B it can be concluded that there was no difference between uni- and bi-molecular SERS primers, when coupled with PCR,

both uni- and bi-molecular SERS primer methods gave a distinct discrimination between negative and positive samples. The bi-molecular SERS primer method contained fewer false negative samples due to a slightly higher reproducibility and therefore lower threshold value. The differences in results between uni- and bi-molecular SERS primers in the synthetic model system and the PCR-based assay can be explained by the fact that in the case of the bi-molecular SERS primer, the FAM labelled ssDNA was not linked to the dsDNA PCR product (which was twice the length of the synthetic model dsDNA) thereby enabling more reproducible adsorption of the FAM labelled ssDNA onto the nanoparticles surface. Nevertheless, bi-molecular as well as uni-molecular SERS primers could successfully be used in coupling PCR and SERS in a separation free assay system significantly reducing the cost of the SERS primers and thereby the overall SERS assay system.

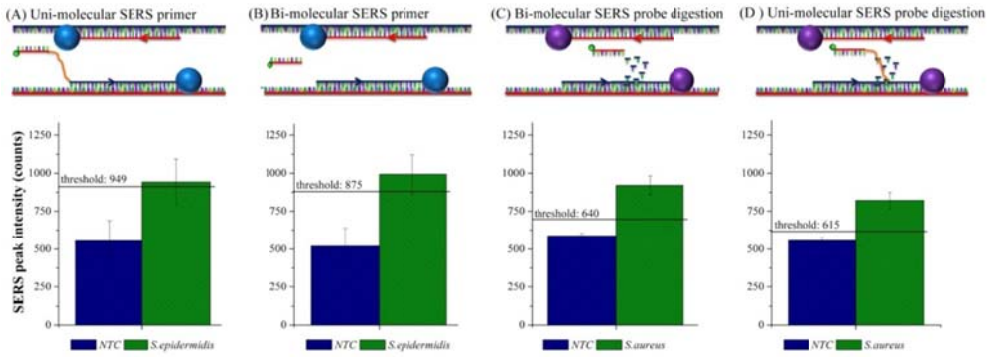

Figure 3.14 Schematic representation and results obtained from SERS primers and SERS probes in PCR reactions. (A) The uni-molecular SERS primer is incorporated into the PCR product, and the blue sphere represents 5'→3' exonuclease deficient DNA polymerase. (B) The bi-molecular SERS primer PCR assay. (C) The bi-molecular SERS probe digested by the 5'→3' exonuclease active DNA polymerase (purple sphere) (D) The uni-molecular SERS probe PCR assay. Error bars represent ± one standard deviation of the sample. Threshold values are the mean plus three times the standard deviation of the negative control sample (NTC).

Moreover, from the previous synthetic experiments, it is known that a higher ratio of target to SERS primer was better for the overall assay performance. Therefore the main challenge in using the SERS primers in a PCR-based SERS

assay was in the yield of the PCR reaction which is typically 50% corresponding to a SERS primer to target ratio of 1 to 0.5.

In an attempt to overcome the PCR yield issue uni- and bi-molecular SERS probes have been incorporated in a PCR reaction where the SERS probes were digested by the 5' → 3' exonuclease activity of the *Taq* DNA polymerase. This approach offers the possibility to partly digest the SERS probe generating ssDNA that is not attached to the dsDNA PCR product (Figure 3.10). An advantage of such a system is the use of an increased PCR primer to SERS probe ratio thereby improving the overall assay performance. The results in Figure 3.14C & D showed clear discrimination between negative and positive samples for both uni- and bi-molecular SERS probes with no false negative results (0/9) which is a significant improvement over the herein reported uni- and bi-molecular SERS primer methods. Reproducibility and discrimination between positive and negative samples are improved which are important parameters for the SERS assay to find practical use.

Additionally, the use of uni-molecular SERS primers and probes only had a performance advantage in direct detection assays such as our synthetic model system. When uni- and bi-molecular SERS primers and probes were coupled with the PCR no clear differences between uni- and bi-molecular approaches were obtained, which significantly reduced the cost of the SERS primers and probes and the overall SERS assay system without compromising the sensitivity or specificity.

3.4 Conclusions

Important factors for the performance of the positive SERS primer assays were investigated utilizing a synthetic model. The demonstration and evaluation of four separation free SERS assays for the specific detection of pathogen DNA has been carried out. These assays prove that SERS is a reliable and competitive technique to fluorescence for direct target DNA detection with or without the use of PCR. Within the synthetic model assays silver citrate and silver EDTA nanoparticles provided the best discrimination between single and double stranded DNA. The use of partly self-complementary uni-molecular oligonucleotide sequences for the SERS primer significantly increased the contrast between positive and negative samples. The results have shown that a SERS primer or probe to target ratio of 0.5 could be detected and when increasing the target to probe ratio significantly higher SERS signals were obtained for all SERS probe models. By increasing the concentration of nanoparticles the assay was fully quantitative up to a DNA concentration of 50 nM. Finally SERS primer overhangs had no significant effect on the performance of the synthetic SERS primer assay. For the detection of PCR products it was best to use the new internal SERS probe digestion assay because with this assay no false negative results were obtained. A significant cost reduction was achieved when using bi-molecular SERS primers and probes coupled to the PCR without any compromises towards sensitivity or selectivity.

Uni-molecular and bi-molecular SERS primers have been used in SERS primer extension and digestion assays. In the following chapter the possibilities of SERS primers in a multiplex reaction will be investigated.

4 SERS PRIMERS AND MULTIPLEX PATHOGEN DETECTION

4.1 Introduction

When SERS primers were used in combination with PCR there was a slight preference for the SERS primer digestion assay and no significant differences between uni-molecular and bi-molecular SERS primers. However multiplex reactions bring a whole new dimension to the assays. Parameters to be considered include specificity of the primers, cross reactions between the SERS primers, and available nanoparticle surface area since more DNA is present in the reactions.

Uni-molecular SERS primers will be designed for both type of assay formats. The decision to use uni-molecular SERS primers was based on the fact that these SERS primers performed with lower detection limits in the synthetic model systems, and a lower number (-1) of individual oligonucleotide sequences was required when compared to a bi-molecular system.

The SERS primer assays are carried out over a temperature range between 95 °C and 20 °C. Therefore the interactions between the oligonucleotides had to be calculated over this temperature range and carefully addressed.

DNA thermodynamics and kinetics are important parameters to be considered for PCR and other DNA hybridisation based assay designs such as the SERS primer assays. Extensive studies on kinetic and thermodynamic properties[102, 117, 130, 131]

have generated strong predictive models for oligonucleotide reactions.[104, 116, 125, 132]

Using fluorescence detection, the multiplexing capabilities in solution are limited by the broad absorption and emission bands of the fluorophores used for the fluorescence detection, and multiple filter sets and / or multiple excitation wavelengths are needed to differentiate fluorescent labels from each other.[133] An alternative technique is surface enhanced Raman scattering (SERS) which produces molecule specific vibrational spectra, and when a Raman reporter is in close proximity to a rough metal surface the technique becomes ultra-sensitive. The advantage of SERS is that it can identify multiple different analytes present in a sample without the need for multiple filter sets or multiple excitation wavelengths. Several groups have reported the multiplexed SERS detection of labelled synthetic oligonucleotides but less work has been reported on SERS based assays.[53-55] Examples of solution based multiplex SERS assays are the molecular sentinels by Vo-Dinh *et al.*[97] and by MacAskill *et al.* the ssDNA / dsDNA assay.[91]

In order to perform multiplexed DNA detection using SERS primers a dye selection was made, followed by oligonucleotide design, and oligonucleotide cross reaction evaluation to investigate the possibilities of the use of SERS primers in multiplex reactions.

4.2 Experimental

Experimental details for Chapter 4 are provided in the sections below. DNA oligonucleotide design, dye selection, and finally oligonucleotide cross reaction analysis.

4.2.1 DNA oligonucleotide design

The *mecA* gene was previously used for identification of methicillin resistance.[23] The whole genome sequence of epidemic methicillin resistant *Staphylococcus aureus* (EMRSA) (NCTC 13142) was obtained from the National Centre of Biotechnology Information (NCBI) website.[124] The oligonucleotide sequence design was carried out using the Primer3Plus online server.[101] Parameters within this software were set to 50 mM monovalent salt, 1.5 mM divalent salt, and 250 nM of DNA. For the table of thermodynamic parameters the setting "Santalucia 1998" was used.[102] For salt correction the formula set by "Owczarzy *et al.* 2004" was used.[103] Internal folding of the sequence region selected by Primer3Plus was analyzed using the DINAMelt webserver[104] and the oligoanalyzer webserver from Integrated DNA Technologies (IDT).[125] Parameters were set to 58°C, 50 mM monovalent salt, 1.5 mM divalent salt, and 250 nM of DNA. Basic Local Alignment (BLAST) was carried out using the BLAST tools from the NCBI website.[126]

4.2.2 Dye selection

SERS spectra of fluorescent dyes were obtained from Renishaw Diagnostics Ltd. SERS spectra were plotted in one graph and a dye selection of three that could be resolved by eye was made.

4.2.3 Cross reaction analysis

Cross reaction analysis between the designed oligonucleotide sequences was carried out using the DINAMelt webserver[104], and the oligoanalyzer webserver from Integrated DNA Technologies (IDT).[125]

Hybridisation between two different strands was modelled using the function "hybridisation between two different strands" on the DINAMelt webserver,

setting applied were 250 nM DNA 50 mM monovalent salts, and 1 mM divalent salt. [104] Utilizing this server the hybridisation between two DNA strands A & B, folding of A and B, and homodimer formation between A & A as well as B & B are considered.

Hairpin folding of an oligonucleotide strands was modelled using the oligoanalyzer from IDT and the hairpin function using the same conditions settings as mentioned above. This function models the formation of a hairpin loop within one strand of DNA for example hairpin folding of strand A. [125]

Hybridisation between two strands A & B was modelled using the function "Two state melt (hybridisation)" on the DINAMelt webserver using the same setting as mentioned above and energy rules for 25°C. Using this setting hybridisation between strand A & B is considered including possible mismatches.

4.3 Results and discussion

The first step towards SERS primer multiplexing was the selection of SERS active dyes that could be resolved by eye. The next step was assay design consisting of SERS primers and normal PCR primers, following by cross reaction analysis of the designed oligonucleotides to explore the possibilities.

4.3.1 Dye selection

Dyes were selected by the following criteria: background fluorescence position and resolvable SERS spectra by eye. The result of the dye selection is shown in Figure 4.1.

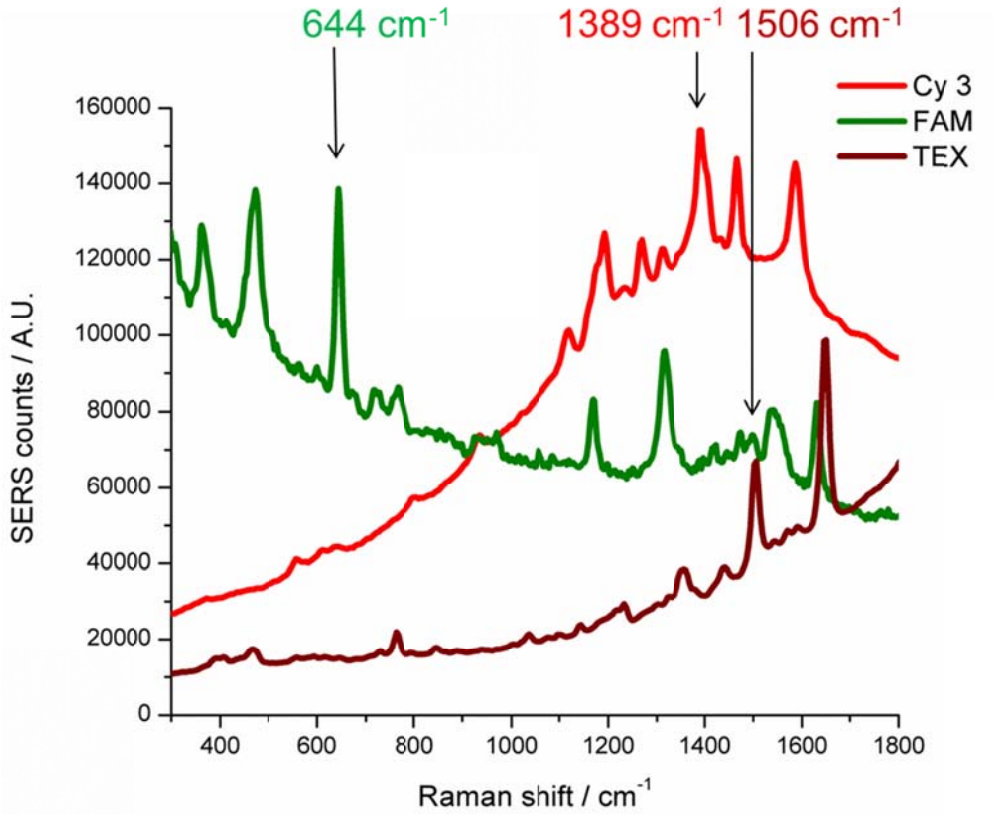

Figure 4.1 SERS spectra of dyes selected for multiplex detection experiments. Green line the SERS spectrum of FAM and the peak at 644 cm^{-1} used for resolving the presence of FAM, Red line the SERS spectrum of Cy3 and peaks at 1389 cm^{-1} can be used for identification of Cy3, Dark red line SERS spectrum of an oligonucleotide labelled with TEX, the 1506 cm^{-1} can be used for identification of the TEX dye.

These dyes emit fluorescence varied over the collection range i.e. FAM emission maximum at 520 nm, Cy3 emission maximum at 564 nm, TEX emission maximum at 613 nm to prevent saturation of the detector at a single position. These dyes can be resolved by eye using the 644 cm^{-1} Raman shift for the FAM dye, the 1389 or the 1466 cm^{-1} peak for Cy3, and the 1506 cm^{-1} peak for the TEX dye.

4.3.2 Assay design

Assay designs were carried out as described in previous experimental sections 2.2.1, 3.2.2, and 4.2.1 and the *femA-SE* and *femA-SA* and the *mecA* genes of *Staphylococcus epidermidis* and *Staphylococcus aureus* were used as model systems for specific DNA gene detection.[23]

The *MecA* gene of *Staphylococcus aureus* was chosen as a third model system for the multiplex work. The sequence of the *MecA* gene gene (gene bank accession number X52593)[23, 134] was obtained from the National Center for Biotechnology Information (NCBI).[100] Primer3 online software was used to generate primers.[102, 103, 113] The primers and amplicon region were selected by the Primer 3 software allowing analysis for internal folding, and for hetro- and homo-dimer formation at 58°C using online software mFold, UNAFold and DINAmelt available from the Rensselaer Polytechnic Institute.[102, 104, 114, 115] Finally the specificity of the primers was checked against other bacteria using NCBI BLAST.[105]

The designed primer sequences are shown in Table 4.1. These sequences are specific to the *MecA* gene and are designed to generate a minimal amount of internal foldings. The T_m values are an indication of the temperature of which half the oligonucleotide strands in a sample are bound to their complements.

Table 4.1 Overview of oligonucleotide sequences selected.

Name	Sequence 5' → 3'
MecA Forward primer	CATTGATCGCAACGTTCAATTT
MecA Reverse primer	TGGTCTTTCTGCATTCCTGGA
MecA Internal probe	TGGAAGTTAGATTGGGATCATAGCGTCAT

The region of genomic DNA selected by the Primer3 software was checked for internal sequence folding at 58 °C containing 50 mM monovalent salt and 1 mM divalent salt and sequence type linear using the DINAMelt Two state folding online software.[104]

The positions of the primers within the *mecA* gene are indicated in yellow, whilst the regions most likely to fold are shown in red in Figure 4.2. The red areas were to be avoided as primer binding regions.

ATGAAAAAGATAAAAATTGTTCCACTTATTTTAATAGTTGTAGTTGTCGGGTTTGGTATATATTTTTATGCTTCAAAAGATA
AAGAAATTAATAATACTATTGATGCAATTGAAGATAAAAATTTCAAACAAGTTTATAAAGATAGCAGTTATATTTCTAAAAG
CGATAATGGTGAAGTAGAAATGACTGAACGTCCGATAAAAATATATAATAGTTTAGGCGTTAAAGATATAAACATTCAGGAT
CGTAAAATAAAAAAAGTATCTAAAAATAAAAAACGAGTAGATGCTCAATATAAAATTAAAACAAACTACGGTAACATTGATC
GCAACGTTCAATTTAATTTTGTTAAAGAAGATGGTATGTGGAAGTTAGATTGGGATCATAGCGTCATTATTCCAGGAATGCA
GAAAGACCAAAGCATACATATTGAAAATTTAAAATCAGAACGTGGTAAAATTTTAGACCGAAACAATGTGGAATTGGCCAAT
ACAGGAACACATATGAGATTAGGCATCGTTCCAAAGAATGTATCTAAAAAAGATTATAAAGCAATCGCTAAAGAACTAAGTA
TTTCTGAAGACTATATCAACAACAAATGGATCAAAATTGGGTACAAGATGATACCTTCGTTCCACTTTAAAACCGTTAAAAA
AATGGATGAATATTTAAGTGATTTCGCAAAAAAATTTCATCTTACAACTAATGAAACAGAAAGTCGTAACTATCCTCTAGAA
AAAGCGACTTCACATCTATTAGGTTATGTTGGTCCCATTAACTCTGAAGAATTAAAACAAAAAGAATATAAAGGCTATAAAG
ATGATGCAGTTATTGGTAAAAAGGGACTCGAAAAACTTTACGATAAAAAGCTCCAACATGAAGATGGCTATCGTGTCACAAT
CGTTGACGATAATAGCAATACAATCGCACATACATTAATAGAGAAAAAGAAAAAAGATGGCAAAGATATTCAACTAACTATT
GATGCTAAAGTTCAAAAGAGTATTTATAACAACATGAAAAATGATTATGGCTCAGGTACTGCTATCCACCCTCAAACAGGTG
AATTATTAGCACTTGTAAGCACACCTTCATATGACGTCTATCCATTTATGTATGGCATGAGTAACGAAGAATATAATAAATT
AACCGAAGATAAAAAAGAACCTCTGCTCAACAAGTTCCAGATTACAACTTCACCAGGTTCAACTCAAAAAATATTAACAGCA
ATGATTGGGTTAAATAACAAAACATTAGACGATAAAACAAGTTATAAAATCGATGGTAAAGGTTGGCAAAAAGATAAATCTT
GGGGTGGTTACAACGTTACAAGATATGAAGTGGTAAATGGTAATATCGACTTAAAACAAGCAATAGAATCATCAGATAACAT
TTTCTTTGCTAGAGTAGCACTCGAATTAGGCAGTAAGAAATTTGAAAAAGGCATGAAAAAACTAGGTGTTGGTGAAGATATA
CCAAGTGATTATCCATTTTATAATGCTCAAATTTCAAACAAAAATTTAGATAATGAAATATTATTAGCTGATTCAGGTTACG
GACAAGGTGAAATACTGATTAACCCAGTACAGATCCTTTCAATCTATAGCGCATTAGAAAATAATGGCAATATTAACGCACC
TCACTTATTAAAAGACACGAAAAACAAAGTTTGGAAGAAAAATATTATTTCCAAAGAAAATATCAATCTATTAAATGATGGT
ATGCAACAAGTCGTAAATAAAACACATAAAGAAGATATTTATAGATCTTATGCAAACTTAATTGGCAAATCCGGTACTGCAG
AACTCAAAATGAAACAAGGAGAAAGTGGCAGACAAATTGGGTGGTTTATATCATATGATAAAGATAATCCAAACATGATGAT
GGCTATTAATGTTAAAGATGTACAAGATAAAGGAATGGCTAGCTACAATGCCAAAATCTCAGGTAAAGTGTATGATGAGCTA
TATGAGAACGGTAATAAAAAATACGATATAGATGAATAA

Figure 4.2 The base numbers 390 till 664 of the *mecA* gene. In red is shown the region with an increased risk of internal folding of the template DNA. In yellow the positions of the selected primers.

Oligonucleotide designs were carried out for both the SERS primer extension assay and the SERS primer digestion assay. Because there was only a slight difference in performance between the two assays and the SERS primer extension assay requires less oligonucleotide sequences (3 vs 4 per target).

The results of the SERS primer digestion assay design which requires a forward and reverse amplification primer and internal SERS primer are shown in Table 4.2.

Table 4.2 Overview of the selected oligonucleotide sequences for the *femA-SE*, *MecA*, and the *femA-SA* gene. Red bases represent mismatched bases. HEG represents an internal hexaethylene spacer molecule. Dye molecules are shown in either; green FAM, yellow Cy3, and dark red for TEX.

Name	Sequence 5' → 3'	T_m (IDT 50mM mono 1mM divalent salt)	Hairpin structure T_m(°C) and number of different structures
femA-SE			
Forward	CAACTCGATGCAAATCAGCAA	60.5	
Reverse	GAACCGCATAGCTCCCTGC	63.5	
Probe	TACTACGCTGGTGGAACTTCAAATCGTTATCG	68.0	
SERS primer	TACTACGCTGGTGGAACTTCAAATCGTTATCG-HEG-ATAAGGATTCGAAGTTCGACCAFAM	68.0	58 -46.5, three structures
MecA			
Forward	CATTGATCGCAACGTTCAATTT	59.6	
Reverse	TGGTCTTTCTGCATTCCTGGA	62.4	
Probe	TGGAAGTTAGATTGGGATCATAGCGTCAT	66.2	
SERS primer	TGGAAGTTAGATTGGGATCATAGCGTCAT-HEG-ATGACACTAGGATCACAATGTAACCy3	66.2	56.7 one structure
femA-SA			
Forward	AACAGCTAAAGAGTTTGGTGCCTTT	64.3	
Reverse	AGTAAGTAAGCAAGCTGCAATGACC	64.1	
Probe	GCATGCCATACAGTCATTTCACGCA	66.5	
SERS primer	GCATGCCATACAGTCATTTCACGCA-HEG-TACTTGAAATGTCTGTATGTEX	66.5	58-46-45.4, multiple structures

Parallel to the SERS primer digestion assay design designs for the SERS primer extension assay were carried out. To make SERS primer design easier cytosine bases in the complementary sequence were replaced by thymine bases creating a 'wobble' pair between thymine and guanidine in the hairpin structure.[135, 136]

These type of base pairs are less favourable than the standard Watson-Crick base pairs,[137] and using these the hairpin structure could be destabilised without creating bulge loops. The results of the SERS primer digestion assay which requires a forward and reverse amplification primer and internal SERS primer are shown in Table 4.3.

Table 4.3 Overview of the oligonucleotide sequences designed for the different assays. Red bases represent mismatched bases to reduce hairpin stability. Green bases represent overhang bases.

Name	Sequence 5' → 3'	T_m (IDT 50mM mono 1mM divalent salt)	Hairpin structure T_m (°C) and number of different structures
femA-SE			
Forward	CAACTCGATGCAAATCAGCAA	60.5	
Reverse	GAACCGCATAGCTCCCTGC	63.5	
SERS Fw primer	GATTTGTATTGATT-HEG-CAACTCGATGCAAATCAGCAA	N/A	49.1 one structure
SERS Rv primer	GAGTTATGTGGT-HEG-GAACCGCATAGCTCCCTG	N/A	55.8 one structure
MecA			
Forward	CATTGATCGCAACGTTCAATTT	59.6	
Reverse	TGGTCTTTCTGCATTCCTGGA	62.4	
SERS Fw primer	GAATGTTGTGATTAA-HEG-CATTGATCGCAACGTTCAATTT	N/A	54.2 one structure
SERS Rv primer	GAATGTAGGGAGATTA-HEG-TGGTCTTTCTGCATTCCTGGA	N/A	47 one structure
femA-SA			
Forward	AACAGCTAAAGAGTTTGGTGCCTTT	64.3	
Reverse	AGTAAGTAAGCAAGCTGCAATGACC	64.1	
SERS Fw primer	CCAAATTTTTTAGTTGTT-HEG-AACAGCTAAAGAGTTTGGTGCCTTT	N/A	48.8 one structure
SERS Rv primer	CATTGTAGTATGTTT-HEG-AGTAAGTAAGCAAGCTGCAATGACC	N/A	46.7 one structure

All designs of the SERS primers form only the preferred hairpin loop which is an improvement over previous designs carried out for the SERS primer digestion assay. The preferred SERS primers have a hairpin T_m of 10-15 °C below the T_m of

the SERS primer priming region. The T_m of the hairpin of the preferred SERS primers is shown in black in Table 4.3.

4.3.3 Cross reaction analysis

After SERS primer designs the next step was cross reaction analysis between the SERS primers and other oligonucleotide sequences present in the reaction. The hybridisation between target and SERS primer needs to be the most preferred event for successful SERS primers, and the SERS primer is not allowed to bind any other oligonucleotides present in the assay, otherwise this might result in either a false positive or a false negative result. A schematic overview of the cross reactions for the SERS primer assays is shown in Figure 4.3.

(A) SERS primer in uni-molecular double stranded form, (B) SERS primer in bi-molecular double stranded form, (C) SERS primer bound to its preferred target DNA, (D) Interaction of two SERS primers via the dye labelled region, this event might cause poor performance of the SERS primer assay, (E) the dye labelled region of the SERS primer interacting with the reverse primer present in the assay. In a single SERS primer reaction this event is not problematic because the reverse primer is mainly build into the PCR product in case of a positive sample when the dye labelled region of the SERS primer is single stranded and free in solution in case of a negative sample, and the SERS primer will be in its closed format not generating strong SERS signals. However this event might cause poor performance of the SERS primer multiplex assay because an opened SERS primer could interact with free reverse primers of a second set present in the multiplex reaction, (F) the priming region of the SERS primer interacts with another primer which might cause problems as explained for event (E). Finally event (G) represents an interaction between the priming regions of two SERS primers and results in a false positive result.

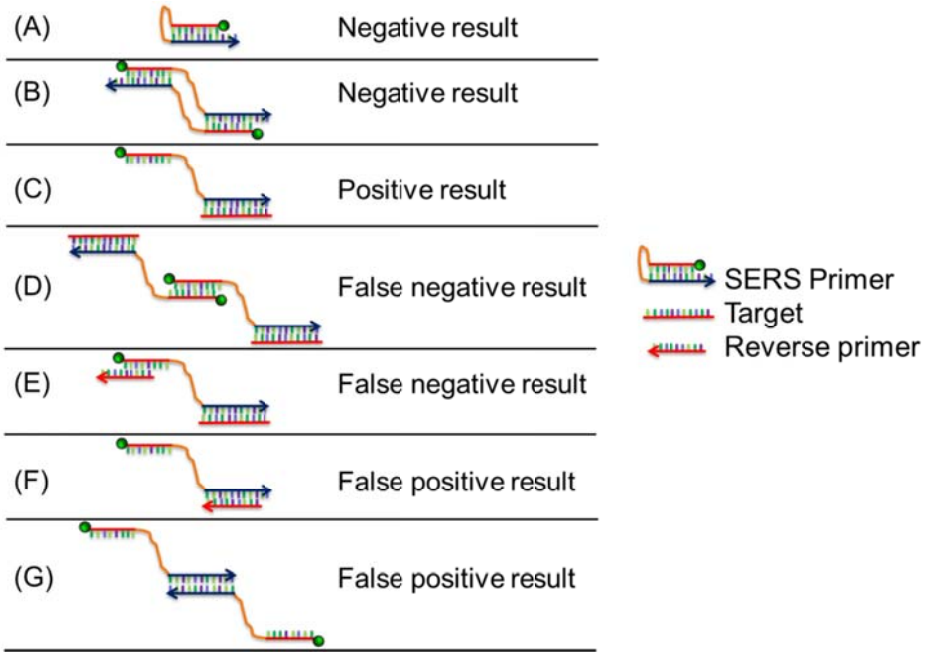

Figure 4.3 Schematic representations of SERS primer interaction and the outcome, T_m represents an indication of the melting temperature. (A) SERS primer in uni-molecular double stranded form, (B) SERS primer in bi-molecular double stranded form, (C) SERS primer bound to its preferred target DNA. (D) Interaction of two SERS primers via the dye labelled region, this event might result in a false negative result. (E) The dye labelled region of the SERS primer interacting with the reverse primer present in the assay. (F) The priming region of the SERS primer interacts with another primer causing a false positive result. Finally event (G) represents an interaction between the priming regions of two SERS primers which results in a false positive result.

A full component analysis of the designed oligonucleotides was carried out for interactions between two oligonucleotide species. Table 4.4 shows the obtained results for the oligonucleotides designed for the SERS primer digestion assay and Table 4.5 shows the results for the SERS primer extension assay. A colour code scheme was made to classify the results and make the results more clear. Red and orange indicate the strongest interactions, and yellow and green represent the weaker interactions.

Table 4.4 Hybridisation T_m absorbance (°C) of two strand hybridisation for the SERS primer digestion assay, modelled via the DINAMelt server function "hybridisation of two different strands". Colour codes; red a T_m above the T_m of the SERS primer hairpin structure i.e. 45 °C, orange when the T_m was 10 °C below the T_m of the SERS primer hairpin structure i.e. between 45 and 35 °C, yellow when the T_m was 20 °C below the T_m of the SERS primer hairpin structure i.e. between 35 and 25 °C, and green when the T_m was below 25 °C.

Hybridisation T_m (°C) of two strands	No.	1	2	3	4	5	6	7	8	9	10	11	12
femA-SE Primer Forward	1	51											
femA-SE Primer Reverse	2	46.7	42.1										
femA-SE SERS Primer Priming Region	3	49.8	46.1	49									
femA-SE SERS Primer Self Complement	4	47.6	42.9	27	43.8								
MecA Primer Forward	5	50.1	48.4	50	48.8	49.9							
MecA Primer Reverse	6	42.8	38.3	43	58.5	47.3	34.7						
MecA SERS Primer Priming Region	7	28.4	27	31	27.4	39.4	25.7	22.7					
MecA SERS Primer Self Complement	8	46.3	42	46	42.8	48.3	38.5	33.3	42				
femA-SA Primer Forward	9	44.5	40.8	44	41.3	47.5	37.6	28	40.8	40			
femA-SA Primer Reverse	10	51.7	47.4	50	48.3	50.4	43.5	28	47	45	52.4		
femA-SA SERS Primer Priming region	11	43.2	39	43	32.5	47.2	35.3	25.8	39.1	38	43.5	36	
femA-SA SERS Primer Self Complement	12	34.7	32.3	37	32.5	43.8	30.1	24.5	33	33	34.8	34	27.4

Table 4.5 Hybridisation T_m absorbance (°C) of two strand hybridisation for the SERS primer extension assay, modelled via the DINAMelt server function "hybridisation of two different strands". Colour codes; red a T_m above the T_m of the SERS primer hairpin structure i.e. 45 °C, orange when the T_m was 10 °C below the T_m of the SERS primer hairpin structure i.e. between 45 and 35 °C, yellow when the T_m was 20 °C below the T_m of the SERS primer hairpin structure i.e. between 35 and 25 °C, and green when the T_m was below 25 °C.

Hybridisation T_m (°C) of two strands	No.	1	2	3	4	5	6	7	8	9
femA-SE Primer Reverse	1	42.1								
femA-SE SERS Primer Forward Self Complement	2	35.3	16.6							
femA-SE SERS Primer Forward Priming Region	3	46.7	12.8	35.4						
MecA Primer Forward	4	48.4	47.9	50.1	49.9					
MecA SERS Primer Reverse Self Complement	5	25.4	18.2	32.3	45	18.8				
MecA SERS Primer Reverse Priming Region	6	38.3	29.9	35	47.3	22.9	34.7			
femA-SA Primer Forward	7	40.8	35	44.5	47.5	30.1	37.6	39.8		
femA-SA SERS Primer Reverse Self Complement	8	27.7	19	30.3	44.2	19.3	25.5	29.1	19.6	
femA-SA SERS Primer Reverse Priming Region	9	47.4	43.9	45.2	50.4	32	43.5	45.1	26.2	52.4

According to these results there is a significant amount of interactions between the oligonucleotides in the mixture. The majority of the calculations was found to be classified as either orange or even red which means an high chance of either false positive or false negative results. From Table 4.4 it can clearly be seen that

when oligonucleotide sequences with numbers 1, 5, and 10 are present in the reaction mixture, high T_m values were obtained. The same results were obtained in the SERS primer extension assay for oligonucleotide sequences with numbers 4 and 9 in Table 4.5.

Importantly these calculations model not only interactions between two oligonucleotide sequences but also folding and dimer formation thereof. Therefore hairpin folding analysis of the oligonucleotide sequences was carried out. Results in Table 4.6 show that oligonucleotide sequences with numbers 1, 5, and 10 possess a T_m for hairpin loop formation as indicated in red, again the same results were obtained for the oligonucleotide sequences numbers 3, 4, and 9 designed for the SERS primer extension assay (Table 4.7).

Table 4.6 Hairpin folding T_m values for the oligonucleotide sequences designed for the SERS primer digestion assay. Colour codes; red a T_m above the T_m of the SERS primer hairpin structure i.e. 45 °C, orange when the T_m was 10 °C below the T_m of the SERS primer hairpin structure i.e. between 45 and 35 °C, yellow when the T_m was 20 °C below the T_m of the SERS primer hairpin structure i.e. between 35 and 25 °C, and green when the T_m was below 25 °C.

Hairpin folding T_m (°C)	No.	1	2	3
femA-SE Primer Forward	1	52.9	45.9	
femA-SE Primer Reverse	2	38.7	30.9	24
femA-SE SERS Primer Priming Region	3	34.7	31.8	32
femA-SE SERS Primer Self Complement	4	39.2	38	
MecA Primer Forward	5	45.6		
MecA Primer Reverse	6	24	22.2	8.6
MecA SERS Primer Priming Region	7	37.4		
MecA SERS Primer Self Complement	8	27.4	21.5	
femA-SA Primer Forward	9	33.2	26.6	23
femA-SA Primer Reverse	10	48.6	48.3	
femA-SA SERS Primer Priming region	11	26.8	22	12
femA-SA SERS Primer Self Complement	12	22.7	22.4	17

Table 4.7 Hairpin folding T_m values for the oligonucleotide sequences designed for the SERS primer extension assay. Colour codes; red a T_m above the T_m of the SERS primer hairpin structure i.e. 45 °C, orange when the T_m was 10 °C below the T_m of the SERS primer hairpin structure i.e. between 45 and 35 °C, yellow when the T_m was 20 °C below the T_m of the SERS primer hairpin structure i.e. between 35 and 25 °C, and green when the T_m was below 25 °C.

Hairpin folding T_m (°C)	No.	1	2	3
femA-SE Primer Reverse	1	38.7	30.9	24.1
femA-SE SERS Primer Forward Self Complement	2	-42.2	-42.7	-42.7
femA-SE SERS Primer Forward Priming Region	3	52.9	45.9	
MecA Primer Forward	4	45.6		
MecA SERS Primer Reverse Self Complement	5	9	-565	
MecA SERS Primer Reverse Priming Region	6	24	22.2	8.6
femA-SA Primer Forward	7	33.2	26.6	23.2
femA-SA SERS Primer Reverse Self Complement	8	16.9	-37.2	
femA-SA SERS Primer Reverse Priming Region	9	48.6	48.3	

These results indicate that the results obtained with the "hybridisation of two strands" analysis are strongly influenced by the formation of hairpin loops within the oligonucleotide structure. This does not directly mean that the SERS primer assays would fail, since hairpin folding of primers is not considered for direct failure of the SERS primer assays.

When a two-state model was applied only considering the hybridisation event of oligonucleotide A & B the results shown in Table 4.8 and Table 4.9 were obtained. From these tables it can clearly be seen that there are no significant interactions between the different oligonucleotide species present in the mixture (light and dark green). Formation of homo-dimers was limited and only for the *femA-SE* SERS primer self complementary region a higher T_m value of 28.5 °C was found, which should not be problematic because the formation of the hairpin loop was previously found to be stronger (T_m 56-48°C). In the worst case this result would lead to a false positive result. Other yellow blocks were interactions found between the SERS primer self-complementary region and its priming region which was as expected.

Table 4.8 Two state melt (hybridisation) analysis of the SERS primer digestion assay. Light green was used for negative T_m values, dark green for T_m values below 25°C and yellow for T_m values between 25 and 35°C.

Two State Melt (Hybridisation) T_m (°C)	No.	1	2	3	4	5	6	7	8	9	10	11	12
femA-SE Primer Forward	1	-20.1											
femA-SE Primer Reverse	2	-11.6	-24										
femA-SE SERS Primer Priming Region	3	-1	-15.9	-33									
femA-SE SERS Primer Self Complement	4	-41.5	-43.9	34	28.5								
MecA Primer Forward	5	9.5	-18	0.2	-14	18.3							
MecA Primer Reverse	6	-14.5	-27.7	-18	-2	-27.7	-6						
MecA SERS Primer Priming Region	7	-5.5	-6.8	20	-32	14.1	-13	-4.2					
MecA SERS Primer Self Complement	8	-41.2	-26.5	-3.8	-34	-1.6	-18	34.5	-4.2				
femA-SA Primer Forward	9	-2.1	-32.4	0.6	-15	-24.4	0.3	-27.4	-34.2	-2			
femA-SA Primer Reverse	10	-4.1	-28.7	-31	-55	-2.5	3.1	-14.2	-29.4	0.8	11.8		
femA-SA SERS Primer Priming region	11	-17	-23.2	0.8	-26	-49.5	-27	-4.9	-10.7	-7.9	11.7	12.7	
femA-SA SERS Primer Self Complement	12	-34.3	-47.3	-21	-32	-27.1	-29	-32.1	-16.1	-29	-9.7	32.7	-46.2

Table 4.9 Two state melt (hybridisation) analysis of the SERS primer extension assay. Light green was used for negative T_m values, dark green for T_m values below 25°C and yellow for T_m values between 25 and 35°C.

Two State Melt (Hybridisation) T_m (°C)	No.	1	2	3	4	5	6	7	8	9
femA-SE Primer Reverse	1	-12								
femA-SE SERS Primer Forward Self Complement	2	-71.2	-111							
femA-SE SERS Primer Forward Priming Region	3	-11.6	13.9	-20.1						
MecA Primer Forward	4	-18	-22.8	9.5	18.3					
MecA SERS Primer Reverse Self Complement	5	18.7	-53.4	-24.9	-18.6	-76.1				
MecA SERS Primer Reverse Priming Region	6	-27.7	-71.2	-14.5	-27.7	3.5	-6			
femA-SA Primer Forward	7	-24.2	-69.2	-2.1	-24.4	-33.8	0.3	-2		
femA-SA SERS Primer Reverse Self Complement	8	-30.7	-85.3	-59.7	-38	-33.9	-38.9	-43.7	-53	
femA-SA SERS Primer Reverse Priming Region	9	-1.5	-13.2	-4.1	-2.5	-32.2	3.1	0.8	7.9	11.8

According to the latest cross reaction analysis results it seems feasible to perform multiplex detection assays using the SERS primers in both types of assays the SERS primer digestion and the SERS primer extension.

4.4 Conclusions

A selection of dyes for multiplex pathogen detection has been made. Assay designs for the SERS primer digestion, and the SERS primer extension assay were made successfully, followed by cross reaction analysis of the oligonucleotides required for the multiplex detection.

With the first model it seemed that there was a very high level off cross reactivity when the SERS primers were analysed in computational models which combined with the positive to negative sample discrimination in the PCR reaction of 2:1 are likely to result in poor performance or in worst case failure of the assay. However after re-analysis using separate models the cross reactivity could be addressed and assigned as not problematic.

After more detailed analysis the results indicate that it is feasible to perform a multiplex detection using both types of assays. However it was decided to postpone the final multiplex detection part of the project and investigate assay systems that requires less complex designs.

5 POSITIVELY CHARGED NANOPARTICLES FOR DNA DETECTION BY SERS

5.1 Introduction

For the analysis of DNA by SERS, negatively charged silver nanoparticles have mainly been used in aqueous solution.[86, 138] In the method developed by Bell *et al.* DNA strands were adsorbed onto metal surfaces with direct interaction of nucleotide chains with the metal surface and the addition of magnesium sulphate facilitated aggregation of the nanoparticle to improve the SERS detection.[86] To improve sensing performance Graham *et al*. added small molecules with positively charged functional groups as aggregating agents and to overcome the electrostatic repulsion between the negatively charged DNA phosphate groups and the metal surface and further enhancing the SERS detection.[139, 140]

Amongst reported aggregating agents, the polyamine spermine offered high SERS sensitivity when used in combination with negatively charged particles acting as a sandwich molecule bringing dye-labelled DNA molecules close to the particle surface and further aggregating the nanoparticles.[141] However, spermine itself can interact with free DNA in solution inducing its agglomeration.[142] On one hand this detection approach offered high sensitivity, however the bi-functional

nature of spermine in this system might lead to over aggregation compromising the stability of the system rendering stable SERS more difficult over time. As such, controlling the aggregation of the nanoparticles[143] and the interparticle distance have become important considerations for SERS analysis.[144]

A more simplified alternative approach for detection of DNA is to use positively charged nanoparticles ensuring electrostatic attraction between the analyte and the enhancing substrate. Several different types of nanoparticles with a positive surface charge have been reported. Gill *et al.* recently employed hexadecyltrimethylammonium bromide (CTAB) capped silver nanoparticles in SERS-based detection of dye-labelled DNA.[145] Although this method brings effective adsorption of the negatively charged analytes, the CTAB double layer surrounding the nanoparticles hampers, on the one hand, the SERS sensitivity due to its intrinsic shell thickness and, on the other hand, limits the nanoparticle stability to the presence of a significant concentration of unbound surfactant in solution. As an alternative, positively charged polymers such as poly-*L*-Lysine (PLL) and polyethyleneimine (PEI) have been employed in the preparation of gold and silver nanoparticles.[146-148] Although polymer coated particles may improve overall stability of the particle ligand shell, large interparticle gaps are formed during the formation of particle clusters substantially limiting the SERS sensing performance. Polymer coated particles can also present high background signals which compromises both the multiplexing potential of SERS and decreases the distinction of the analyte signals from the particle background.

In chapters two and three it has been shown that negatively charged silver nanoparticles (EDTA and citrate) in combination with SERS detection could be used for discrimination between ds and ssDNA with an increased SERS response. In order to generate a signal upon the presence of a DNA target molecule a double stranded SERS probe was used. In this system the target DNA sequence was in competition with the labelled part of the SERS probe. A more intense SERS

response was generated when more DNA target molecules compared to SERS primer molecules were present.

In this chapter the possibilities of using positively charged silver nanoparticles in order to invert the signalling system and use a single stranded SERS probe that only has to bind to the target sequence to become double stranded and thereby generate an increased SERS response will be explored. Figure 5.1 demonstrates a schematic representation of cationic polymer (sticks) coated nanoparticles (grey spheres) interacting with ssDNA labelled with a dye (green) molecule.

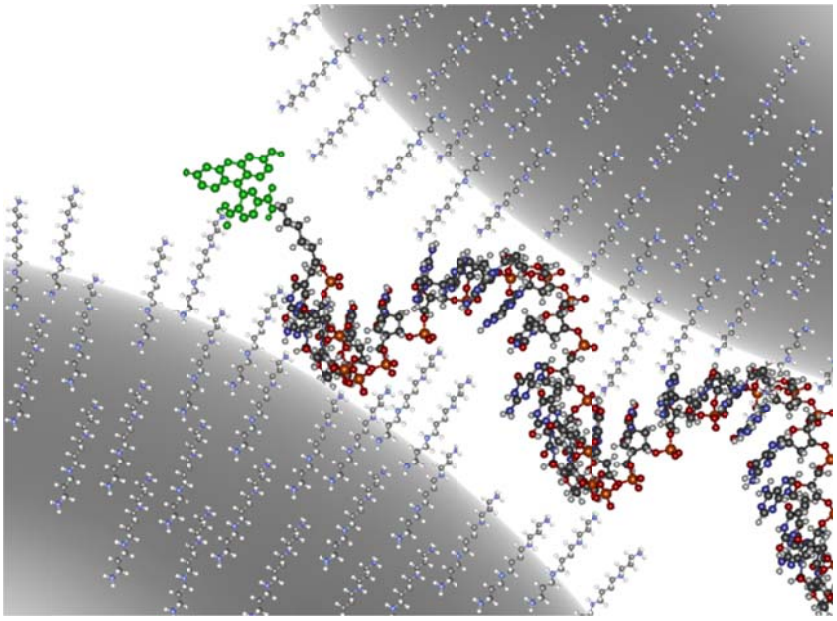

Figure 5.1 A schematic representation of cationic polymer (sticks) coated nanoparticles (grey spheres) interacting with ssDNA labelled with a dye (green) molecule.

The cationic polymer on the nanoparticle interacts with the DNA, bringing the DNA close to the nanoparticle surface and aggregation of the nanoparticles occurs. In this chapter multiple cationic nanoparticles will be tested in order to develop a simplified and more sensitive pathogen detection system without the use of a competitive DNA molecule (SERS primer and its self complementary region).

5.2 Experimental

5.2.1 Materials

All materials were obtained from Sigma Aldrich unless stated otherwise.

5.2.2 Buffers

Phosphate buffered saline (PBS) was obtained from Oxoid Limited (Basingstoke, Hampshire, England). One tablet was dissolved in 100 mL Milli Q water, and the solution was sterilised in an autoclave for 15 min at 121°C.

5.2.3 Oligonucleotide sequences

Oligonucleotide sequences were HPLC purified and obtained from ATD Bio (Southampton) and dissolved in DEPC treated water (Bioline). An overview is provided in Table 5.1.

Table 5.1 An overview of oligonucleotide sequences used. (T* is 5-propargylamine-2'-deoxyuridine).

No.	5'→3'	5' label
1	TGCTTGAAATGTCTGTATGGGATGC	FAM
2	GCATCCCATACAGACATTTCAAGCA	
3	T*CT*CT*CT*CT*CT*CGCGTCATCGTATACACAGGAGCAG	Cy5

5.2.4 Glassware preparation for positively charged nanoparticles preparation and storage

To prevent attachment of positively charged nanoparticles to glass surfaces, vials used for particle preparation and storage were coated with polyethyleneimine (PEI).[149] Briefly, prior to use all glassware was cleaned with chromic acid overnight and extensively rinsed with milli-Q water and dried in N_2 flow. The glassware was then filled with 0.2% w/w PEI aqueous solution and incubated for 2h. Vials were then rinsed once with milli-Q water and dried with N_2 flow.

5.2.5 Preparation of positively charged Silver nanoparticles

To 10 mL aqueous $AgNO_3$ (1 mM) 0.1 M spermine hydrochloride was added (5 µL) and the mixture was degassed for 30 min under N_2 flow, protected from light. Subsequently, under vigorous stirring, 25 µL of aqueous $NaBH_4$ (0.1 M) was

quickly added to the solution and stirred for 20 min. Particle formation was immediately observed as the colour of the dispersion turned bright yellow. Formation of the particles was verified by UV-visible spectroscopy observing a typical plasmon resonance peak in the 390-400 nm wavelength range.

Following this preparation method, silver nanoparticles (AgNPs) stabilised with branched PEI (bPEI), spermidine, and ethylenedioxydiethylamine were prepared.

5.2.6 Poly-*L*-Lysine Stabilised AgNPs

Au-Ag core/shell nanoparticles of 45 nm diameter were prepared following the two-step particle seeded growth method.[150] Briefly, 40 µmoles of $AgNO_3$ were added to 125 mL of milli-Q water and heated to boiling, protected from light. Subsequently, 5 mL of gold nanoparticles (14 nm gold seeds) were added, followed by addition of 1% w/w aqueous trisodium citrate (22 µmol). The mixture was refluxed for 30 min under vigorous stirring. Subsequently, to further stabilize the particles, 5 mL of 1% w/w aqueous trisodium citrate was added and further refluxed for 1h. The particles were filtered through a 0.45 µm Millipore® filter and further centrifuged (500·g, 10 min) to remove any large aggregates before further functionalization with thioctic acid.

Citrate stabilised Au-Ag nanoparticles were further functionalized with thioctic acid in a ligand exchange reaction. Typically, to 10 mL nanoparticle dispersion, methanolic solution of thioctic acid (2.5 µL, 40 mM) was added and left stirring for 3 h protected from light. The excess ligand was removed by centrifugation (1073·g, 15 min) and re dispersion in milli-Q water.

The attachment of poly-*L*-lysine (PLL) was achieved by EDC/sulfo-NHS coupling reaction. Briefly, 600 µL of the nanoparticle dispersion was diluted in 10 mL of milli-Q water and 1.5 µL of an aqueous (*N*-(3-dimethylaminopropyl)-*N*'-ethylcarbodiimide hydrochloride) (EDC) 200 mM solution was added along with 50 mM aqueous *N*-hydroxysulfosuccinimide (sulfo-NHS) in 1:1 molar ratio and left for 30 min protected from light in order to activate the COOH functionality.

Subsequently the sample was divided into smaller aliquots and to each aliquot containing 0.8 mL of activated COOH 0.05% w/w aqeous solution of PLL was added (200 μL) and left overnight. Particles were then purified by centrifugation (2415·g, 20 min) and redispersed in milli-Q water.

5.2.7 Cetyltrimethylammonium bromide stabilised AgNPs

Cetyltrimethylammonium bromide (CTAB) stabilised silver nanoparticles (Ag-CTAB) were prepared according to literature reference.[151] Briefly, two solutions were prepared: A) 20 mL of an aqueous solution containing 2 mM $AgNO_3$, 0.4 M NH_4OH, 0.5 mM CTAB and B) 20 mL of an aqueous solution containing 8 mM $NaBH_4$ and 0.5 mM CTAB. The solutions A and B were then cooled for 10 min in an ice bath. Subsequently under vigorous stirring solution B was added dropwise to solution A in an ice bath. After 2 min the solution turned yellow indicating the formation of the Ag-CTAB nanoparticles and left stirring for further 3h protected from light. Subsequently the particle dispersion was brought to boil rapidly, refluxed for 10 min and then cooled to room temperature.

5.2.8 Silver citrate nanoparticles

All glassware was cleaned with aqua regia and thoroughly rinsed with distilled water. Ag-citrate nanoparticles were prepared according to the Lee & Meisel procedure.[70] A clean three necked round bottom flask was filled with 500 mL of Milli Q water. The solution was heated to 45 °C with a Bunsen burner under continuous stirring with a glass stirrer. Then silver nitrate (90 mg dissolved in 10 mL of Milli Q water) was added. The solution was heater further to 98 °C. Tri-sodium citrate (100 mg in 10 mL Milli Q waer) was added and the solution was kept at 98 °C for 90 min and afterwards allowed to cool to room temperature.

5.2.9 Characterisation of Ag-nanoparticles

5.2.9.1 Dynamic light scattering

The hydrodynamic radius of the nanoparticles were measured by DLS on a Malvern HPPS particle sizer. Fifteen replicate measurements were taken from

each sample and the average value reported. A standard sample consisting of commercially available Nanosphere™ Size Standards (Thermo Scientific Fremont CA.) 40 nm polymer microspheres in water were used as a standard before each set of measurements.

5.2.9.2 Scanning electron microscopy

For the particle sample depositions silicon wafers (Agar Scientific) were cleaned with methanol and oxygen plasma (Diener electronic femto oxygen plasma cleaner, 72 cm^3/min gas flow) to produce a negatively charged surface for better adhesion of the cationic particles. Imaging was carried out on a Sirion 200 Schottky field-emission electron microscope (FEI) operating at an accelerating voltage of 5 kV. Image analysis was carried out using Image J, v1.43u.

5.2.9.3 UV-Visible spectroscopy

UV-Vis spectroscopy was carried out on a Varian Cary 300 BIO spectrophotometer using 1 cm path quartz cells. Nanoparticle concentrations were calculated by Beers law using the extinction coefficient for silver nanoparticles (diameter of 30 nm) of $1.85 \cdot 10^{10}$ M^{-1} cm^{-1}, derived from literature.[106]

5.2.9.4 ζ-potential

The ζ (Zeta) potential measurements were carried out using a Malvern 2000 Zetasizer, using the default method protocol and a minimum sample volume of 3 mL. Before each measurement a standard solution of -63.0 ± 6.8 mV was measured.

5.2.10 Surface enhanced Raman scattering

Samples were prepared with 90 µL of the nanoparticles and 10 µL of the DNA solution in water, these samples were prepared in triplicate in PMMA micro-cuvettes and analysed using an Avalon probe system Ramanstation R3 optical fibre with a 532 nm diode laser excitation with approximately 24 mW laser power at the sample. Typical integration times were 1 second and 3

accumulations. Data analysis was carried out using the xanthene ring C-C stretch[110, 111] of the fluorescent dye 5-carboxyfluorescein (5-FAM) at 1632 cm^{-1} in the spectrum.

5.2.11 Preparation of double stranded DNA

Double stranded DNA was made by adding 5 µL of FAM labelled DNA (400 nM) to 5 µL of its complementary DNA (400 nM) in 10 µL PBS (140 mM sodium chloride, 5.11 mM potassium, 8.1 mM Na_2HPO_4,and 1.47 mM KH_2PO_4 pH 7.4) and in case of single stranded DNA 5 µL water was used. These samples were hybridised in a thermo-cycler (Agilent Stratagene MX3005P) by 95°C for 5 min and cooling to room temperature by 2 degrees per second. Afterwards these samples were transferred to PMMA microcuvettes and 180 µL of Ag-spermine nanoparticles was added followed by SERS analysis.

5.2.12 Laser intensity measurements

The laser intensity measurements were carried out using a Thorlabs PM100D laser intensity meter equipped with a Thorlabs S130C sensor. The laser intensity at the sample was ~ 24 mW.

5.3 Results and discussion

Firstly, silver nanoparticles reported in literature as well as novel positively charged silver nanoparticles were prepared. This was followed by characterisation of the nanoparticles. Then detection of DNA was carried out to investigate the SERS performance of the different types of nanoparticles, and finally detection of ds and ssDNA detection to determine the discrimination between double and single stranded DNA with the optimised Ag-positive particles.

5.3.1 Nanoparticles synthesis

Preparation of stable positively charged silver nanoparticles using cationic ligands as the stabilising molecules, which prevents interparticle aggregation via electrostatic repulsion producing a stable colloid in aqueous solution was carried out. This allows the creation of a ligand shell with an overall positive surface charge. The following nanoparticles were prepared according to the different procedures reported in the experimental section; Ag-CTAB, Ag-bPEI, Ag-PLL, Ag-spermine, Ag-spermidine, and Ag-ethylenedioxydiethylamine.

These particles bring several advantages. Firstly, by anchoring cationic ligands onto the particle surface, the negatively charged analyte adsorbs onto the nanoparticle surface *via* controlled electrostatic interaction through charged secondary amine moieties readily available on the particle surface with either the phosphate backbone and/or DNA bases.[152, 153] Secondly, the addition of aggregation agents is no longer needed in order to obtain SERS signals. The DNA induces nanoparticle aggregation allowing straightforward DNA detection by SERS. In this way reducing the number of variables and aggregation dynamics are more controlled, rendering these particles very attractive for quantitative DNA analysis by SERS. Thirdly, as DNA sequences are positioned in the interparticle hot spots and close to the nanoparticle surface, high SERS sensing performance, in terms of sensitivity, is efficiently provided.

5.3.2 Silver nanoparticle characterisation

Characterisation of the different types of silver nanoparticles was carried out by dynamic light scattering (DLS) for determination of the hydrodynamic radius of the nanoparticles, scanning electron microscopy (SEM) to determine the average nanoparticle core size, UV-Vis spectroscopy to determine the concentration of the nanoparticles, and **ζ** potential measurements to determine the nanoparticle surface charge. Finally the SERS background of the nanoparticles was investigated.

5.3.2.1 Determination of the hydrodynamic radius of the nanoparticles

The hydrodynamic radius of the nanoparticles was obtained with dynamic light scattering (DLS) measurements. In Table 5.2 positively charged silver nanoparticles found in the literature, as well as novel silver nanoparticles stabilised with similar length ligands; spermine, spermidine, ethylenedioxydiethylamine. All hydrodynamic diameters were between 45 and 77 nm.

Table 5.2 Hydrodynamic radius of the silver nanoparticles used.

	Mean Count Rate $kcps^{-1}$	**Peak $d.nm^{-1}$**
Ag-citrate	231.1	63
Ag-bPEI	440.7	75.7
Ag-CTAB	153	76.3
Ag-PLL	368	54.5
Ag-ethylenedioxydiethylamine	338.5	45.1
Ag-spermidine	386.3	47.4
Ag-spermine	209.7	55.4

5.3.2.2 Scanning electron microscopy

Figure 5.2 shows SEM images of positively charged silver nanoparticles (Ag-spermine and Ag-bPEI). According to the SEM images these nanoparticles possess the same spherical morphology.

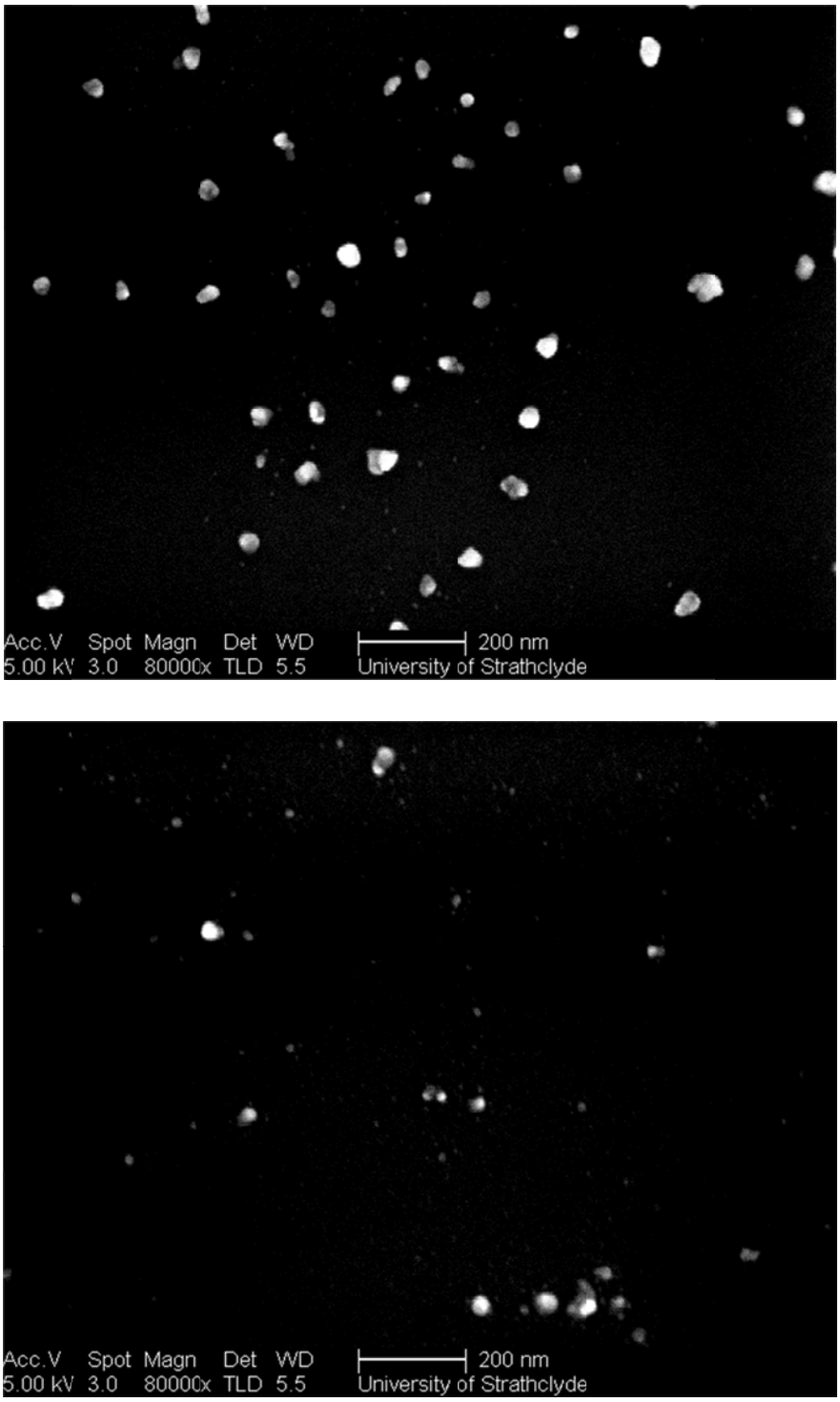

Figure 5.2 SEM image of Spermine coated silver nanoparticles (top), and bPEI coated nanoparticles (bottom).

Silver nanoparticles with a diameter of 26.8 ± 6.0 nm (n=225) were prepared via a sodium borohydride reduction in aqueous solution using spermine hydrochloride as a stabilising ligand molecule (Figure 5.3).

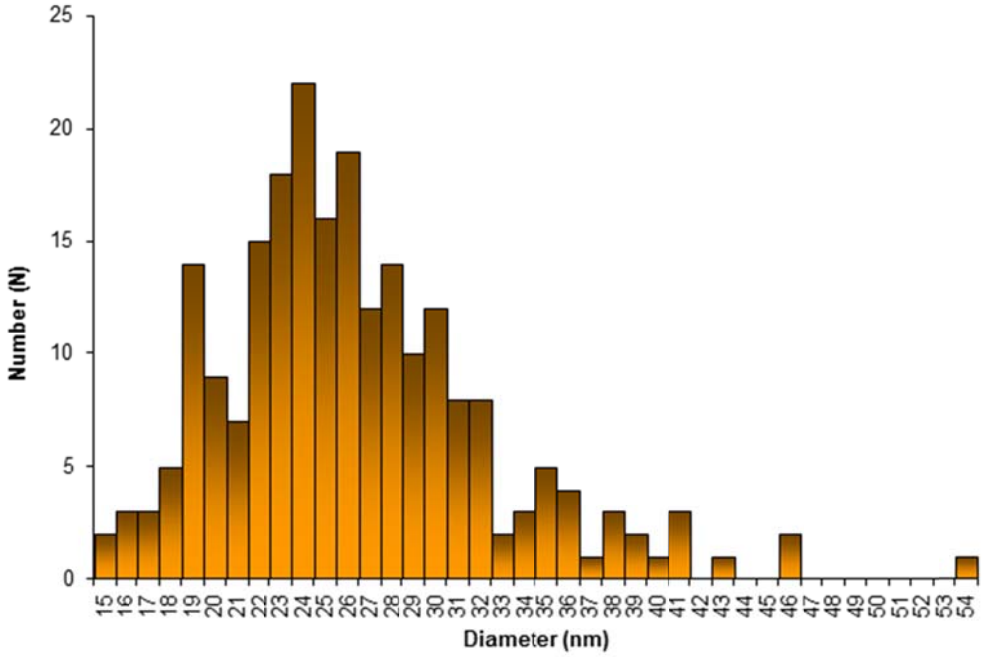

Figure 5.3 Ag-spermine nanoparticle distribution determined by SEM (N=225). The average size was 26.8 ± 6 nm (1 standard deviation).

The nanoparticle diameter determined by SEM was approximately half the size of the hydrodynamic diameter determined by DLS measurements. Differences in size between SEM and DLS measurements can be explained, SEM measures the size of the metal core, and with DLS the hydrodynamic radius including the ligand shell is measured, and larger particles have a greater scattering contribution compared to smaller particles in the DLS measurement.

5.3.2.3 UV-Visible

UV-Vis spectra obtained from silver nanoparticles are presented in Figure 5.4. The λ_{max} values for all nanoparticles were very similar and between 394 and 405 nm, except for Ag-PLL which had a λ_{max} of 420 nm which indicates most nanoparticles were similar in size of about 30 nm.

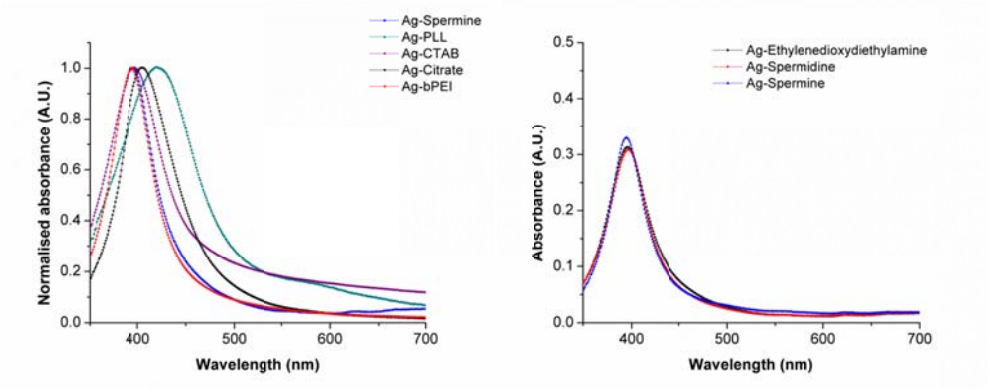

Figure 5.4 UV-Vis traces of silver nanoparticles coated with different ligands (left). The obtained λ max value for Ag-spermine was 395 nm, for Ag-PLL λ max was 420 nm, for Ag-CTAB λ max was 397 nm, for Ag-Citrate λ max was 405 nm, and for Ag-bPEI λ max was 394 nm. UV-Vis spectra obtained from the similar length ligand silver nanoparticles are presented (right). Samples were ten times diluted in water prior to analysis. The observed λ max value for Ag-Ethylenedioxydiethylamine was 395 nm, for Ag-Spermidine λ max was 397 nm, for Ag-spermine λ max was 395 nm.

Finally each of the different types of nanoparticles were brought to similar concentrations by adjusting the optical density (OD), nanoparticles had similar sizes (ESI), providing nanoparticle concentrations of ~190 pM. However, we are comparing different systems where the nanoparticle sizes are different (25-45 nm) as well as several other variables that cannot be carefully controlled (surface chemistry, aggregation dynamics, interparticle distances at the generated hot-spots). Therefore it was decided to carry out the experiment using a fixed excitation wavelength and nanoparticle concentration. Since Ag-spermine belongs to the group of the smallest nanoparticles (Figure 5.4) of the nanoparticles investigated, by fixing the nanoparticle concentration we chose a rather conservative approach to evaluate their sensing ability as compared to bigger nanoparticles (i.e. the metal surface available in the Ag-spermine samples is lower than that for bigger particles). These ligands vary with respect to their internal chemistry and overall charge, however the λ_{max} of the functionalised nanoparticles determined by UV-Vis and the size of these nanoparticles as determined by DLS was found to be very similar.

5.3.2.4 ζ-potential

The surface charge of the nanoparticles was determined with ζ potential measurements, the obtained results are shown in .

Table 5.3.

Table 5.3 ζ potential measurements

Nanoparticles	Zeta (mV)	Error ±
Ag-Citrate	-37.7	± 2.0
Ag-bPEI	+42.0	± 7.04
Ag-CTAB	+18.0	± 1.9
Ag-PLL	+37.0	± 0.8
Ag-ethylenedioxydiethylamine	+42.4	± 11.4
Ag-spermidine	+44.2	± 13.3
Ag-spermine	+46.7	± 7.97

All particles prepared had a surface charge of at least + 35 mV which means the colloidal solution is stable, an exception were the Ag-CTAB nanoparticles that had a surface charge of + 18 mV which means these particles were less stable. The negatively charged Ag-Citrate nanoparticles had a surface charge of – 35 mV which also means these particles were a stable colloid.

5.3.2.5 Polymer coating leakage test by SERS

Importantly, nanoparticle synthesis was performed in glass vials that were pre-coated with a positively charged polymer (bPEI) to prevent binding of the positive nanoparticles to the normally negatively charged glass walls.

A leakage test was carried out to determine the carryover of PEI coating polymer to the nanoparticles synthesised in the glass by SERS. Glass vials coated with bPEI were tested for leakage by analysing the washing and comparing it to a reference sample containing bPEI. Significant SERS signals were obtained from the

reference bPEI sample and no bPEI peaks were obtained from the washing sample (Figure 5.5) indicating stable coating of the glass vials.

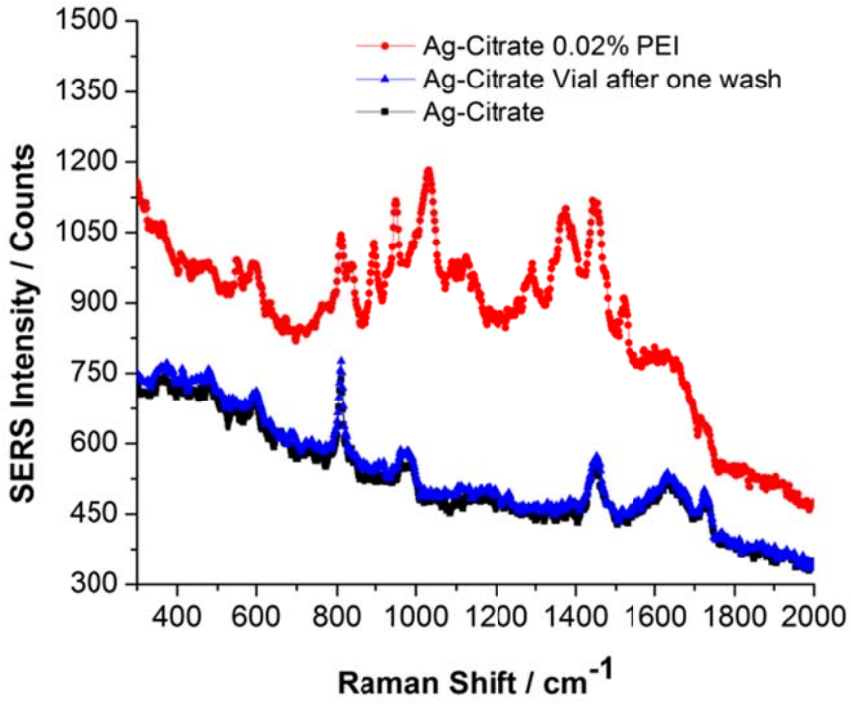

Figure 5.5 Investigation of bPEI leakage from the vial by SERS. A 532 nm laser excitation of approximately 24 mW at the sample was used (three accumulations of 1 second).

5.3.2.6 Nanoparticle SERS background

The background SERS signal of the positively charged silver nanoparticles was determined. These results show that there was little background for most types of nanoparticles, except for Ag-bPEI which possessed a strong background signal between Raman shift 800 and 1700 cm^{-1} of approximately 2000 counts (Figure 5.6), rendering sensitive detection of multiple analytes simultaneously more difficult.

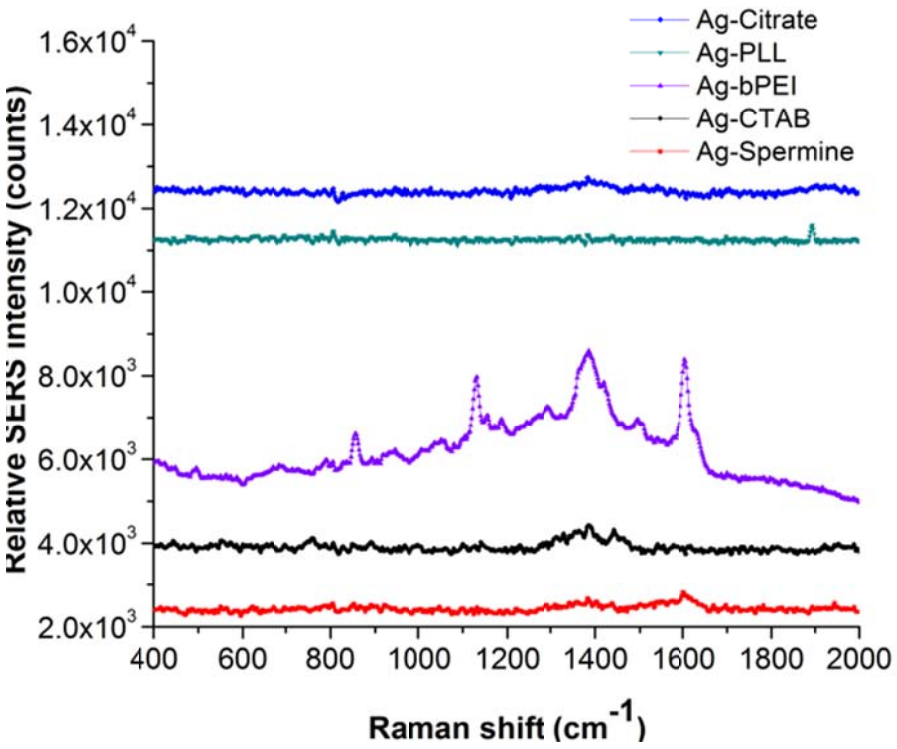

Figure 5.6 SERS background of the different types of positively charged silver nanoparticles. SERS measurements were three accumulations for 10 s using a 532 nm laser excitation of approximately 24 mW at the sample. The spermine coated nanoparticles showed as little background as the poly-*L*-lysine stabilised nanoparticles, the bPEI stabilised nanoparticles showed higher background possibly due to partial aggregation.

A SERS spectrum was taken of aggregated and un-aggregated Ag-spermine particles to obtain the background signal of Ag-spermine nanoparticles (Figure 5.7). There was little background for Ag-spermine nanoparticles when compared to the PMMA cuvette and water control sample, however upon aggregation with PBS a strong bump appeared within the Raman shift region of 1000 - 1800 cm^{-1} with a peak height of approximately 1000 counts.

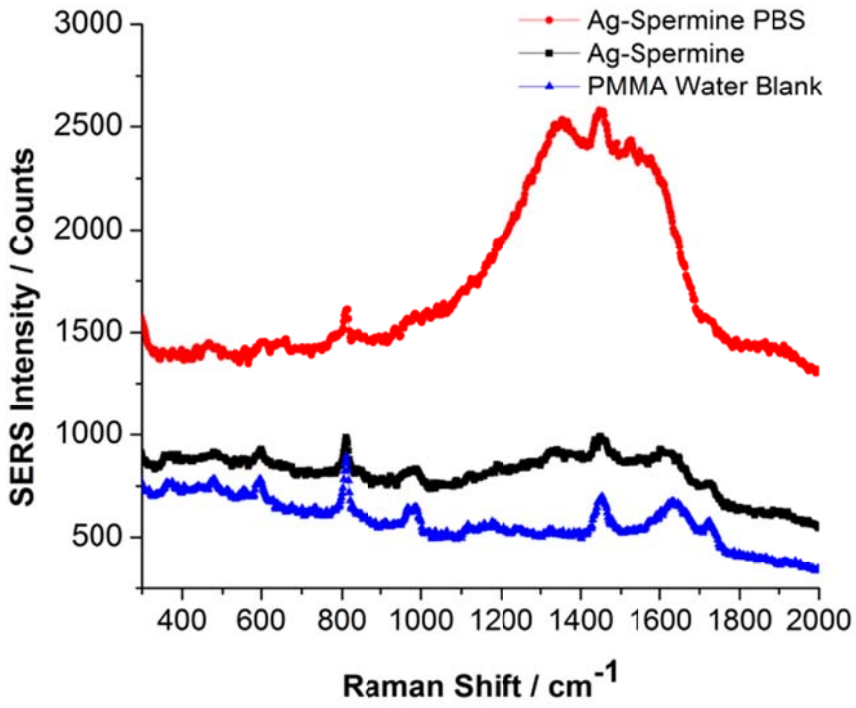

Figure 5.7 Investigation of background signal from Ag-spermine nanoparticles un-aggregated and aggregated. A 532 nm laser excitation of approximately 24 mW at the sample and three accumulations of 1 second was used.

5.3.3 SERS sensing performance

The SERS sensing performance of spermine stabilised nanoparticles was compared to other silver nanoparticles stabilised with poly-*L*-lysine, CTAB, citrate and branched PEI. As a Raman reporter, 5-carboxyfluorescein covalently attached to a 25-*mer* DNA sequence was utilised (Figure 5.8).

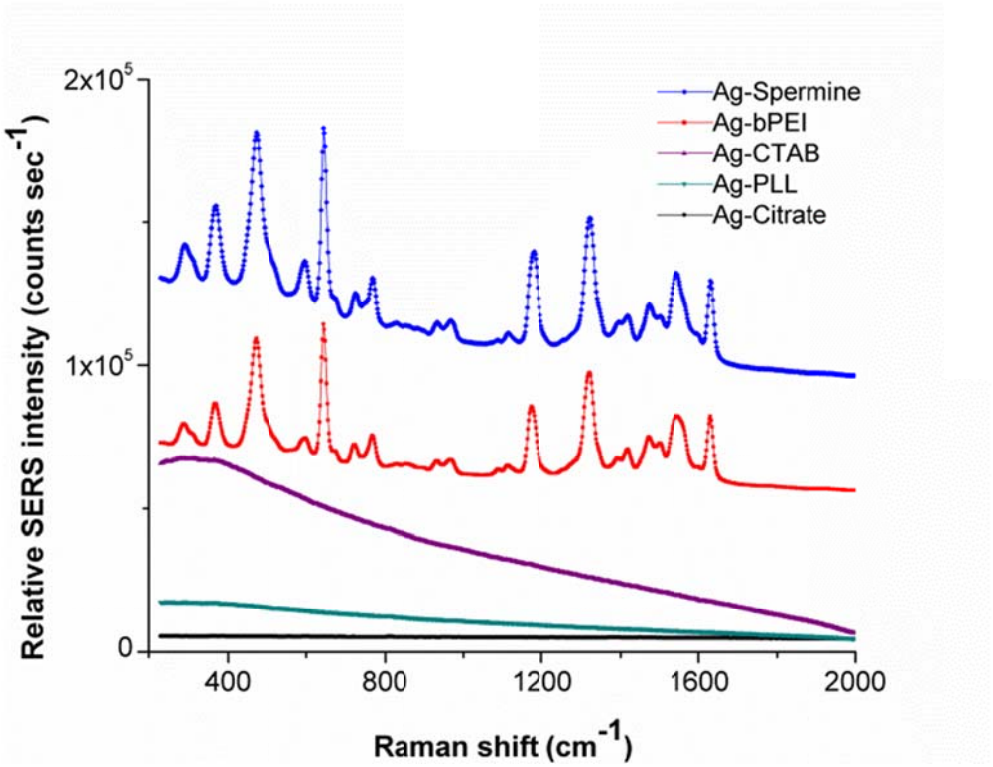

Figure 5.8 SERS spectra obtained from 10 nM FAM labelled DNA. Spectra are off set. Silver nanoparticles with spermine (blue), PLL (cyan), CTAB (purple), negative citrate particles (black), and branched PEI (red). A 532 nm laser excitation of approximately 24 mW at the sample and three accumulations of 1 second was used.

The spermine stabilised nanoparticles offered highest performance, in terms of SERS sensitivity (Figure 5.8). For CTAB coated nanoparticles, signal could only be obtained when the nanoparticles were diluted. This indicates that the SERS signal appearance was a result of the CTAB molecules displacement from the particle surface leading to a high degree of uncontrolled particle aggregation.[145] Otherwise when the CTAB layer was intact, a surface enhanced fluorescence (SEF) background was obtained with an approximate factor of 350 times (Figure 5.9).

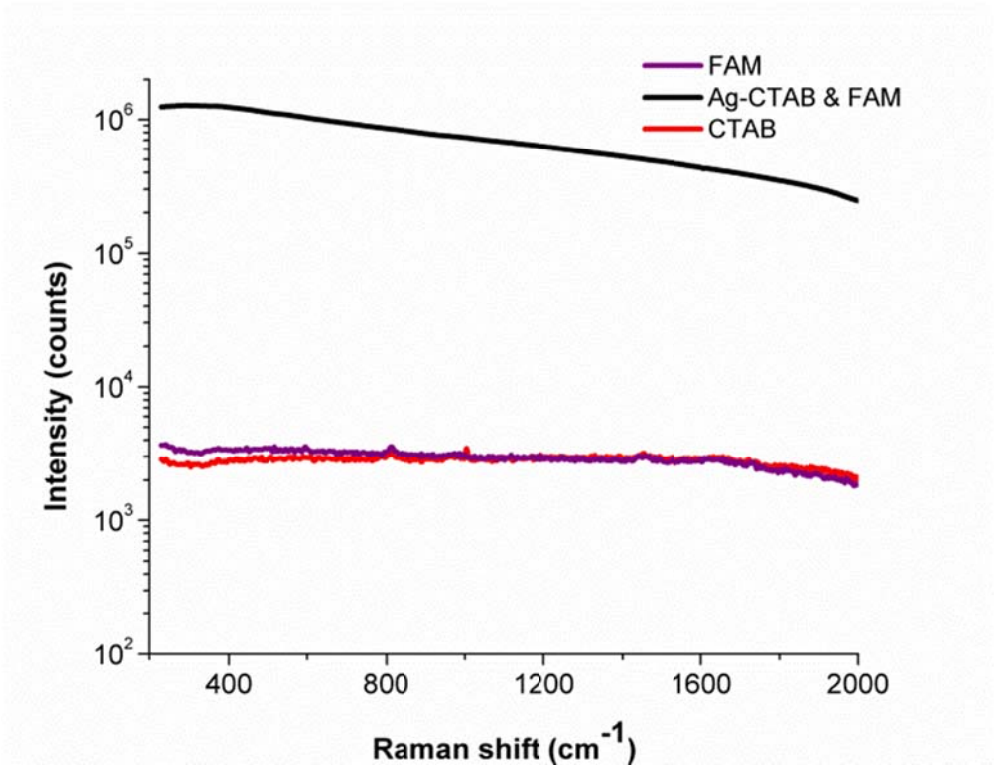

Figure 5.9 SEF of FAM on Ag-CTAB nanoparticles (black line), FAM fluorescence (purple line), Ag-CTAB signal (red line). A 532 nm laser excitation of approximately 24 mW at the sample and three accumulations of 1 second was used.

Detection of dye labelled DNA at 10 nM was not achieved with PLL-coated nanoparticles, while PEI functionalised surfaces allowed the detection of the target analyte, although with SERS signal approximately three times less intense after 30 min than those reported for the spermine functionalised nanoparticles (Figure 5.10).

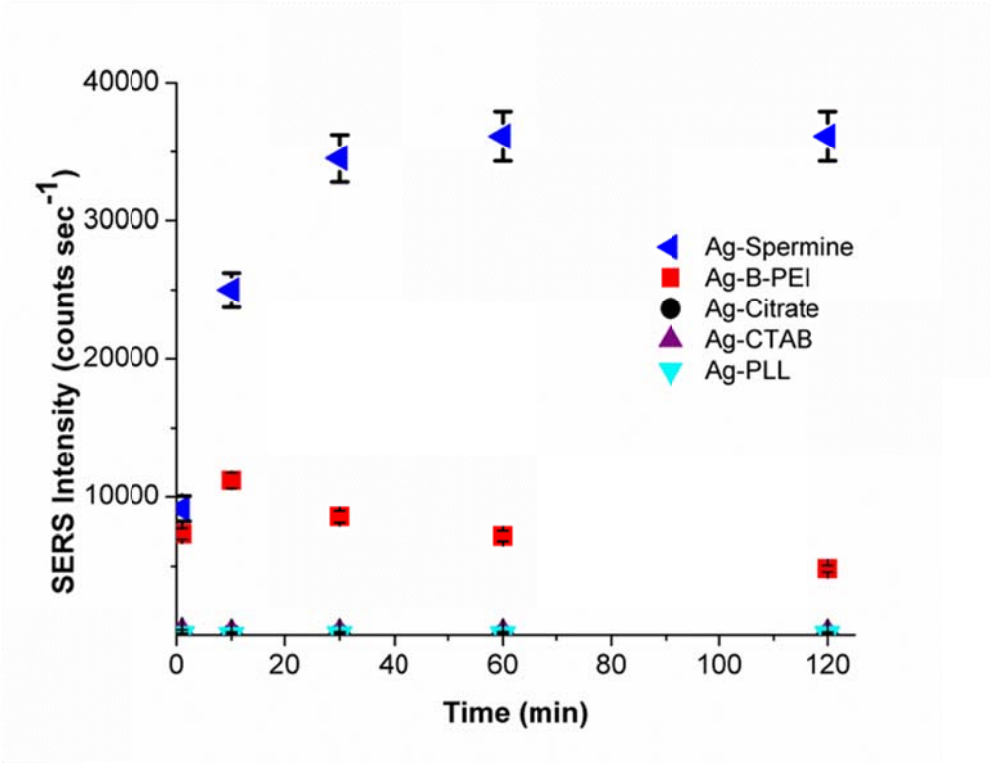

Figure 5.10 SERS signal stability over a time period of 120 min. Silver nanoparticles with branched PEI (red squares), negative citrate particles (black circles), CTAB (purple upwards pointed triangle), PLL (cyan downwards pointed triangle), and spermine (blue leftwards pointed triangle). Error bars represent ± one standard deviation. A 532 nm laser excitation of approximately 24 mW at the sample and three accumulations of 1 second was used. Error bars represent ± one standard deviation of three separate samples.

We suggest that the use of branched polyamines and surfactants as nanoparticle coatings induces larger distances between the adsorbed analyte and the metal surface, leading to significantly lower enhancements of the dye signal. The lowest observable concentration of dye labelled DNA in the case of spermine-stabilised nanoparticles was 1 nM. In addition spermine stabilised nanoparticles produced a lower background signal when compared to branched PEI-stabilised nanoparticles (Figure 5.6).

The stability of the samples was measured over a time period of 120 min (Figure 5.10) confirming the higher stability of Ag-spermine stabilised particles over

longer periods of time. This makes spermine stabilised particles attractive for analysis within an automated system.

Additionally the effect of the ligand charge on the SERS peak intensity using three similar length ligands was investigated. The chemical structure of the similar length ligands for SERS experiments; spermine, spermidine, and ethylenedioxydiethylamine are shown in Figure 5.11 these ligands differ with respect to their positive charge, 4+, 3+ and 2+ respectively.

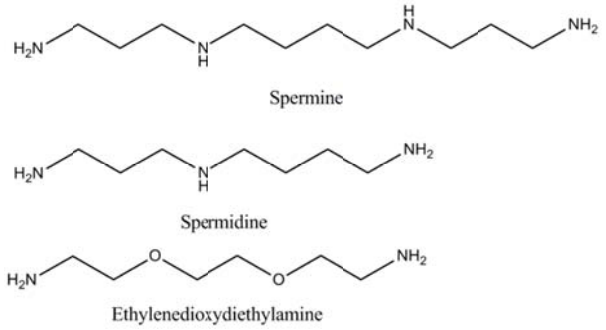

Figure 5.11 Chemical structures of the ligands used for nanoparticle stabilisation.

Ligand charge was found to be directly proportional to the observed SERS peak intensity of the dye labelled DNA, with more positive charge on the ligand providing more intense SERS signals (Figure 5.12).

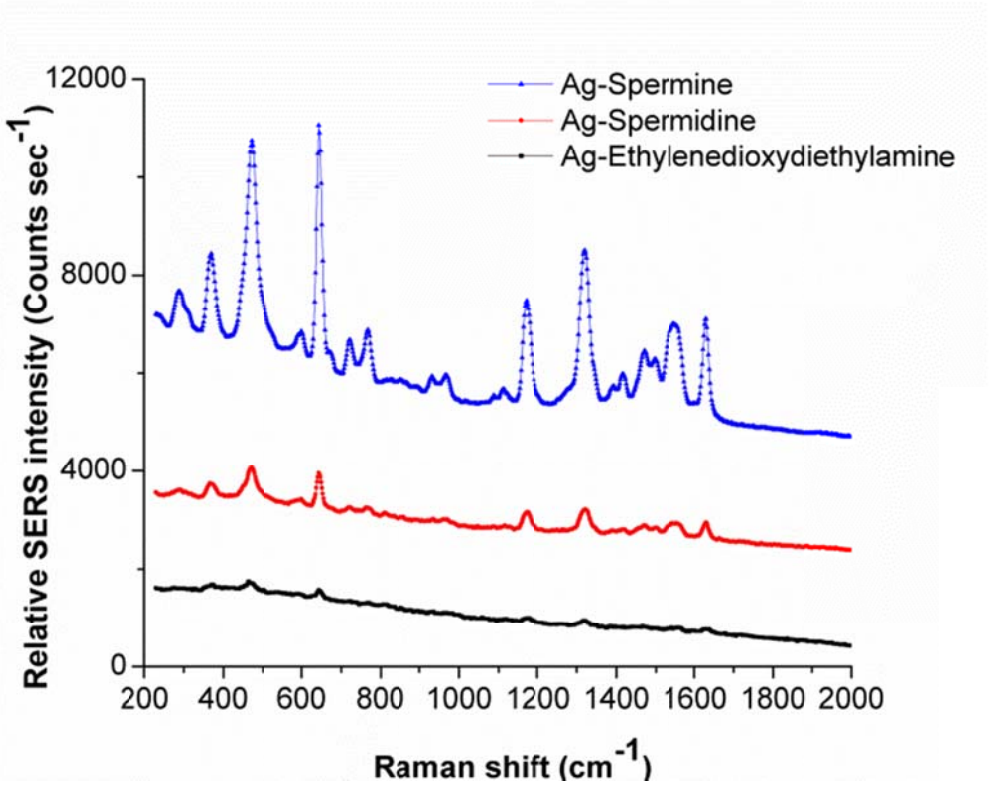

Figure 5.12 Off set relative SERS signal intensity of 1 nM FAM labelled DNA, using silver nanoparticles with Ethylenedioxydiethylamine (black), Spermidine (red), or Spermine (blue) ligands.

The affinity of the spermine for the interaction with single stranded DNA resulted in highly effective SERS active silver nanoparticles. These data are in agreement with previous studies reporting the greatest SERS enhancements of dye labelled DNA using spermine.[139, 154] These results showed that the Ag-spermine nanoparticles were the most sensitive positively charged silver nanoparticles used within this study.

Aggregation caused by adsorption of dye-labelled ssDNA onto the silver nanoparticles was analysed colourimetrically. Different concentrations of ssDNA were added (ranging from 0.05 to 10 nM) to 33 pM silver colloidal dispersions.[106] Addition of ssDNA caused aggregation of the nanoparticles evidenced by colour change and a decrease in absorbance at 395 nm and an increase in absorbance at 550 nm (Figure 5.13).

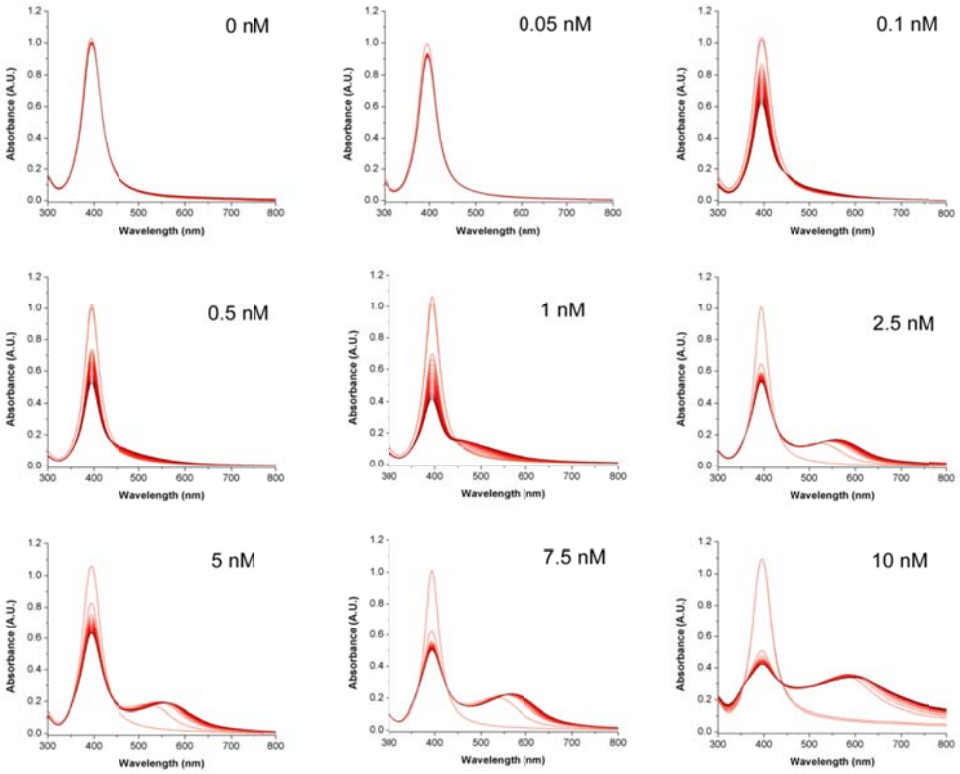

Figure 5.13 The surface plasmon red shift of the Ag-spermine nanoparticles after addition of DNA in the concentration range of 0-10 nM (from left to right and from top to bottom) was measured every 10 min over a time period of 120 min. Samples contained 40 µL of Ag-spermine nanoparticles, 320 µL water, and 40 µL of DNA solution.

These results confirmed the stable aggregation state of the nanoparticles over a time period of 120 min.

The hydrodynamic radius of the Ag- Spermine nanoparticle after addition of DNA was measured over time (Figure 5.14).

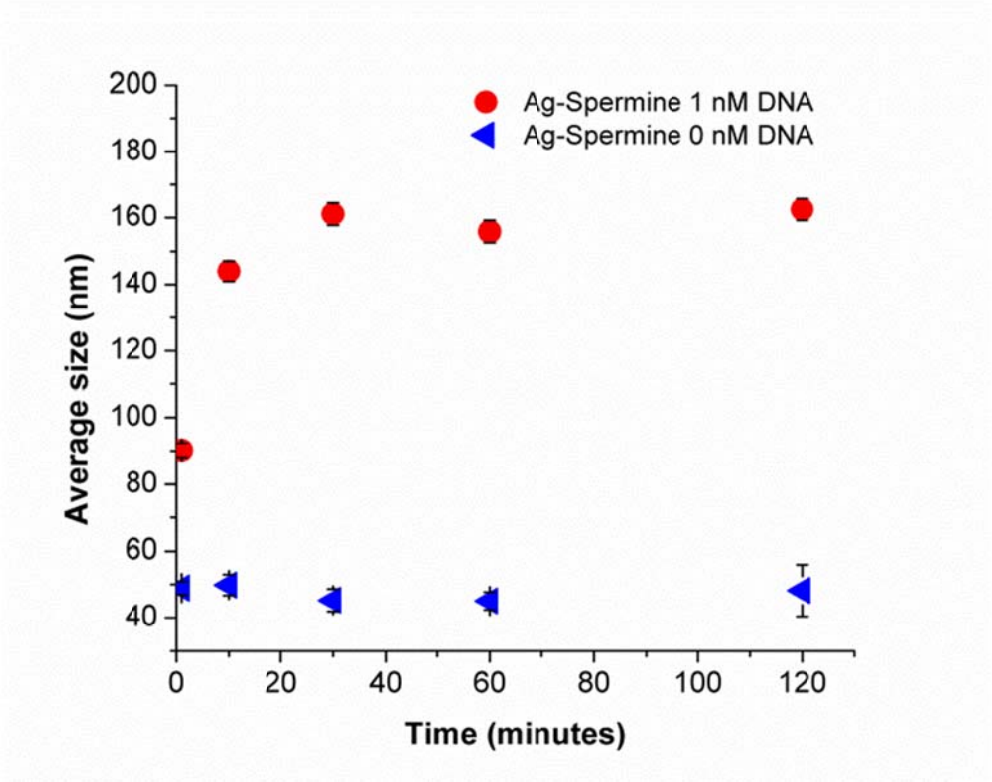

Figure 5.14 Average nanoparticle size without (red circles) and with (blue triangles) 1 nM DNA present in the sample measured over a time period of 120 min. Samples contained 120 µL of Ag-spermine nanoparticles, 960 µL water, and 120 µL of 10 nM DNA solution or water in case of the control sample. Error bars represent ± one standard deviation of three measurements.

The Ag-spermine nanoparticle size without (red circles) and with (blue triangles) 1 nM DNA present in the sample measured over a time period of 120 min. The average Ag-spermine nanoparticle size increased after the addition of DNA and reached the plateau phase after 30 min which corresponds to the presented UV-Vis and SERS data.

The negative charge of the dye (FAM) had limited contribution to the DNA adsorption, because DNA labelled with a positive dye (Cy5) could easily be detected (Figure 5.15).[155, 156]

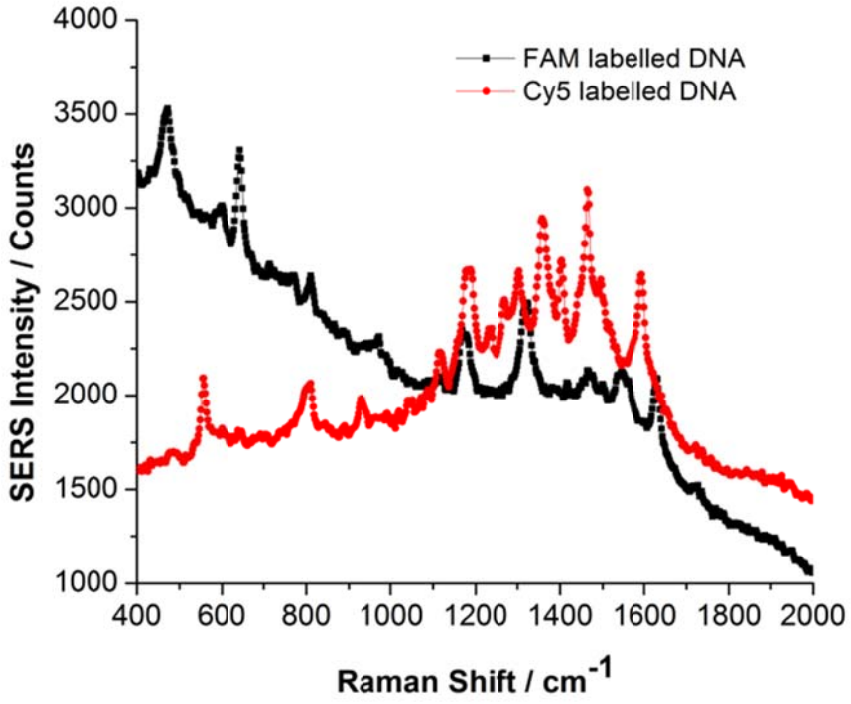

Figure 5.15 Detection of positively charged dye (Cy5) labelled DNA and negatively charged dye (5'FAM) labelled DNA by SERS. A 532 nm laser excitation of approximately 24 mW at the sample and three accumulations of 1 second was used.

5.3.4 Double stranded DNA detection

Ag-spermine nanoparticles possessed the most intense SERS spectra and were applied to double stranded and single stranded DNA detection. Detection of double and single stranded DNA was compared and intensities were found to be very similar (Figure 5.16).

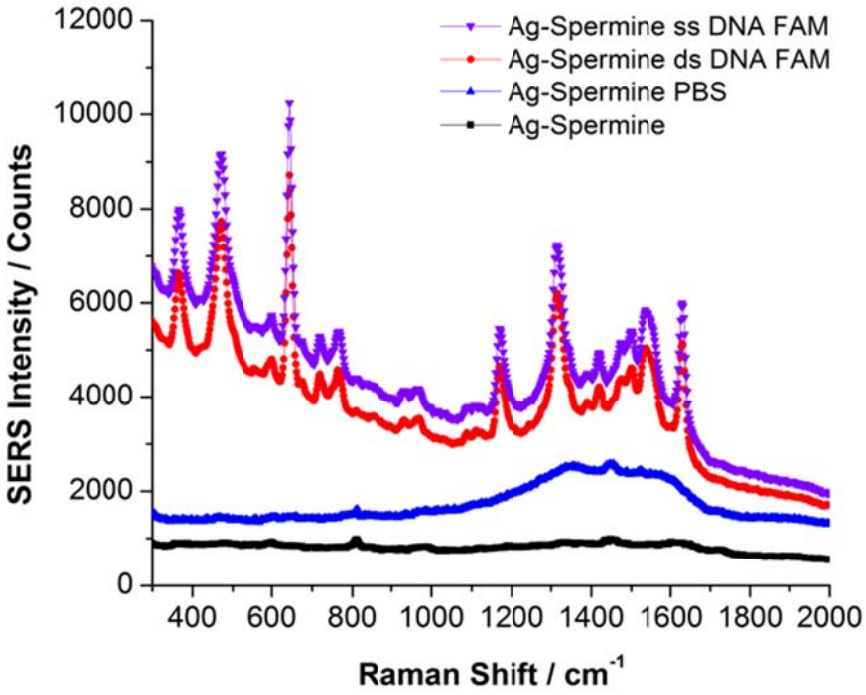

Figure 5.16 Detection of dye labelled double and single stranded DNA. A 532 nm laser excitation of approximately 24 mW at the sample was used (three accumulations of 1 second).

A scanning kinetics SERS experiment measuring FAM labelled double and single stranded DNA over time showed similar SERS intensities for double and single stranded DNA with overall slightly higher intensities for double stranded DNA.

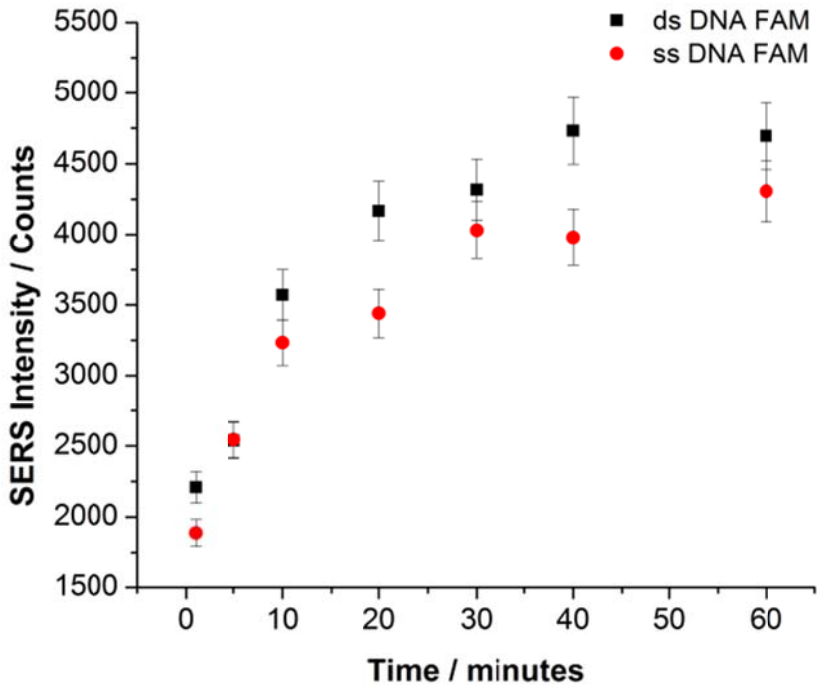

Figure 5.17 SERS intensity of the FAM 1632 cm^{-1} peak measured over time for double and single stranded DNA. A 532 nm laser excitation of approximately 24 mW at the sample was used (three accumulations of 1 second). Error bars represent ± one standard deviation of three separate samples.

The discrimination between ds and ssDNA with the Ag-spermine nanoparticles was found to be 1.2 in the best cases, and thereby less than the in Chapter two and three presented assays with the negatively charged silver nanoparticles which had a ss / dsDNA ratio off at least 2.

5.4 Conclusions

In conclusion, spermine stabilised silver particles with a positive surface charge are particularly suitable as platforms for detection of dye labelled DNA with surface enhanced Raman scattering. Ag-spermine particles for the direct detection of negatively charged 5-carboxyfluorescein labelled DNA, and compared them to other positively charged nanoparticles found in the literature. Introduction of the analyte to the Ag-spermine nanoparticles resulted in their aggregation giving rise to intense and stable SERS spectra for up to at least 120 min. Addition of aggregating agents or diluents were not required significantly simplifying quantitative SERS analysis. In addition the Ag-spermine nanoparticles showed a limited background signal, which is of particular importance for sensitive analysis of multiple analytes in solution. The affinity of the spermine functionalised particles for ssDNA was found to be greater than ligands of similar length with lower charge.

When comparing the SERS intensities of dye labelled ds and ssDNA slightly higher intensities were found for dsDNA, however the discrimination between ds and ssDNA with the Ag-spermine nanoparticles was found to be less when compared to the negatively charged nanoparticles presented in Chapter two and three. Therefore negatively charged nanoparticles are thus far the preferred nanoparticles for DNA detection assays exploiting the discrimination between ds and ssDNA.

6 CONCLUSIONS

From Chapter 2 SERS primers we can conclude that SERS primers can used to specifically detect DNA sequences with or without the use of the PCR.

A new positive SERS assay that can discriminate between target and no target DNA in a homogenous sample without additional separation steps was developed. Starting from a bacterial culture, DNA was isolated, a specially designed primer was incorporated into the PCR products and the presence or lack of target was identified within two hours. The high multiplexing capabilities of SERS make this a very promising approach for future DNA analysis. This method has the potential for single molecule detection of nucleic acid targets in a positive manner when SERS is combined with PCR and this is the first step towards a highly competitive SERS based molecular diagnostic assay.

In Chapter 3 The mode of action of SERS primers and probes we concluded that the use of the SERS primers as internal probes being digested by the 5' → 3' exonuclease activity of the DNA polymerase leads to higher reproducibility.

Important factors for the performance of the positive SERS primer and probe assays were investigated utilizing a synthetic model. The demonstration and evaluation of four novel separation free SERS assays for the specific detection of pathogen DNA has been carried out. These assays prove that SERS is a reliable and competitive technique to fluorescence for direct target DNA detection with or without the use of PCR. The use of partly self-complementary uni-molecular oligonucleotide sequences for the SERS primer significantly increased the contrast between positive and negative samples within the synthetic assay. The results have shown that a SERS primer or probe to target ratio of 0.5 could be detected and when increasing the target to probe ratio significantly higher SERS signals were obtained for all SERS probe models. For the detection of PCR products it was best to use the internal SERS probe digestion assay because with

this assay no false negative results were obtained. A significant cost reduction was achieved when using bi-molecular SERS primers and probes coupled to the PCR without any compromises towards sensitivity or selectivity.

In Chapter 4 it was shown that multiplexed pathogen detection using SERS primers seems to be feasible according to the cross reaction analysis. A selection of dyes for multiplex pathogen detection was made. Assay designs for the SERS primer digestion, and the SERS primer extension assay were made successfully, followed by cross reaction analysis of the oligonucleotides required for the multiplex detection. The results indicate that it is feasible to perform a multiplex detection using both types of assays. However it was decided to postpone the final multiplex detection part of the project and investigate assay systems that require less complex designs.

In Chapter 5 spermine stabilised silver particles with a positive surface charge are particularly suitable as platforms for detection of dye labelled DNA with surface enhanced Raman scattering. Herein we have used these particles for the direct detection of negatively charged 5-carboxyfluorescein labelled DNA, and compared them to other positively charged nanoparticles found in the literature. Introduction of the analyte to the Ag-spermine nanoparticles resulted in their aggregation giving rise to intense and stable SERS spectra for up to 120 min. Addition of aggregating agents or diluents were not required significantly simplifying quantitative SERS analysis. In addition the Ag-spermine nanoparticles showed a limited background signal, which is of particular importance for sensitive analysis of multiple analytes in solution. The affinity of the spermine functionalised particles for ssDNA was found to be greater than ligands of similar length with lower charge. These particles may even be useful for detection of unlabelled DNA obtaining the Raman specific bands of the DNA bases.

Due to their ease of preparation and herein described advantages, these particles might find widespread use in the detection of other negatively charged analytes, improving sensitivity and allowing direct SERS analysis, circumventing

the need for additional aggregating agents, and this providing extended sample stability over the conventional SERS methods.

Overall conclusions, to make best use of the SERS multiplex capabilities for DNA detection, it is important to develop an assay method that is sensitive towards the analytes, has low risk of sample contamination, and multiplex capabilities are not limited by other factors in the assay method. A closed tube real time PCR SERS project could be a method that is closed tube, with PCR-based sensitivity and offers fully quantitative SERS multiplex capabilities. The ultimate goal of closed tube PCR less detection of biomolecules requires further work, on the sensitivity of the assays.

7 FURTHER WORK

The SERS primers incorporated into PCR product and when used as an internal digestion probe in the PCR, perform as expected. However discrimination between positive and negative samples obtained was 4:1 in the best cases, therefore optimisations and new investigations into the discrimination might improve overall assay performances. When using the SERS primers as internal probes an extra level of specificity was created, therefore universal primers can be used to minimize the number of oligonucleotide sequences needed to detect multiple targets. The latter method was not investigated in this study but is considered for further work. Additionally, the multiplexed pathogen detection using the SERS primer assays should be performed.

Cationic nanoparticles have been successful for the detection of ssDNA and dsDNA by SERS. However little SERS signal intensity difference was observed between ds and ssDNA when compared to the assay system using negatively charged silver nanoparticles. Therefore a further investigation of the spermine and DNA interaction needs to be performed to investigate sequence dependencies. Finally an investigation of the possibilities of label free detection using these particles might be a very interesting opportunity.

In future, a closed tube real time PCR SERS project could be a method that is closed tube, with PCR-based sensitivity and offers fully quantitative SERS multiplex capabilities.

A schematic representation of a proposed assay to make a real time PCR SERS assay is demonstrated together with the detection system in Figure 7.1. This assay consists of the Plexor PCR assay introduced in the introduction modified onto nanoparticles to create a SERS active complex upon DNA amplification. Primer sequences were bound to silver nanoparticles and upon extension of the

primers a Dabcyl labelled iso dGTP nucleotide is brought in close proximity to the silver nanoparticle surface. This event creates a SERS active complex which is directly proportional to the amount of DNA amplified, resulting in a fully quantitative and closed tube real time Plexor SERS assay. The setup for real time PCR SERS detection combining a Raman spectrometer and a thermo cycler PCR instrument was created.

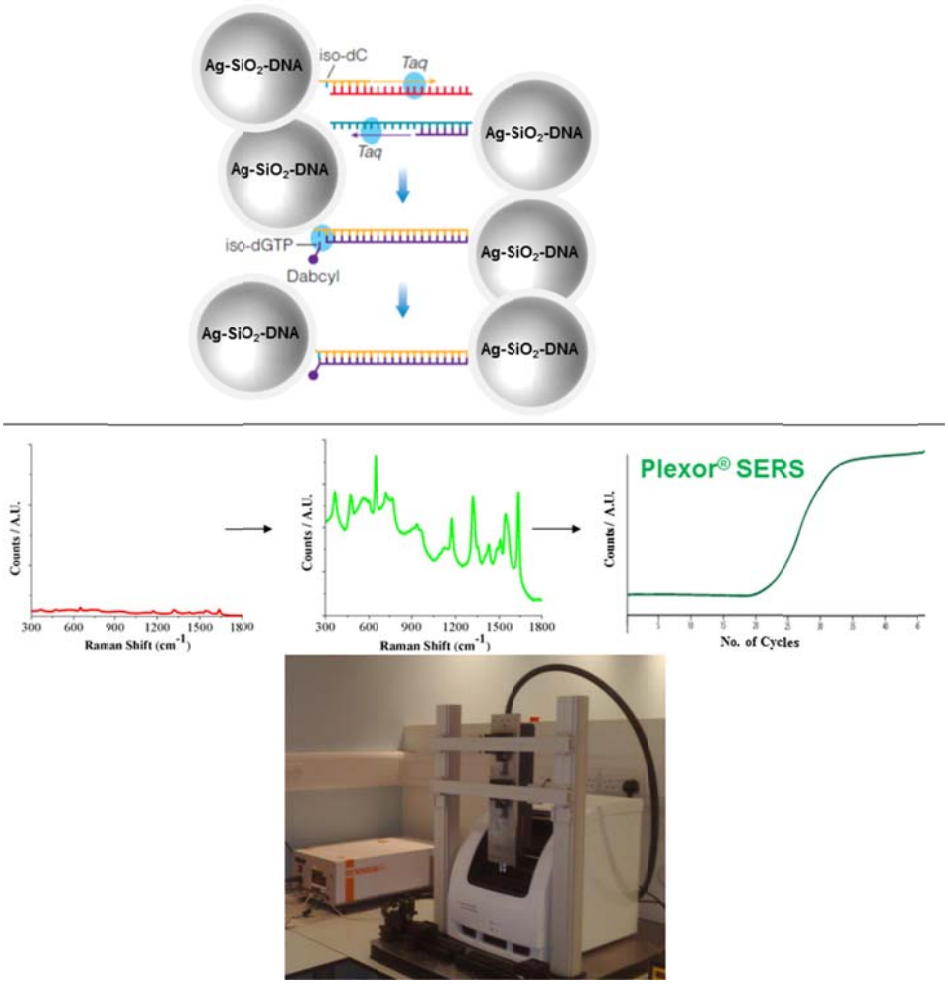

Figure 7.1 Top: A schematic representation of the proposed Plexor based real time detection of DNA amplification by SERS. Primer sequences are bound to silver nanoparticles and upon extension of the primers a Dabcyl labelled iso dGTP nucleotide is brought in close proximity to the silver nanoparticle surface. This event creates a SERS active complex which is directly proportional to the amount of DNA amplified, resulting in a fully quantitative and closed tube real time Plexor SERS assay. Bottom: Picture of the setup for real time PCR SERS detection where a Raman spectrometer was coupled to a thermo cycler PCR instrument.

Initial experiments on the PlexSERS assay were not successful possibly due to multiple reasons including non-optimised functionalised nanoparticles, and SERS conditions. In further work, focus on the nanofabrication while continuously monitoring the effects on SERS is advised.

Alternatively detection of pathogens without target amplification remains interesting, this approach would reduce the risk of contamination and the time to result. The ultimate goal of closed tube PCR less detection of biomolecules requires further work, on the sensitivity of the assays.

8 REFERENCES

1. J. G. Bartlett, *Annals of Internal Medicine*, 2006, **145**, 758-764.
2. T. Kievits, B. Vangemen, D. Vanstrijp, R. Schukkink, M. Dircks, H. Adriaanse, L. Malek, R. Sooknanan and P. Lens, *Journal of Virological Methods*, 1991, **35**, 273-286.
3. P. G. Kelley, E. A. Grabsch, B. P. Howden, W. Gao and M. L. Grayson, *Journal of Clinical Microbiology*, 2009, **47**, 3769-3772.
4. J. Kim, M. Johnson, P. Hill and B. K. Gale, *Integrative Biology*, 2009, **1**.
5. W. W. Navarre and O. Schneewind, *Microbiology and Molecular Biology Reviews*, 1999, **63**, 174-229.
6. G. Francius, O. Domenech, M. P. Mingeot-Leclercq and Y. F. Dufrêne, *Journal of Bacteriology*, 2008, **190**, 7904-7909.
7. B. A. Andrews and J. A. Asenjo, *Trends in Biotechnology*, 1987, **5**, 273-277.
8. Z. Lin and Z. Cai, *Biotechnology Journal*, 2009, **4**, 210-215.
9. R. Boom, C. J. A. Sol, M. M. M. Salimans, C. L. Jansen, P. M. E. Wertheimvandillen and J. Vandernoordaa, *Journal of Clinical Microbiology*, 1990, **28**, 495-503.
10. B. Van Gemen, P. Van De Wiel, R. Van Beuningen, P. Sillekens, S. Jurriaans, C. Dries, R. Schoones and T. Kievits, *PCR primer: A laboratory manual*, 1995, 667-677.
11. P. Gill and A. Ghaemi, *Nucleosides Nucleotides & Nucleic Acids*, 2008, **27**, 224-243.
12. J. Compton, *Nature*, 1991, **350**, 91-92.
13. K. Mullis, F. Faloona, S. Scharf, R. Saiki, G. Horn and H. Erlich, *Cold Spring Harbor Symposia on Quantitative Biology*, 1986, **51**, 263-273.
14. R. K. Saiki, S. Scharf, F. Faloona, K. B. Mullis, G. T. Horn, H. A. Erlich and N. Arnheim, *Science*, 1985, **230**, 1350-1354.
15. R. K. Saiki, T. L. Bugawan, G. T. Horn, K. B. Mullis and H. A. Erlich, *Nature*, 1986, **324**, 163-166.
16. K. B. Mullis and F. A. Faloona, *Methods in Enzymology*, 1987, **155**, 335-350.
17. R. K. Saiki, D. H. Gelfand, S. Stoffel, S. J. Scharf, R. Higuchi, G. T. Horn, K. B. Mullis and H. A. Erlich, *Science*, 1988, **239**, 487-491.
18. K. B. Mullis, *Scientific American*, 1990, **262**, 56-65.
19. U. o. Leicester, Schematic overview PCR proces, http://www2.le.ac.uk/departments/emfpu/genetics/explained/images/PCR-process.gif, Accessed 2010-05-05.
20. H. Zipper, H. Brunner, J. Bernhagen and F. Vitzthum, *Nucleic Acids Research*, 2004, **32**.
21. C. T. Wittwer, M. G. Herrmann, A. A. Moss and R. P. Rasmussen, *Biotechniques*, 1997, **22**, 130-&.

22. K. M. Ririe, R. P. Rasmussen and C. T. Wittwer, *Analytical Biochemistry*, 1997, **245**, 154-160.
23. P. Francois, D. Pittet, M. Bento, B. Pepey, P. Vaudaux, D. Lew and J. Schrenzel, *Journal of Clinical Microbiology*, 2003, **41**, 254-260.
24. M. Holfelder, U. Eigner, A. M. Turnwald, W. Witte, M. Weizenegger and A. Fahr, *Clinical Microbiology and Infection*, 2006, **12**, 1163-1167.
25. G. M. Hogg, J. P. McKenna and G. Ong, *Diagnostic Microbiology and Infectious Disease*, 2008, **61**, 446-452.
26. D. Lleres, S. Swift and A. I. Lamond, *Curr Protoc Cytom*, 2007, **Chapter 12**, Unit12.10.
27. T. Förster, *Annalen der Physik*, 1948, **437**.
28. K. E. Sapsford, L. Berti and I. L. Medintz, *Angewandte Chemie-International Edition*, 2006, **45**, 4562-4588.
29. S. A. E. Marras, F. R. Kramer and S. Tyagi, *Nucleic Acids Research*, 2002, **30**.
30. P. M. Holland, R. D. Abramson, R. Watson and D. H. Gelfand, *Proceedings of the National Academy of Sciences of the United States of America*, 1991, **88**, 7276-7280.
31. M. Weidmann, K. Armbruster and F. T. Hufert, *Journal of Clinical Virology*, 2008, **42**, 326-334.
32. S. Tyagi and F. R. Kramer, *Nature Biotechnology*, 1996, **14**, 303-308.
33. S. Tyagi, D. P. Bratu and F. R. Kramer, *Nature Biotechnology*, 1998, **16**, 49-53.
34. C. T. Wittwer, K. M. Ririe, R. V. Andrew, D. A. David, R. A. Gundry and U. J. Balis, *Biotechniques*, 1997, **22**, 176-181.
35. G. Leone, H. van Schijndel, B. van Gemen, F. R. Kramer and C. D. Schoen, *Nucleic Acids Research*, 1998, **26**, 2150-2155.
36. A. Raj, P. van den Bogaard, S. A. Rifkin, A. van Oudenaarden and S. Tyagi, *Nature Methods*, 2008, **5**, 877-879.
37. S. Tyagi, Designing Molecular Beacons, Accessed 2009-12-21.
38. D. Whitcombe, J. Theaker, S. P. Guy, T. Brown and S. Little, *Nature Biotechnology*, 1999, **17**, 804-807.
39. N. Thelwell, S. Millington, A. Solinas, J. Booth and T. Brown, *Nucleic Acids Research*, 2000, **28**, 3752-3761.
40. J. A. Piccirilli, S. A. Benner, T. Krauch and S. E. Moroney, *Nature*, 1990, **343**, 33-37.
41. S. C. Johnson, C. B. Sherrill, D. J. Marshall, M. J. Moser and J. R. Prudent, *Nucleic Acids Research*, 2004, **32**, 1937-1941.
42. C. B. Sherrill, D. J. Marshall, M. J. Moser, C. A. Larsen, L. Daudé-Snow, S. Jurczyk, G. Shapiro and J. R. Prudent, *Journal of the American Chemical Society*, 2004, **126**, 4550-4556.
43. S. C. Johnson, D. J. Marshall, G. Harms, C. M. Miller, C. B. Sherrill, E. L. Beaty, S. A. Lederer, E. B. Roesch, G. Madsen, G. L. Hoffman, R. H. Laessig, G. J. Kopish, M. W. Baker, S. A. Benner, P. M. Farrell and J. R. Prudent, *Clin Chem*, 2004, **50**, 2019-2027.

44. P. Corporation, Plexor qPCR System- Technical Manual, http://www.promega.com/resources/protocols/technical-manuals/0/plexor-qpcr-system-protocol/, Accessed 2011-01-19.
45. BitesizeBio.com, 2009.
46. Cepheid, 2010.
47. Qiagen, Corbett Rotor Gene Six Excitation wavelengths, http://www.qiagen.com/products/rotor-geneq.aspx#tab4, Accessed 2009-11-12.
48. L. H. Augenlicht and D. Kobrin, *Cancer Res*, 1982, **42**, 1088-1093.
49. M. Schena, D. Shalon, R. W. Davis and P. O. Brown, *Science*, 1995, **270**, 467-470.
50. K. R. Everett, J. Rees-George, I. P. S. Pushparajah, B. J. Janssen and Z. Luo, *New Zealand Plant Protection*, 2010, **63**, 1-6.
51. H.-Y. Park, J. Driskell, K. Kwarta, R. Lipert, M. Porter, C. Schoen, J. Neill and J. Ridpath, eds. K. Kneipp, M. Moskovits and H. Kneipp, Springer Berlin / Heidelberg, 2006, pp. 427-446.
52. I. A. Larmour and D. Graham, *Analyst*, 2011, **136**, 3831-3853.
53. K. Faulds, F. McKenzie, W. E. Smith and D. Graham, *Angewandte Chemie International Edition*, 2007, **46**, 1829-1831.
54. L. Sun, C. X. Yu and J. Irudayaraj, *Analytical Chemistry*, 2007, **79**, 3981-3988.
55. K. Faulds, R. Jarvis, W. E. Smith, D. Graham and R. Goodacre, *Analyst*, 2008, **133**, 1505-1512.
56. C. V. Raman, Krishnan K.S., *Nature*, 1928, **121**, 501-502.
57. P. C. White, *Science & Justice*, 2000, **40**, 113-119.
58. R. Brown, W. E. Smith and D. Graham, *Tetrahedron Letters*, 2001, **42**, 2197-2200.
59. H. P. J. a. M. A. J. FLEISCHMANN M, *Chemical Physics Letters*, 1974, **26**, 163 - 166.
60. D. L. Jeanmaire and R. P. Van Duyne, *Journal of Electroanalytical Chemistry*, 1977, **84**, 1-20.
61. M. G. Albrecht and J. A. Creighton, *Journal of the American Chemical Society*, 1977, **99**, 5215-5217.
62. M. Moskovits, *Reviews of Modern Physics*, 1985, **57**, 783-826.
63. E. E. Le Ru, Pablo *Principles of Surface Enhanced Raman Spectroscopy and related plasmonic effects*, Elsevier Radarweg 29, PO Box 211, 1000 AE Amsterdam, The Netherlands Linacre House, Jordan Hill, Oxford OX2 8DP, UK, 2009.
64. G. Braun, S. J. Lee, M. Dante, T. Q. Nguyen, M. Moskovits and N. Reich, *Journal of the American Chemical Society*, 2007, **129**, 6378-+.
65. C. H. Munro, W. E. Smith, M. Garner, J. Clarkson and P. C. White, *Langmuir*, 1995, **11**, 3712-3720.
66. C. H. Munro, W. E. Smith and P. C. White, *Analyst*, 1995, **120**, 993-1003.
67. A. M. Stacy and R. P. Vanduyne, *Chemical Physics Letters*, 1983, **102**, 365-370.

68. S. Nie and S. R. Emory, *Science*, 1997, **275**, 1102-1106.
69. A. Kudelski and J. Bukowska, *Chemical Physics Letters*, 1996, **253**, 246-250.
70. P. C. Lee and D. Meisel, *Journal of Physical Chemistry*, 1982, **86**, 3391-3395.
71. S. P. Mulvaney, M. D. Musick, C. D. Keating and M. J. Natan, *Langmuir*, 2003, **19**, 4784-4790.
72. J. F. Li, Y. F. Huang, Y. Ding, Z. L. Yang, S. B. Li, X. S. Zhou, F. R. Fan, W. Zhang, Z. Y. Zhou, D. Y. Wu, B. Ren, Z. L. Wang and Z. Q. Tian, *Nature*, 2010, **464**, 392-395.
73. A. Fabrikanos, Athanass.S and K. H. Lieser, *Zeitschrift Fur Naturforschung Part B-Chemie Biochemie Biophysik Biologie Und Verwandten Gebiete*, 1963, **B 18**, 612-&.
74. N. Leopold and B. Lendl, *The Journal of Physical Chemistry B*, 2003, **107**, 5723-5727.
75. J. A. Creighton, C. G. Blatchford and M. G. Albrecht, *Journal of the Chemical Society-Faraday Transactions Ii*, 1979, **75**, 790-798.
76. D. Graham, K. Faulds and W. E. Smith, *Chemical Communications*, 2006, 4363-4371.
77. K. Faulds, W. E. Smith and D. Graham, *Analyst*, 2005, **130**, 1125-1131.
78. K. Faulds, R. E. Littleford, D. Graham, G. Dent and W. E. Smith, *Analytical Chemistry*, 2004, **76**, 592-598.
79. R. Jin, *Angewandte Chemie International Edition*, 2010, **49**, 2826-2829.
80. K. L. Wustholz, A.-I. Henry, J. M. McMahon, R. G. Freeman, N. Valley, M. E. Piotti, M. J. Natan, G. C. Schatz and R. P. V. Duyne, *Journal of the American Chemical Society*, 2010, **132**, 10903-10910.
81. C. A. Mirkin, R. L. Letsinger, R. C. Mucic and J. J. Storhoff, *Nature*, 1996, **382**, 607-609.
82. Y. W. C. Cao, R. C. Jin and C. A. Mirkin, *Science*, 2002, **297**, 1536-1540.
83. D. Graham, D. G. Thompson, W. E. Smith and K. Faulds, *Nature Nanotechnology*, 2008, **3**, 548-551.
84. L. Guerrini, F. McKenzie, A. W. Wark, K. Faulds and D. Graham, *Chemical Science*, 2012, **3**, 2262-2269.
85. E. C. Le Ru and P. G. Etchegoin, *Principles of Surface-Enhanced Raman Spectroscopy*, Elsevier, Amsterdam, 2009.
86. S. E. J. Bell and N. M. S. Sirimuthu, *Journal of the American Chemical Society*, 2006, **128**, 15580-15581.
87. X. Dou, T. Takama, Y. Yamaguchi, K. Hirai, H. Yamamoto, S. Doi and Y. Ozaki, *Applied Optics*, 1998, **37**, 759-763.
88. H. X. Li and L. J. Rothberg, *Journal of the American Chemical Society*, 2004, **126**, 10958-10961.
89. H. X. Li and L. Rothberg, *Proceedings of the National Academy of Sciences of the United States of America*, 2004, **101**, 14036-14039.
90. H. Li and L. J. Rothberg, *Analytical Chemistry*, 2004, **76**, 5414-5417.

91. A. MacAskill, D. Crawford, D. Graham and K. Faulds, *Anal Chem*, 2009, **81**, 8134-8140.
92. M. B. Wabuyele and T. Vo-Dinh, *Analytical Chemistry*, 2005, **77**, 7810-7815.
93. K. Faulds, L. Fruk, D. C. Robson, D. G. Thompson, A. Enright, W. E. Smith and D. Graham, *Faraday Discussions*, 2006, **132**, 261-268.
94. P. B. Monaghan, K. M. McCarney, A. Ricketts, R. E. Littleford, F. Docherty, W. E. Smith, D. Graham and J. M. Cooper, *Analytical Chemistry*, 2007, **79**, 2844-2849.
95. M. H. Harpster, H. Zhang, A. K. Sankara-Warrier, B. H. Ray, T. R. Ward, J. P. Kollmar, K. T. Carron, J. O. Mecham, R. C. Corcoran, W. C. Wilson and P. A. Johnson, *Biosensors and Bioelectronics*, 2009, **25**, 674-681.
96. H. Zhang, M. H. Harpster, H. J. Park, P. A. Johnson and W. C. Wilson, *Analytical Chemistry*, 2011, **83**, 254-260.
97. H.-N. Wang and T. Vo-Dinh, *Nanotechnology*, 2009, **20**, 065101.
98. D. Graham, B. J. Mallinder, D. Whitcombe, N. D. Watson and W. E. Smith, *Analytical Chemistry*, 2002, **74**, 1069-+.
99. T. Vo-Dinh, K. Houck and D. L. Stokes, *Analytical Chemistry*, 1994, **66**, 3379-3383.
100. NCBI, National Center for Biotechnology Information http://www.ncbi.nlm.nih.gov/, Accessed 2009-10-01.
101. A. Untergasser, H. Nijveen, X. Rao, T. Bisseling, R. Geurts and J. A. M. Leunissen, *Nucleic Acids Research*, 2007, **35**, W71-W74.
102. J. SantaLucia, *Proceedings of the National Academy of Sciences of the United States of America*, 1998, **95**, 1460-1465.
103. R. Owczarzy, Y. You, B. G. Moreira, J. A. Manthey, L. Y. Huang, M. A. Behlke and J. A. Walder, *Biochemistry*, 2004, **43**, 3537-3554.
104. N. R. Markham and M. Zuker, *Nucleic Acids Research*, 2005, **33**, W577-W581.
105. NCBI, 2010.
106. J. Yguerabide and E. E. Yguerabide, *Analytical Biochemistry*, 1998, **262**, 137-156.
107. J. Yguerabide and E. E. Yguerabide, *Analytical Biochemistry*, 1998, **262**, 157-176.
108. K. De Gussem, J. De Gelder, P. Vandenabeele and L. Moens, *Chemometrics and Intelligent Laboratory Systems*, 2009, **95**, 49-52.
109. C. A. Lieber and A. Mahadevan-Jansen, *Applied Spectroscopy*, 2003, **57**, 1363-1367.
110. P. Hildebrandt and M. Stockburger, *Journal of Raman Spectroscopy*, 1986, **17**, 55-58.
111. L. Wang, A. Roitberg, C. Meuse and A. K. Gaigalas, *Spectrochimica Acta, Part A: Molecular and Biomolecular Spectroscopy*, 2001, **57**, 1781-1791.
112. W. E. Alborn, J. A. Hoskins, S. Unal, J. E. Flokowitsch, C. A. Hayes, J. E. Dotzlaf, W. K. Yeh and P. L. Skatrud, *Gene*, 1996, **180**, 177-181.
113. S. Rozen and H. Skaletsky, *Methods Mol Biol*, 2000, **132**, 365-386.

114. R. A. Dimitrov and M. Zuker, *Biophysical Journal*, 2004, **87**, 215-226.
115. N. R. Markham and M. Zuker, *Methods in Molecular Biology:VOLUME II: STRUCTURE, FUNCTION AND APPLICATIONS*, 2008, 3-31.
116. J. SantaLucia, Jr., *Methods in Molecular Biology*, 2007, 3-33.
117. J. SantaLucia, H. T. Allawi and A. Seneviratne, *Biochemistry*, 1996, **35**, 3555-3562.
118. J. J. SantaLucia, in *Methods in Molecular Biology, vol. 402: PCR Primer Design Edited by: A. Yuryev © Humana Press, Totowa, NJ*, pp. 3-33.
119. W. A. Kibbe, Oligo Calc: Oligonucleotide Properties Calculator, http://www.basic.northwestern.edu/biotools/oligocalc.html, Accessed 2009-09-12.
120. C. Rodger, W. E. Smith, G. Dent and M. Edmondson, *Journal of the Chemical Society, Dalton Transactions*, 1996, 791-799.
121. Qiagen, *Genomic DNA handbook*, 2001.
122. Nanodrop, *Technical Support bulletin*, 2007.
123. D. van Lierop, K. Faulds and D. Graham, *Analytical Chemistry*, 2011, **83**, 5817-5821.
124. Zhang YQ, Ren SX, Li HL, Wang YX, Fu G, Yang J, Qin ZQ and W. W. Miao YG, Chen RS, Shen Y, Chen Z, Yuan ZH, Zhao GP, Qu D, Danchin A, Wen YM., *Mol Microbiol.*, 2003, **49**, 1577-1593.
125. R. Owczarzy, A. V. Tataurov, Y. Wu, J. A. Manthey, K. A. McQuisten, H. G. Almabrazi, K. F. Pedersen, Y. Lin, J. Garretson, N. O. McEntaggart, C. A. Sailor, R. B. Dawson and A. S. Peek, *Nucleic Acids Research*, 2008, **36**, W163-W169.
126. S. F. Altschul, W. Gish, W. Miller, E. W. Myers and D. J. Lipman, *Journal of Molecular Biology*, 1990, **215**, 403-410.
127. M. W. Meyer and E. A. Smith, *Analyst*.
128. P. L. Stiles, J. A. Dieringer, N. C. Shah and R. R. Van Duyne, *Annual Review of Analytical Chemistry*, 2008, **1**, 601-626.
129. B. Bergerbachi, L. Barberismaino, A. Strassle and F. H. Kayser, *Molecular & General Genetics*, 1989, **219**, 263-269.
130. S. Schreiber-Gosche and R. A. Edwards, *Journal of Chemical Education*, 2009, **86**, 644-650.
131. S. Bommarito, N. Peyret and J. SantaLucia, *Nucleic Acids Research*, 2000, **28**, 1929-1934.
132. M. Mitsuhashi, *Journal of Clinical Laboratory Analysis*, 1996, **10**, 277-284.
133. C. T. Wittwer, M. G. Herrmann, C. N. Gundry and K. S. J. Elenitoba-Johnson, *Methods*, 2001, **25**, 430-442.
134. C. Ryffel, F. H. Kayser and B. Bergerbachi, *Antimicrobial Agents and Chemotherapy*, 1992, **36**, 25-31.
135. F. H. C. Crick, *Journal of Molecular Biology*, 1966, **19**, 548-555.
136. T. A. Early, J. Olmsted, D. R. Kearns and A. G. Lezius, *Nucleic Acids Research*, 1978, **5**, 1955-1970.
137. M. F. Goodman, *Proc Natl Acad Sci U S A*, 1997, **94**, 10493-10495.

138. K. Faulds, W. E. Smith and D. Graham, *Analytical Chemistry*, 2004, **76**, 412-417.
139. D. Graham, W. E. Smith, A. M. T. Linacre, C. H. Munro, N. D. Watson and P. C. White, *Analytical Chemistry*, 1997, **69**, 4703-4707.
140. S. E. J. Bell and N. M. S. Sirimuthu, *Chemical Society Reviews*, 2008, **37**, 1012-1024.
141. D. Graham and K. Faulds, *Chemical Society Reviews*, 2008, **37**, 1042-1051.
142. B. C. Hoopes and W. R. McClure, *Nucleic Acids Research*, 1981, **9**, 5493-5504.
143. I. A. Larmour, K. Faulds and D. Graham, *Journal of Physical Chemistry C*, 2010, **114**, 13249-13254.
144. F. McKenzie and D. Graham, *Chemical Communications*, 2009, **45**, 5757-5759.
145. A. McLintock, N. Hunt and A. W. Wark, *Chemical Communications*, 2011, **47**, 3757-3759.
146. M. Thomas and A. M. Klibanov, *Proceedings of the National Academy of Sciences*, 2003, **100**, 9138-9143.
147. Y. Ma, Y. Guo, J. Li, J. Guan, L. Xu and W. Yang, *Chemistry-a European Journal*, 2009, **15**, 13135-13140.
148. B. L. Frey and R. M. Corn, *Analytical Chemistry*, 1996, **68**, 3187-3193.
149. S. F. D'Souza and J. S. Melo, *Enzyme and Microbial Technology*, 1991, **13**, 508-511.
150. Z. e. Krpetić, P. Nativo, V. Sée, I. A. Prior, M. Brust and M. Volk, *Nano Letters*, 2010, **10**, 4549-4554.
151. Z. M. Sui, X. Chen, L. Y. Wang, L. M. Xu, W. C. Zhuang, Y. C. Chai and C. J. Yang, *Physica E*, 2006, **33**, 308-314.
152. B. G. Feuerstein, N. Pattabiraman and L. J. Marton, *Nucleic Acids Research*, 1990, **18**, 1271-1282.
153. H. Deng, V. A. Bloomfield, J. M. Benevides and G. J. T. Jr, *Nucleic Acids Research*, 2000, **28**, 3379-3385.
154. R. J. Stokes, A. Macaskill, P. J. Lundahl, W. E. Smith, K. Faulds and D. Graham, *Small*, 2007, **3**, 1593-1601.
155. V. Zanker and W. Peter, *Chemische Berichte*, 1958, **91**, 572-580.
156. R. Gill and G. W. Lucassen, *Analytical Methods*, 2010, **2**, 445-447.

9 LIST OF PUBLICATIONS

Peer reviewed publications

- D. van Lierop, K. Faulds, D. Graham, Separation Free DNA Detection Using Surface Enhanced Raman Scattering. Anal. Chem. 2011, 83. 5817-5821
- D. van Lierop, I. A. Larmour, K. Faulds, D. Graham, SERS Primers and Their Mode of Action for Pathogen DNA Detection. Anal. Chem. 2013, 85. 1408-1414
- D. van Lierop, Ž. Krpetić, L. Guerrini, I. A. Larmour, J. A. Dougan, K. Faulds, D. Graham, Positively charged silver nanoparticles and their effect on surface-enhanced Raman scattering of dye-labelled oligonucleotides. Chem. Commun. 2012, 48, 8192-8194.

Conference contributions

- Danny van Lierop, Karen Faulds, Duncan Graham, "Novel methods for surface enhanced Raman scattering based pathogen DNA detection", Annual departmental section meeting, June 17th 2011, Glasgow, Scotland, (Oral presentation)
- Danny van Lierop, Karen Faulds, Duncan Graham, Graeme McNay, Ewen Smith, "Separation free multiplexed pathogen detection using silver nanoparticles and surface enhanced Raman spectroscopy", EMRS conference, 9-13th of May 2011, Nice, France, (poster presentation)
- Danny van Lierop, Karen Faulds, Duncan Graham, Graeme McNay, Ewen Smith, "Separation free multiplexed pathogen detection using silver nanoparticles and surface enhanced Raman spectroscopy", SPIRIT conference, May 25th 2011, St. Andrews, Scotland, (poster presentation)

analytical chemistry

LETTER

pubs.acs.org/ac

Separation Free DNA Detection Using Surface Enhanced Raman Scattering

Danny van Lierop, Karen Faulds, and Duncan Graham*

Centre for Molecular Nanometrology, WestCHEM, Pure and Applied Chemistry, University of Strathclyde, 295 Cathedral Street, Glasgow, G1 1XL, United Kingdom

Supporting Information

ABSTRACT: Surface enhanced raman scattering (SERS) based molecular diagnostic assays for the detection of specific DNA sequences have been developed in recent years to compete with the more common fluorescence based approaches. Current SERS assays either require time-consuming separation steps that increase assay cost and can also increase the risk of contamination or they are negative assays, where the signal intensity decreases in the presence of target DNA. Herein, we report a new separation free SERS assay with an increase in signal intensity when target DNA is present using a specifically designed SERS primer. The presence of specific bacterial DNA from *Staphylococcus epidermidis* was detected using polymerase chain reaction (PCR) and SERS and indicates a new opportunity for exploration of SERS assays requiring minimal handling steps.

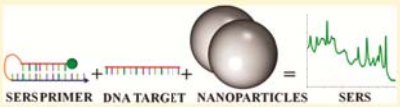

In the field of molecular diagnostics, patient samples such as blood, urine, feces, nasal swabs, and various other samples are tested for the presence of diseases. Early diagnosis can save lives and minimize healthcare costs due to more effective treatment. The current gold standard for testing in hospitals is based on culturing pathogens. Although this process is a sensitive technique, pathogen identification based on culturing the strains can take up to 2 to 3 days.[1,2] A recently more favored method is the detection of gene specific deoxyribonucleic acid (DNA) sequences using real time polymerase chain reaction (rtPCR), which usually takes less than 2 h;[3] therefore, the fast turnaround of PCR based approaches are preferred for many diagnostic screens. The same techniques can also be applied to screen patients for genetic diseases as well as infections. However, the multiplexing capabilities in solution of these systems are limited by the broad absorption and emission bands of the fluorophores used for the fluorescence detection.

Using fluorescence spectroscopy, multiple filter sets and/or multiple excitation wavelengths are needed to differentiate fluorescent labels from each other.[4] An alternative technique is surface enhanced Raman spectroscopy (SERS) which produces molecule specific vibrational spectra, and when a Raman reporter is in close proximity to a rough metal surface, the technique becomes ultrasensitive. Detection limits of dye labeled oligonucleotide probes have been calculated down to a concentration of 7.5×10^{-13} M using SERS which was significantly lower than the observed limit of detection by fluorescence.[5] The choice of Raman reporter molecule, metal surface, excitation wavelength, and surface chemistry are important because detection limits can vary using different experimental conditions.[5−8]

The advantage of SERS is that it can identify multiple different analytes present in a sample without the need for multiple filter sets or multiple excitation wavelengths. Several groups have reported the multiplexed SERS detection of labeled synthetic oligonucleotides but less work has been reported on SERS based assays.[9−11] Dluhy et al. reported the direct detection and identification of viruses on nanorod substrates using SERS and partial least squares-discriminant analysis (PLS−DA) data analysis.[12,13] Herein, no genetic information was obtained. A method to obtain gene specific information is by the sensitive detection of DNA labeled with a SERS active dye. This requires the negative backbone of the DNA to be neutralized to aid in its adsorption onto negatively charged metal nanoparticles, using polyamines such as spermine.[14] Recently, Gill et al. circumvented these issues using positively charged nanoparticles which adsorb DNA without the need of an additional aggregating agent.[15]

For the successful detection of pathogenic DNA, an assay method is required to detect and identify specific DNA sequences. Currently, SERS assays for the detection of unlabeled target DNA have some drawbacks, they either require separation steps using magnetic beads[16] or are so-called "negative assays" where the signal decreases when the target is present.[17−21] Separation steps are labor intensive, expensive, and increase the risk of sample contamination. Negative assays have the disadvantage that it can be difficult to judge if a reduction in signal is due to poor assay performance or the target being present, and an internal performance control target also lowers, or even disappears, during the assay. This could potentially be solved by having two internal controls, one to check the reagents are functioning, which will give a high signal, and the other to check that the assay is functioning correctly, which will give a low signal. However, this would make the assay overly complex. Therefore, it is more

Received: February 28, 2011
Accepted: April 25, 2011
Published: April 25, 2011

advantageous to design an assay which increases signal upon presence of target DNA.

In this Letter, we present a new assay for the detection of gene specific DNA targets from biological samples. The assay generates an increased SERS response upon hybridization of target DNA without the need for additional separation steps and is fully compatible with PCR. This positive assay could be further extended in future studies to take advantage of the high multiplexing capabilities of SERS previously demonstrated. The work reported here is the first step toward the next generation of SERS based molecular diagnostics.

EXPERIMENTAL SECTION

Oligonucleotide Design. The *femA* gene of *Staphylococcus epidermidis* was targeted; this gene was previously used for bacterial identification of *Staphylococcus epidermidis* and *Staphylococcus aureus*.[22] The sequence of the whole genome including the *femA* gene of *Staphylococcus epidermidis* National Culture Type Collection (NCTC) strain NCTC 13360 was obtained from the National Centre of Biotechnology Information (NCBI) Web site.[23] The *FemA-SE* assay design was carried out using the Primer3Plus online server.[24] Parameters within this software were set to 50 mM monovalent salt, 1.5 mM divalent salt, and 250 nM DNA. For the table of thermodynamic parameters, the setting "Santalucia 1998" was used.[25] For salt correction, the formula set by "Owczarzy et al." was used.[26] Internal folding of the sequence region selected by Primer3Plus was analyzed using the DINAMelt server.[27] Parameters were set to 58 °C, 50 mM monovalent salt, 1.5mM divalent salt, and 250 nM DNA. Basic local alignment (BLAST) was carried out using the BLAST tools from the NCBI Web site[28]

The designed oligonucleotides are shown in Table S1 (Supporting Information). The forward (Fw) primer selected in the previous section was modified with a self-complementary probe sequence with a melting temperature (T_m) that was 15 °C lower than that of the primer sequence using four mismatches in the self-complementary sequence. Oligonucleotides were HPLC purified and obtained from ATD Bio (Southampton).

Reagents. All reagents were obtained from Sigma Aldrich (United Kingdom) unless stated otherwise.

SERS Analysis. Silver ethylenediaminetetraacetic acid (EDTA) nanoparticles were synthesized using a previously reported method.[17] The basic native pH of the colloid (pH 11) was adjusted by the addition of TRIZMA hydrochloride (0.5 mL of 200 mM, pH 7.0) and Tween 20 (0.5 mL of 0.2%) to 9 mL of the as prepared colloid. This reduced the pH to 7 preventing the denaturation of dsDNA into ssDNA. The λ_{max} of the buffered colloid was 421 ± 2 nm, and the full width half-maximum (fwhm) was 85 ± 2 nm, indicating no significant changes or aggregation effects due to buffering the colloid (Figure S1, Supporting Information).[29] The size of the silver EDTA nanoparticles was determined with dynamic light scattering using a Malvern HPPS particles sizer. The hydrodynamic radius of the particles was measured as 90 ± 1 nm. The concentration of nanoparticles was calculated to be 22 ± 1 pM.

UV−vis spectroscopy was carried out on a Varian Cary 300 BIO spectrophotometer with Peltier thermal control cycling from 10 to 90 °C and back with 1 °C increments per minute, and the UV absorbance was measured at 260 nm every minute. Samples were prepared using 50 μL of SERS primer (10 μM), 50 μL of diethylpyrocarbonate (DEPC) treated water (Bioline, London, United Kingdom), target or nontarget DNA (10 μM), and 400 μL of 1× phosphate buffered saline (PBS) obtained from Oxoid (Hampshire, United Kingdom).

Afterward, three replicates of each sample were used for the SERS limit of detection experiment. A volume of 2.5 μL of DNA sample (100−5 nM) was mixed with 125 μL of 1× PBS, 10 μL of 0.01 M spermine tetrahydrochloride, and 137.5 μL of buffered silver EDTA colloid in a microtiter plate. Each sample was analyzed 1 min after preparation using a Raman Microscope (Renishaw inVia using 514.5 nm laser excitation with ~10 mW laser power, coupled with a 20×/0.40 long working distance objective). SERS spectra were analyzed using Matlab 2008b, spectra were imported using the free GSTools toolbox from Gussem et al.[30] Fluorescence background subtraction was carried out according to Lieber et al.[31] SERS signal peak intensities at 1632 cm^{-1} were plotted against the concentration of DNA.

For experiments where the target concentration was varied, SERS analysis was carried out using 2.5 μL of 100 nM SERS primer and 2.5 μL of its complementary sequence as target in 110 μL of PBS buffered at pH 7.3 ± 0.2 as a positive control and a 20 base pair long nonsense DNA sequence as a negative control, prehybridized for 10 min at 95 °C and 10 min at 20 °C using a Stratagene MX4000 thermocycler. The target concentrations were varied over a range of concentrations from 0.1 to 5 nM final concentration after the addition of 10 μL of 0.01 M spermine tetrahydrochloride and 125 μL of silver EDTA nanoparticles. Samples were mixed in microcuvettes and analyzed within 1 min using a Raman Probe (Renishaw system coupled to a 514.5 nm Melles Griot laser with ~6 mW laser power using a 20×/0.35 long working distance objective). Typical integration times were between 1 and 10 s and 3 accumulations. The fluorescent dye attached to the 5′-terminus of the SERS primer was 5-(and 6)-carboxyfluorescein (5,6-FAM) which has a λ_{max} of 490 nm. Data analysis was carried out using the strong peak in the spectrum at 1632 cm^{-1} which represents the xanthene ring C−C stretch.[32,33] Matlab 2006b and a fluorescence background subtraction method published by Lieber et al. were used for data analysis.[31]

Bacterial Culturing. Bacterial strains of *Staphylococcus epidermidis* (NCTC 13360) and *Staphylococcus aureus* (NCTC 8325) were obtained from the national health protection agency culture collections (HPACC Salisbury, UK) and cultured in sterile Tryptone Soy Broth (Oxoid). The cells were centrifuged at 16.110*g* for 10 min at 4 °C; the supernatant was then removed, and 1 mL of Lysostaphin was added. The suspension was incubated for 30 min at 37 °C to lyse the cells. DNA was extracted according to the manufacturer's protocol from the lysate using a QIAamp DNA minikit (Qiagen, Crawley, UK).

Polymerase Chain Reactions. PCR reactions were setup in a total volume of 25 μL for each reaction. Each reaction contained 0.5 μL of 2 U μL^{-1} DNA polymerase Phusion Hot Start II (New England Biolabs, UK), 5 μL of 5× Phusion HF buffer (New England Biolabs, UK), 0.5 μL of deoxynucleoside triphosphates (dNTP's), 10 mM each (New England Biolabs, UK). Two microliters of 2.5 μM forward and 2 μL of 2.5 μM reverse primer were used. Volumes were made up to a total volume of 15 μL using DEPC treated water, and finally, 10 μL of 0.09 ng μL^{-1} genomic template DNA was added. Thermal cycling was carried out using a Stratagene MX4000 Real Time PCR machine. The cycling protocol was as follows: 30 s at 98 °C; thereafter, 30 repeats of 10 s at 98 °C, 60 s at 62 °C, and 60 s at 72 °C; and a final extension at 72 °C for 1 min. After cycling, the sample was cooled to 20 °C.

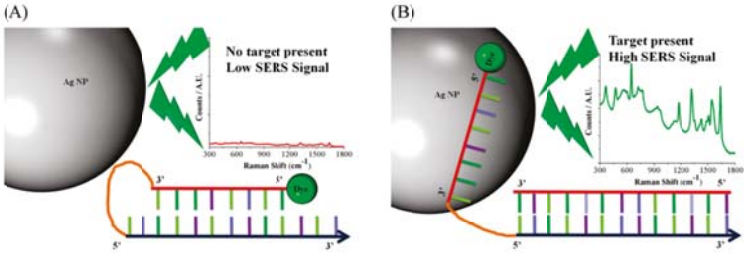

Figure 1. Schematic representation of the SERS probe. Ag NP represents a silver nanoparticle. (A) In the case of a negative sample (when target DNA is absent), the SERS primer is closed and predominantly dsDNA. This means it does not adsorb onto the negatively charged nanoparticle, resulting in a low SERS response. (B) In the case of a positive sample, the complementary target DNA displaces the partly self-complementary region of the SERS primer which is destabilized using mismatches and consists of a dye labeled ssDNA region which is then free to adsorb onto the negatively charged nanoparticle surface resulting in a high SERS response.

Capilary Gel Electrophoresis. Capillary gel electrophoresis was carried out using an Agilent Bioanalyzer and DNA1000 kit including microfluidic chips and reagents (Agilent Technologies, UK). All procedures were carried out following the manufacturer's protocol.

SERS Analysis of PCR samples. PCR samples were analyzed in the SERS assay as follows: 1 μL of the PCR sample was added to 499 μL of PBS buffer. Sample (115 μL) was mixed with 10 μL of 0.01 M spermine hydrochloride and 125 μL of five times concentrated silver EDTA nanoparticles buffered in 10 mM TRIZMA hydrochloride and 0.01% Tween 20. SERS analysis was carried out as discussed above.

■ RESULTS AND DISCUSSION

The assay reported here relies on the difference in adsorption between double stranded and single stranded DNA (dsDNA and ssDNA) onto negatively charged silver nanoparticles. The differential adsorption of ssDNA onto gold nanopartides was first observed by Li and Rothberg.[20] Several assay formats have been previously investigated using salt aggregation approaches, colorimetric detection, fluorescence, and SERS.[20,21,34−36] The investigated assays were all colorimetric assays not capable of multiplexing, negative assays, or fluorescence assays whose multiplexing capability is limited by spectral overlap.

In order to make a positive SERS assay, a SERS primer was designed which contained a dye labeled segment which was rendered single stranded upon hybridization to a target sequence (Figure 1). This single stranded region will have a higher affinity for the metal surface than double stranded, resulting in an increase in the SERS signal. The SERS primer can be used to detect target DNA directly or as a primer when used in combination with PCR.

UV−vis spectroscopy was used to monitor the hybridization profile of the SERS primer in the presence of complementary target DNA and nontarget DNA (e.g., reverse primer). The absorbance at 260 nm was monitored against temperature and shows the formation of single stranded DNA (Figure S2, Supporting Information). The SERS primer (blue triangles) denatures and becomes ssDNA, when heated above 50 °C, and when cooled in the presence of target DNA (green squares), forms a duplex before the partly self-complementary part of the SERS primer can hybridize back to itself. This results in a duplex between the target and the SERS primer with a region of single stranded dye labeled DNA attached. In the case of nontarget DNA (red diamonds), the SERS primer did not form a duplex with the added ssDNA and forms a duplex with its partly self-complementary sequence. The water control (cyan circles) showed no increase in absorbance upon heating.

The UV−vis data showed that the target DNA hybridized to the SERS primer before the self-complementary region of the SERS primer hybridized back to itself. In the presence of nontarget DNA, the SERS primer closed itself at the same temperature as without target DNA proving that the SERS primer is specific to its complementary target.

Figure 2 shows the SERS response for this positive assay. When no target or nonsense DNA is present, a low SERS signal intensity was observed (blue triangles, red diamonds), and when the SERS primer hybridized to its target sequence, an increase in SERS signal intensity was observed (green squares). The blank control (cyan circles) showed no SERS signal as expected. Spermine hydrochloride was used to aggregate the silver EDTA nanoparticles and enhance the SERS response of the FAM labeled DNA. Without the use of spermine hydrochloride, no SERS response was observed from the FAM labeled DNA.

A dilution series of the SERS primer and target with a ratio of 1:1 was conducted in order to find the limit of detection. A positive signal was observed from just 90.9 pM of SERS primer and target. It is clear that below this level discrimination between target and nontarget is not obvious by the eye (Figure S3, Supporting Information). The ratio of SERS primer to target needed to afford a clear discrimination between target and nontarget DNA was, therefore, investigated by keeping the SERS primer concentration constant at 1 nM and varying the concentration of target and nontarget DNA over a range of 0.01−5 nM (Figure 2).

The ratio between SERS primer and target was found to be important in the discrimination between a positive and a negative sample. Reliable discrimination between target and nontarget DNA becomes problematic below a 1:1 ratio. Meanwhile, the upper limit of the dynamic range was dictated by the available surface area on the nanoparticles. However, when there is a need for an extended dynamic range, the nanoparticles can be concentrated to increase the available metal surface area.

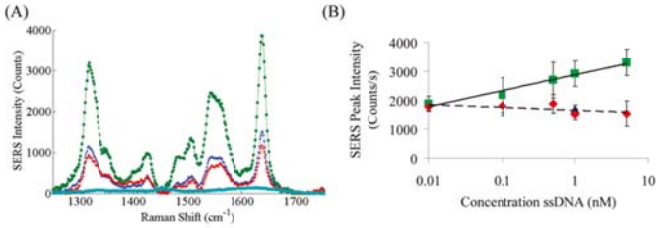

Figure 2. (A) SERS spectra of 1 nM SERS primer (blue triangles), SERS primer and 1 nM perfect match (green squares), SERS primer and 1 nM nontarget DNA (red diamonds), and blank (cyan circles). Exposure time was 1 s using 3 accumulations. (B) SERS intensities of SERS primer with a concentration of 1 nM and different concentrations of target and nontarget DNA. For the three repeats of the samples, the peak at 1632 cm^{-1} was monitored following 3 accumulations of 1 s exposure. SERS primer 1 nM no DNA was added (blue triangle), SERS primer 1 nM and different concentrations of complementary target DNA (green squares), and SERS primer 1 nM and different concentrations of single stranded nontarget DNA (red diamonds). Each point represents the mean of 3 replicates, and error bars represent the standard deviation. The detection limit of target DNA was 1 nM, using 1 nM of SERS primer (3 times standard deviation of the control).

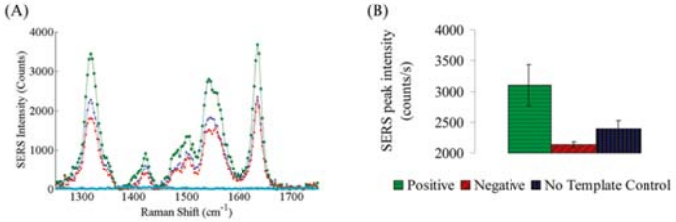

Figure 3. (A) SERS of PCR products, no template control PCR (blue triangles), positive PCR sample (green squares), negative PCR sample (red diamonds), and blank (cyan circles). (B) Average SERS signal peak intensity at 1632 cm^{-1} and standard deviation for three positive (*Staphylococcus epidermidis*) PCR samples (green horizontal shading), three negative (*Staphylococcus aureus*) PCR samples (red diagonal shading), and three no template control (NTC) PCR samples (blue vertical shading).

PCR Products. To show the full compatibility of the SERS primer with biological samples, 1 ng of genomic DNA from *Staphylococcus epidermidis* was amplified using the SERS primer in PCR. The schematic mechanism is shown in the Supporting Information (Figure S4). After the PCR reaction, capillary electrophoresis showed specific amplification of the *femA-SE*gene of *Staphylococcus epidermidis* with a yield of 57.5% (product output (nM)/primer input (nM)*100%) (Figure S5, Supporting Information). Amplification of DNA was not observed when 1 ng of *Staphylococcus aureus* DNA or the no template control (NTC) was used, Supporting Information (Figure S6, Figure S7). Nanoparticles were added after the PCR reaction to avoid unwanted artifacts such as adsorption of PCR components onto the nanoparticles during the PCR and aggregation of the nanoparticles by salts present in the PCR.

When the SERS assay is applied to PCR products, it is important that the yield of the PCR reaction is above 50% in order to discriminate between target and nontarget DNA. Furthermore, the single stranded reverse primer, dNTPs, and other components in the PCR reaction could compete for adsorption onto the silver nanoparticle surface, thereby hindering the adsorption of the SERS primer. To overcome this problem, five times concentrated colloid was used to increase the available surface area. Figure 3 shows the spectra obtained from the samples that underwent the PCR cycling process. The most intense SERS response was observed from the positive sample (green squares); lower intensities were observed for the negative samples (blue triangles, red diamonds).

This system is a unique approach that allows the first direct detection of DNA sequences and PCR product using SERS in a positive assay. The extension of this methodology to the previously shown multiplexing capabilities of SERS will make this assay a useful tool for high degree multiplexing of DNA sequences.

CONCLUSION

We have shown a new positive SERS assay that can discriminate between target and no target DNA in a homogeneous sample without additional separation steps. Starting from a bacterial culture, DNA was isolated; a specially designed primer was incorporated into the PCR products, and the presence or lack of target was identified within 2 h. The high multiplexing capabilities of SERS make this a very promising approach for future DNA analysis. This method has the potential for single molecule detection of nucleic acid targets in a positive manner when SERS is combined with PCR, and this is the first step toward a highly competitive SERS based molecular diagnostic assay.

■ ASSOCIATED CONTENT

Supporting Information. Additional information as noted in text. This material is available free of charge via the Internet at http://pubs.acs.org.

■ AUTHOR INFORMATION

Corresponding Author
*E-mail: Duncan.Graham@strath.ac.uk.

■ ACKNOWLEDGMENT

The authors thank Renishaw Diagnostics Ltd. and the Scottish Funding Council for funding to D.v.L. through a SPIRIT award and the Royal Society for a Wolfson Research Merit award to D. G.

■ REFERENCES

(1) Davies, S.; Zadik, P. M.; Mason, C. M.; Whittaker, S. J. *Br. J. Biomed. Sci.* **2000**, *57* (4), 269–272.
(2) Wertheim, H.; Verbrugh, H. A.; van Pelt, C.; de Man, P.; van Belkum, A.; Vos, M. C. *J. Clin. Microbiol.* **2001**, *39* (7), 2660–2662.
(3) Huletsky, A.; Lebel, P.; Picard, F. J.; Bernier, M.; Gagnon, M.; Boucher, N.; Bergeron, M. G. *Clin. Infect. Dis.* **2005**, *40* (7), 976–981.
(4) Wittwer, C. T.; Herrmann, M. G.; Gundry, C. N.; Elenitoba-Johnson, K. S. J. *Methods* **2001**, *25* (4), 430–442.
(5) Stokes, R. J.; Macaskill, A.; Lundahl, P. J.; Smith, W. E.; Faulds, K.; Graham, D. *Small* **2007**, *3*, 1593–1601.
(6) Faulds, K.; Barbagallo, R. P.; Keer, J. T.; Smith, W. E.; Graham, D. *Analyst* **2004**, *129* (7), 567–568.
(7) Macaskill, A.; Chernonosov, A. A.; Koval, V. V.; Lukyanets, E. A.; Fedorova, O. S.; Smith, W. E.; Faulds, K.; Graham, D. *Nucleic Acids Res.* **2007**, *35* (6), 8134–8140.
(8) Sabatte, G.; Keir, R.; Lawlor, M.; Black, M.; Graham, D.; Smith, W. E. *Anal. Chem.* **2008**, *80* (7), 2351–2356.
(9) Faulds, K.; Jarvis, R.; Smith, W. E.; Graham, D.; Goodacre, R. *Analyst* **2008**, *133* (11), 1505–1512.
(10) Faulds, K.; McKenzie, F.; Smith, W. E.; Graham, D. *Angew. Chem., Int. Ed.* **2007**, *46* (11), 1829–1831.
(11) Sun, L.; Yu, C. X.; Irudayaraj, J. *Anal. Chem.* **2007**, *79* (11), 3981–3988.
(12) Shanmukh, S.; Jones, L.; Driskell, J.; Zhao, Y.; Dluhy, R.; Tripp, R. A. *Nano Lett.* **2006**, *6* (11), 2630–2636.
(13) Hoang, V.; Tripp, R. A.; Rota, P.; Dluhy, R. A. *Analyst* **2010**, *135* (12), 3103–3109.
(14) Graham, D.; Smith, W. E.; Linacre, A. M. T.; Munro, C. H.; Watson, N. D.; White, P. C. *Anal. Chem.* **1997**, *69* (22), 4703–4707.
(15) Gill, R.; Lucassen, G. W. *Anal. Method* **2010**, *2* (5), 445–447.
(16) Monaghan, P. B.; McCarney, K. M.; Ricketts, A.; Littleford, R. E.; Docherty, F.; Smith, W. E.; Graham, D.; Cooper, J. M. *Anal. Chem.* **2007**, *79* (7), 2844–2849.
(17) MacAskill, A.; Crawford, D.; Graham, D.; Faulds, K. *Anal. Chem.* **2009**, *81* (19), 8134–8140.
(18) Faulds, K.; Fruk, L.; Robson, D. C.; Thompson, D. G.; Enright, A.; Smith, W. E.; Graham, D. *Faraday Discuss.* **2006**, *132*, 261–268.
(19) Vo-Dinh, T.; Houck, K.; Stokes, D. L. *Anal. Chem.* **1994**, *66* (20), 3379–3383.
(20) Li, H. X.; Rothberg, L. *Proc. Natl. Acad. Sci. U.S.A.* **2004**, *101* (39), 14036–14039.
(21) Li, H. X.; Rothberg, L. J. *J. Am. Chem. Soc.* **2004**, *126* (35), 10958–10961.
(22) Zhang, Y. Q.; Ren, S. X.; Li, H. L.; Wang, Y. X.; Fu, G.; Yang, J.; Qin, Z. Q.; Miao, YG, W. W; Chen, R. S.; Shen, Y.; Chen, Z.; Yuan, Z. H.; Zhao, G. P.; Qu, D.; Danchin, A.; Wen, Y. M. *Mol. Microbiol.* **2003**, *48* (6), 1577–1593.
(23) NCBI U.S. National Library of Medicine: Bethesda MD, 2010; Vol 2010.
(24) Untergasser, A.; Nijveen, H.; Rao, X.; Bisseling, T.; Geurts, R.; Leunissen, J. A. M. *Nucleic Acids Res.* **2007**, *35* (suppl 2), W71–W74.
(25) SantaLucia, J. *Proc. Natl. Acad. Sci. U.S.A.* **1998**, *95* (4), 1460–1465.
(26) Owczarzy, R.; You, Y.; Moreira, B. G.; Manthey, J. A.; Huang, L. Y.; Behlke, M. A.; Walder, J. A. *Biochemistry* **2004**, *43* (12), 3537–3554.
(27) Markham, N. R.; Zuker, M. *Nucleic Acids Res.* **2005**, *33*, W577–W581.
(28) Altschul, S. F.; Madden, T. L.; Schäffer, A. A.; Zhang, J.; Zhang, Z.; Miller, W.; Lipman, D. J. *Nucleic Acids Res.* **1997**, *25* (17), 3389–3402.
(29) Rodger, C.; Smith, W. E.; Dent, G.; Edmondson, M. *J. Chem. Soc., Dalton Trans.* **1996**, *5*, 791–799.
(30) De Gussem, K.; De Gelder, J.; Vandenabeele, P.; Moens, L. *Chemom. Intell. Lab.* **2009**, *55* (1), 49–52.
(31) Lieber, C. A.; Mahadevan-Jansen, A. *Appl. Spectrosc.* **2003**, *57* (11), 1363–1367.
(32) Hildebrandt, P.; Stockburger, M. *J. Raman Spectrosc.* **1986**, *17* (1), 55–58.
(33) Wang, L.; Roitberg, A.; Meuse, C.; Gaigalas, A. K. *Spectrochim. Acta, Part A: Mol. Biomol. Spectrosc.* **2001**, *57* (9), 1781–1791.
(34) Li, H.; Liang, R.; Turner, D. H.; Rothberg, L. J.; Duan, S. *Rna-a Publication of the RNA Society* **2007**, *13*, 2034–2041.
(35) Li, H. X.; Nelson, E.; Pentland, A.; Van Buskirk, J.; Rothberg, L. *Plasmonics* **2007**, *2* (4), 165–171.
(36) Li, H. X.; Rothberg L. *Anal. Chem.* **2005**, *77* (19), 6229–6233.

analytical chemistry

Article

pubs.acs.org/ac

SERS Primers and Their Mode of Action for Pathogen DNA Detection

Danny van Lierop, Iain A. Larmour, Karen Faulds, and Duncan Graham*

Centre for Molecular Nanometrology, WestCHEM, Pure and Applied Chemistry, University of Strathclyde, 295 Cathedral Street, Glasgow G1 1XL, United Kingdom

Supporting Information

ABSTRACT: SERS primers have been used to directly detect specific PCR products utilizing the difference in adsorption of single-stranded and double-stranded DNA onto nanoparticle surfaces. Herein, seven parameters important for improved positive SERS assays for real applications were investigated. First, we applied a model system for optimization experiments, followed by a PCR assay to detect pathogen DNA, and then the introduction of a new assay that utilizes the 5′→3′ exonuclease activity of *Taq* DNA polymerase to partly digest the SERS probe, generating dye-labeled single-stranded DNA increasing the SERS signals for detection of pathogen DNA. Applying the model system, it was found that uni-molecular SERS primers perform better than bi-molecular SERS primers. However, within the PCR assays, it was found that uni- and bi-molecular SERS primers performed very similarly, and the most reproducible results were obtained using the 5′→3′ exonuclease digestion assay. These SERS-based assays offer new routes over conventional fluorescence-based techniques without compromising sensitivity or selectivity.

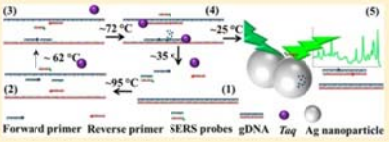

Simultaneous detection of multiple diseases where sample volume and concentrations are limited remains a challenge in the field of molecular diagnostics. Sensitive and fast detection of specific gene markers are based on target or signal amplification in combination with fluorescence detection.[1−3] An approach that competes with these existing approaches is surface enhanced Raman scattering (SERS). Because of the 10−100 times narrower Raman bands of the labels compared to absorption and emission bands of fluorophores,[4,5] simultaneous detection of analytes could be increased.[6−8] However, for successful detection of multiple diseases, an assay system is required to link the Raman reporter signal to a specific disease. Over the past 15 years, multiple SERS-based DNA detection assays have been developed. Unfortunately, there are drawbacks with these assays: either no genetic information was obtained due to the nonspecific intercalation of DAPI,[9] multiple washing steps were required that increase the number of labor intensive handling steps and the risk of sample contamination,[10−12] or the assay resulted in a reduced signal in the presence of the target molecule,[13−15] making the judgment of the assay performance more difficult because of the lack of signal when target DNA was present. An advancement was carried out by Graham et al. who developed a DNA detection assay that utilized the coupling of DNA modified nanoparticles via target DNA resulting in an increased SERS response of the Raman reporter dye attached to the nanoparticle surface.[16] A ssDNA concentration of 1.25 nM was detected using that method. To be clinically useful, a method is required with lower detection limits; an increase in SERS signal intensity in the presence of the target and without separation or washing steps is the preferred method. Recently, SERS primers have been incorporated into polymerase chain reaction (PCR) products to detect pathogen deoxyribonucleic acid (DNA) directly using a surface enhanced Raman spectroscopy (SERS)-based detection approach.[17] SERS primers consist of double-stranded DNA labeled with a SERS active molecule. When SERS primers interact with target DNA, a dye-labeled part of the SERS primer becomes single-stranded DNA (ssDNA) and interacts with a nanoparticle surface, resulting in an increase in the SERS response.

In this approach (Figure S1, Supporting Information), SERS primers are incorporated into PCR products, exposing the fluorophore-labeled ssDNA, allowing adsorption onto the nanoparticles surface resulting in an increased SERS response, thereby detecting the specific gene of a pathogen.

The aims of this study were to investigate the performance of SERS primers in a uni- and bi-molecular manner using a synthetic model system and the introduction of a new SERS assay that utilizes the 5′→3′ exonuclease activity of *Taq* DNA polymerase to partly digest the SERS probe, generating dye-labeled single-stranded DNA increasing the SERS signals for separation free detection of pathogen DNA by SERS.

EXPERIMENTAL PROCEDURES

Materials. All materials were obtained from Sigma Aldrich unless stated otherwise.

DNA Oligonucleotide Design. DNA oligonucleotide design and characterization methods can be obtained from the Supporting Information.

Received: August 8, 2012
Accepted: December 30, 2012
Published: January 11, 2013

dx.doi.org/10.1021/ac302254h | Anal. Chem. 2013, 85, 1408−1414

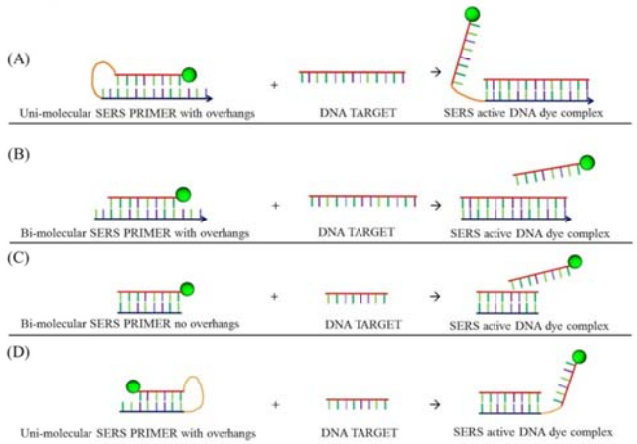

Figure 1. Schematic representation of the synthetic model assay formats investigated. (A) Uni-molecular SERS primer where the dye-labeled region of the SERS primers is attached via a HEG linker to the 5′ terminal end of the primer region of the SERS primer with overhangs. Stepwise, the uni-molecular SERS primer addition of target DNA binding of the target to the uni-molecular SERS primer opens the uni-molecular SERS primer, which then becomes a SERS active DNA dye complex, and after addition of nanopartides creates an increase in the SERS signal. (B) Bi-molecular SERS primer where the dye-labeled region was not attached to the primer region of the SERS primers with overhangs. Stepwise, the bi-molecular SERS primer binding to the target producing more dye-labeled SERS active single-stranded DNA. (C) Bi-molecular SERS primer where the primer region is without overhangs. (D) Uni-molecular SERS probe with mirrored orientation, where the dye-labeled region is linked to the 3′ terminal end of the priming region via a HEG linker.

UV–Vis Spectroscopy. UV−vis spectroscopy was carried out on a Varian Cary 300 BIO spectrophotometer with Peltier thermal control cycling from 10 to 90 °C and back with 1 °C increments per minute, and the UV absorbance was measured at 260 nm every minute. Samples were prepared using 50 μL of SERS primer (10 μM), 50 μL of diethylpyrocarbonate (DEPC)-treated water (Bioline, London, U.K.), or target or nontarget DNA (10 μM), and 250 μL of 1 × phosphate buffered saline (PBS) obtained from Oxoid (Hampshire, U.K.). Finally, the volume was made up to 500 μL with DEPC water.

Bacterial Culturing. Bacterial strains of *Staphylococcus epidermidis* (NCTC 13360) and *Staphylococcus aureus* (NCTC 8325) were obtained from the national health protection agency culture collections (HPACC Salisbury, U.K.) and cultured for 24 h in 10 mL sterile Tryptone Soy Broth (Oxoid). The cells were centrifuged at 16,110×g for 10 min at 4 °C, the supernatant was then removed, and 1 mL of Lysostaphin was added to the remaining pellet. The suspension was incubated for 30 min at 37 °C to lyse the cells. DNA was extracted according to the manufacturer's protocol from the lysate using a QIAamp DNA minikit (Qiagen, Crawley, U.K.).

Polymerase Chain Reactions. PCR reactions were set up in a total volume of 25 μL for each reaction. Each reaction contained 0.5 μL of 2 U μL^{-1} 5′→3′ exonuclease deficient DNA polymerase Phusion Hot Start II (New England Biolabs, U.K.), and for the 5′→3′ exonuclease digestion assay, 0.5 μL of 2 U μL^{-1} DyNAZyme II Hot Start DNA polymerase (New England Biolabs, UK), 5 μL of 5× Phusion HF buffer (New England Biolabs, UK), and 0.5 μL of deoxynucleoside triphosphates (dNTPs) 10 mM each (New England Biolabs, UK) were used. Teh reactions used 2.5 μM forward and 2 μL of 2.5 μM reverse primer, and for the exonuclease assay, 1 μL of 2.5 μM premixed probes was used. Volumes were made to a total volume of 15 μL using DEPC-treated water, and finally, 10 μL of 0.01 ng μL^{-1} genomic template DNA was added. Thermal cycling was carried out using a Stratagene MX3005P thermo cycler. The cycling protocol was 30 s at 98 °C, thereafter 30 repeats of 10 s at 98 °C, 60 s at 62 °C, and 60 s at 72 °C, and a final extension at 72 °C for 1 min. After cycling, the sample was cooled to 20 °C.

Gel Electrophoresis. Capillary electrophoresis of the PCR products was carried out using an Agilent Bioanalyzer and DNA1000 reagent kit, and handling procedures were carried out according to the manufacturers protocol.

Nanoparticles. Nanoparticle synthesis and characterization methods can be obtained from the Supporting Information.

Surface Enhanced Raman Spectroscopy. For the model system experiments where the target concentration was varied, SERS analysis was carried out using 2.5 μL of 100 nM SERS primer and 2.5 μL of its complementary sequence (10−1000 nM) in 110 μL of PBS buffered at pH 7.3 ± 0.2 as a positive sample and a 20−25 base pairs long nontarget DNA sequences as a negative sample, prehybridized for 10 min at 95 °C and 10 min at 20 °C using a thermocycler (Agilent MX3005P). The target concentrations were varied from 0.1 to 10 nM final concentration after the addition of 10 μL of 0.01 M spermine tetrahydrochloride and 125 μL of concentrated silver EDTA nanoparticles (approximately 250 pM).

dx.doi.org/10.1021/ac302254h | Anal. Chem. 2013, 85, 1408−1414

PCR samples were analyzed in the SERS assay as follows: 1 μL of the PCR sample was added to 499 μL of PBS buffer; 115 μL of this sample was then mixed with 10 μL of 0.01 M spermine hydrochloride and 125 μL of concentrated silver EDTA nanoparticles (approximately 500 pM) buffered to pH 7 in 10 mM TRIZMA hydrochloride and 0.01% Tween20.

All samples were prepared in at least triplicate in PMMA microcuvettes and analyzed within 1 min using an Avalon probe system Ramanstation R3 optical fiber equipped with a 532 nm diode laser excitation and laser power of approximately 24 mW at the sample. Typical exposure time was 3 s (1 s integration and 3 accumulations). Data analysis was carried out using the xanthene ring C−C stretch[18,19] of the fluorescent dye carboxyfluorescein (FAM) at 1632 cm^{-1} minus the 1660 cm^{-1} position in the spectrum. The threshold line was plotted and used to find the detection limits, which were calculated using the mean plus three times the standard deviation of the control samples.

■ RESULTS AND DISCUSSION

The performance of the SERS primers in the positive assay was investigated in several different ways. A model system for optimization experiments was applied, followed by application to a PCR assay to detect pathogen specific DNA. A schematic representation of the synthetic model systems (Figure 1) shows the variation in the structure of the SERS primers used in this study. These models were applied to investigate SERS primer performance using uni- and bi-molecular SERS primers with and without overhangs and the mirrored orientation of the uni-molecular SERS primer.

The following seven factors were considered with respect to the assay performance. (1) SERS primer design: The correct folding of a SERS primer will be affected majorly by the sequence composition. The hairpin folding of the SERS primers was modeled using computational software, and the effect of this folding on the assay was investigated with a synthetic model. (2) Type of silver nanoparticles: In order to test the robustness of the ssDNA VS dsDNA assay and the importance of the surface stabilizing layer, three types of nanoparticles were tested in the assay, i.e., EDTA, citrate, and sodium borohydride reduced silver nanoparticles. (3) Nanoparticle and analyte concentration effects: To ensure a fully quantitative assay, dose response curves with respect to the nanoparticle and analyte concentrations on the SERS response were assessed. (4) SERS primer to target molecule ratio: Because of the competitive nature of the SERS primers, the effect of the SERS primer to target ratio was investigated to determine if higher target to SERS primer ratios could increase the SERS signal intensity by opening more SERS primers, which could then significantly improve the performance of the assay. (5) Uni-molecular and bi-molecular SERS primers: The use of a bi-molecular over a uni-molecular system reduces the cost of the SERS primer, which makes the commercialization and implementation of these probes more attractive. Uni-molecular and bi-molecular Scorpion primers in combination with fluorescence detection have been reported[20] and intensively studied by Thellwell et al., who concluded that uni-molecular probes result in a more sensitive method.[21] However, for SERS detection, there still appears the question of whether ssDNA attached to dsDNA hinders the adsorption and thereby the achievable SERS intensity. This also leads to an investigation of the closure of the SERS primer to minimize background signal and maximize displacement of the fluorophore-labeled self-complementary sequence by the target to ensure maximum signal generation in a synthetic SERS model. (6) Terminal overhangs on the SERS primer: The first SERS primer developed[17] had terminal overhangs of ssDNA when in closed conformation. These overhangs were in contradiction with the theory of DNA adsorption, in which ssDNA adsorbs with higher affinity onto the nanoparticle surface then dsDNA,[22] and therefore SERS primers without these overhangs were investigated. (7) Orientation of the SERS primer: In order to use SERS primers in 5′→3′ exonuclease digestion assays, a mirrored SERS primer was developed that had the 5′ terminus free for digestion by *Taq* DNA polymerase. This was then used as an intermolecular probe and introduced in a new assay that utilizes the 5′→3′ exonuclease activity of *Taq* DNA polymerase to partly digest the SERS probe and release the dye-labeled ssDNA, which was then detected by SERS. This method might have several advantages; one of them is the generation of more target than SERS probe by using a higher concentration of primers to SERS probes. When using the SERS probes, an extra level of specificity was created; therefore, universal primers can be used to minimize the number of oligonucleotide sequences needed to detect multiple targets. The latter method was not investigated in this study but will be considered for further work.

SERS Primer Design. Clearly, for the most successful SERS primers, the affinity for the target has to be higher than for the hairpin formation. This was optimized for target binding by incorporation of mismatches and a reduced number of bases in the hairpin folding region of the SERS primer. Mismatches and base reductions were chosen such that they minimized the number of alternative hairpin structures. UV−vis spectroscopy was used to investigate the hybridization profiles of the hairpins in combination with target and nontarget DNA and provided good insights into the performance of the SERS primers in a uni- and bi-molecular fashion. The data shown in Figure S2 of the Supporting Information shows the preferred binding of the SERS primer to the target. When no or nontarget DNA was present, the closure of the self-complementary region onto the SERS primer was observed. The melting temperatures for the SERS primers to their targets are very similar as expected because these were exactly the same DNA sequences. When the closure of the SERS primers was measured, there were differences in melting temperatures between uni- and bi-molecular SERS primers due to the complete different nature of these SERS primers. These experiments were the first steps toward successful SERS primers.

Type of Silver Nanoparticles. Three types of silver nanoparticles (silver citrate, silver EDTA, and silver sodium borohydride) were tested with respect to assay performance. Characterization of these nanoparticles can be found in Table S2 and Figure S3 of the Supporting Information.

Data in Figure 2 and Table S3 (Supporting Information) shows that EDTA and citrate-reduced silver nanoparticles performed in a similar fashion with a ratio of ssDNA:dsDNA of 2.1:2.4, and slightly more intense signals (approximately 5313 versus 5328 counts) were observed when citrate-reduced silver nanoparticles were used. These slight differences were possibly due to the ease of citrate displacement and slight differences in nanoparticles size, where silver citrate nanoparticles had on average a bigger diameter of about 6 nm compared to silver EDTA nanoparticles. Sodium borohydride-reduced silver nanoparticles performed with lower discrimination between double- and single-stranded DNA with a ssDNA:dsDNA ratio

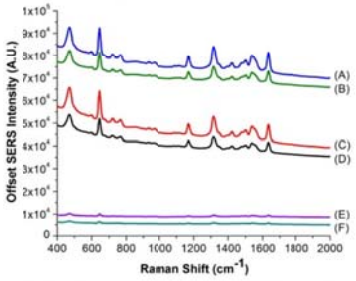

Figure 2. Offset SERS intensity from FAM-labeled single-stranded and double-stranded DNA (1 nM) and silver nanoparticles (20 pM) with different surface chemistry using 532 nm laser excitation and three accumulations of 1 s. (A) Blue line, Ag citrate with ssDNA. (B) Green line, Ag citrate with dsDNA. (C) Red line, Ag EDTA with ssDNA. (D) Black line, Ag EDTA with dsDNA. (E) Purple line, Ag BH_4 with ssDNA. (F) Cyan line, Ag BH_4 with dsDNA.

of ~1.4, and the SERS peak intensity was less intense (~500 counts) when compared to the EDTA and citrate nanoparticles, possibly due to the smaller size of the nanoparticles.[23,24] From these experiments, we conclude that from the types of nanoparticles used, silver citrate nanoparticles and silver EDTA nanoparticles were most successful for this assay with a slight preference for EDTA silver nanoparticles due to the ease of nanoparticle preparation and strong SERS peak intensity.

Nanoparticle and Analyte Concentration Effects. The nanoparticle concentration was optimized (Figure S4, Supporting Information), and in the further model assay studies, a final nanoparticle concentration of 125 pM was used to take advantage of the extended analyte concentration range with a linear response. Further discussion can be obtained from the Supporting Information. In the model system, the SERS primers were exposed to increasing concentrations (0.1−10 nM) of either target or nontarget DNA. After hybridization, the addition of spermine and nanoparticles was followed by SERS analysis of the 1632 cm^{-1} peak intensity of FAM dye.

SERS Primer to Target Molecule Ratio. The hairpin folding of the SERS primer is a uni-molecular event and therefore kinetically more favorable, whereas the binding of the target DNA to the SERS primer is a bi-molecular event in competition with the SERS primer hairpin folding. Therefore, our hypothesis was that when the target to SERS primer ratio was increased a higher discrimination between target DNA and control samples would be obtained due to an increased occurrence of opened SERS primers. The importance of SERS primer to target ratio was investigated following a synthetic experimental model approach (Figure 1).

Following this model system, it was possible to carefully study the behavior of the SERS primer in the assay when more target and nontarget DNA was added. As expected addition of more target DNA resulted in an increase in SERS peak intensity, whereas the addition of more nontarget DNA did not result in an increase in SERS peak intensity. Although it was possible to detect target concentrations 0.5 times lower than the SERS primer concentration, the best contrast between positive and negative samples was obtained when the target to SERS primer ratio was greater than one and preferably five to ten times higher than the SERS primer concentration (Figure 3A). These results are in agreement with our theoretical hypothesis that a higher target concentration was needed to open more SERS primers due to the competitive and bi-molecular nature of the events.

This knowledge can be used in practical design of an assay by using a SERS primer concentration that suits the application and relevant target concentrations. These results also indicate that it might be important for a PCR-based system to run the PCR reaction until all sample concentrations reach the plateau phase and incorporating as much of the SERS primers as possible.

Uni-Molecular and Bi-Molecular SERS Primers. Uni-molecular SERS primers are more likely to fully form double-stranded DNA structures than bi-molecular events. Bi-molecular SERS primers are commercially more attractive due to the significant reduction in cost (Figure 1). Therefore, the use of bi-molecular SERS primers was investigated in a synthetic SERS model assay. Uni-molecular probes had a slightly higher reproducibility and a highly reduced rate of false positives and false negatives resulting in lower detection limits (Figure 3A vs B and C vs D). The reduced performance with bi-molecular SERS primers might be due to a cross reaction between oligonucleotide sequences at 20 °C.

As a result, uni-molecular SERS primers were chosen as the preferred SERS primers over bi-molecular SERS primers due to their lower detection limits and higher reproducibility in the synthetic model assay. Bi-molecular SERS primers might still be useful in PCR-based detection assays because other assay parameters such as the free availability of the dye-labeled ssDNA sequence might also play an important role; however, in this case, the performance of the uni-molecular SERS primer is the leading factor.

Terminal Overhangs of the SERS Primer. The influence of the overhangs in the SERS primer was investigated in bi-molecular manner (Figure 3B vs C). There was no significant effect observed on the SERS assay performance from the 17 (5 + 12) bases overhang with respect to sensitivity, and only a slightly lower background signal was observed.

Orientation of SERS Primer. In order to use the SERS primer as a SERS probe that can be digested by the 5′→3′ exonuclease activity of the DNA polymerase, the positions of the fluorescent molecule and HEG linker were changed to leave the 5′ terminus of the probing sequence free for digestion (Figure 4). First, a SERS probe sequence was designed that contained a 3′ terminus FAM fluorophore and an internal HEG linker molecule. Then the performance of this SERS probe with mirrored orientation was investigated in our synthetic model, and the results in Figure 3D showed that this SERS probe performs with similar sensitivity as the uni-molecular SERS primer shown in Figure 3A.

These results confirm that the fluorophore can be either positioned at the 3′ terminal end of the SERS primer as well as at the 5′ terminal end of the SERS probe with no significant changes in the performance of the SERS primers or probes.

SERS Primers and Probes in PCR-Based SERS Assay. The previous parameters have all been investigated with synthetic models. In this section, our results were transferred to the identification of bacterial cultures by coupling PCR-based DNA amplification with SERS detection. First, the performance of the uni- and bi-molecular SERS primers coupled with PCR

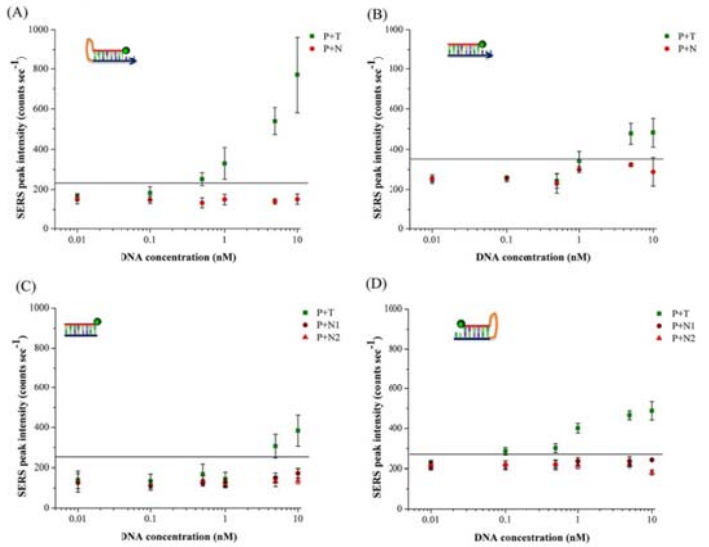

Figure 3. Response of the uni-molecular SERS primer (P) with increasing concentration of target (T) and nontarget (N, N1, and N2) DNA. The horizontal line in each graph represents the threshold values set as three times the standard deviation of the negative control sample. (A) Uni-molecular SERS primer: Intense SERS signals were obtained when the ratio of SERS primer to target was greater than 0.5. (B) Performance of the bi-molecular SERS primer (P) with 3′ terminus overhang. (C) Performance of the bi-molecular SERS probe (P) without overhangs. (D) Performance of the uni-molecular SERS probe (P) with different dye orientation. In the case of SERS primers (A and B), one nontarget sequence (N) was used because in the following PCR experiments this sequence was used as the reverse primer. In the case of the SERS probes experiments (C and D), two nontarget sequences were used because in the following PCR experiments these SERS probes were used in combination with reverse (N1) and forward (N2) primers. A 532 nm laser excitation and three accumulations of 1 s were used. Error bars represent ±1 standard deviation of three individual samples. Threshold values are the mean plus three times the standard deviation of the negative control sample (NTC). Threshold values were 215 (A), 346 (B), 264 (C), and 270 (D), respectively.

were investigated. The PCR yield was similar for both SERS primers with only a slight difference in length of the PCR product in the case of the uni-molecular SERS primers due to the HEG linker and ssDNA attached to the PCR product influencing the electrophoretic properties of the PCR product (data shown in Figure S6, Supporting Information). The optimal spermine concentration for direct detection and positive/negative sample discrimination in the SERS primer PCR SERS assay was determined to be 400 μM as a final concentration (data shown in Figure S7, Supporting Information).

From the results in Figure 4A and B, we concluded that there was no difference between uni- and bi-molecular SERS primers when coupled with PCR; both uni- and bi-molecular SERS primer methods gave a distinct discrimination between negative and positive samples. The bi-molecular SERS primer method contained fewer false negative samples due to a slightly higher reproducibility and therefore lower threshold value. The differences in results between uni- and bi-molecular SERS primers in the synthetic model system and the PCR-based assay can be explained by the fact that in the case of the bi-molecular SERS primer, the FAM labeled ssDNA was not linked to the dsDNA PCR product (which was twice the length of the synthetic model dsDNA) thereby enabling more reproducible adsorption of the FAM-labeled ssDNA onto the nanoparticles surface. Nevertheless, bi-molecular as well as uni-molecular SERS primers could successfully be used in coupling PCR and SERS in a separation free assay system significantly reducing the cost of the SERS primers and thereby the overall SERS assay system.

Moreover, from our synthetic experiments, it is known that a higher ratio of target to SERS primer was better for the overall assay performance. Therefore, the main challenge in using the SERS primers in a PCR-based SERS assay was in the yield of the PCR reaction, which is typically 50% corresponding to a SERS primer to target ratio of 1:0.5.

In an attempt to overcome the PCR yield issue, we have incorporated uni- and bi-molecular SERS probes in a PCR reaction where the SERS probes were digested by the 5′ → 3′ exonuclease activity of the *Taq* DNA polymerase. This method offers the possibility to partly digest the SERS probe generating ssDNA that is in this case not attached to the dsDNA PCR

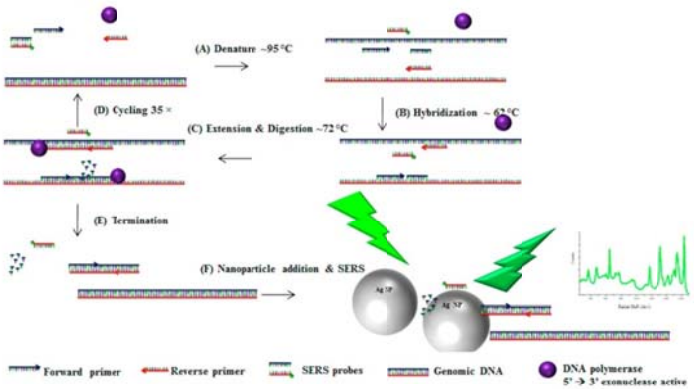

Figure 4. Schematic representation of a PCR reaction incorporating the SERS primer as an internal probe to be partly digested by the polymerase. (A) Denaturation of the DNA using heat: Generation of single-stranded SERS primer and target DNA occurs. (B) Hybridization by cooling the sample: Specific hybridization of the primers and SERS probe occurs. (C) Extension phase: DNA polymerase extends the 3′ prime ends of the primers and digests the target binding sequence of the SERS probe generating dy- labeled single-stranded DNA that results in an increased SERS signal. Repeating step (A) until (C): Multiple copies of product can be generated (D). (E) After the reaction, a double-stranded PCR product is generated and short single-stranded dye-labeled sequences. (F) After addition of nanoparticles, SERS can be obtained from the single-stranded piece of DNA. In the case of a negative sample, the SERS probe remains double-stranded resulting in low SERS of the dye.

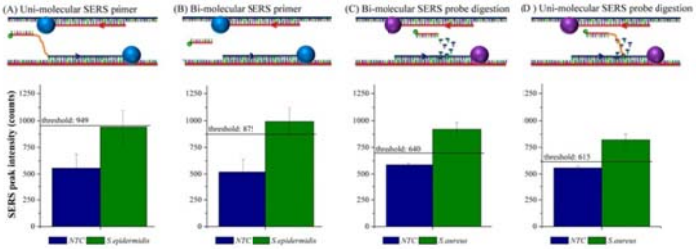

Figure 5. Schematic representation and results obtained from SERS primers and SERS probes in PCR reactions. (A) Uni-molecular SERS primer is incorporated into the PCR product (Figure S1, step C, Supporting Information) and the blue sphere represents 5′→3′ exonuclease deficient DNA polymerase. (B) Bi-molecular SERS primer PCR assay. (C) Bi-molecular SERS probe digested by the 5′→3′ exonuclease active DNA polymerase (purple sphere) (D) Uni-molecular SERS probe PCR assay. Error bars represent ±1 standard deviation of the sample. Threshold values are the mean of three individual negative control samples (NTC) plus three times the standard deviation thereof.

product (Figure 4). An advantage of such a system is the use of an increased PCR primer to SERS probe ratio thereby improving the overall assay performance. Our results in Figure 5C and D showed clear discrimination between negative and positive samples for both uni- and bi-molecular SERS probes with no false negative results, which is a significant improvement over the herein reported uni- and bi-molecular SERS primer methods. Reproducibility and discrimination between positive and negative samples are improved, which are important parameters for the SERS assay to find practical use.

Additionally, the use of uni-molecular SERS primers and probes only had a performance advantage in direct detection assays such as our synthetic model system. When uni- and bi-molecular SERS primers and probes were coupled with the PCR, no clear differences between uni- and bi-molecular approaches were obtained, which significantly reduced the cost of the SERS primers and probes and the overall SERS assay system without compromising the sensitivity or specificity.

■ CONCLUSIONS

Important factors for the performance of the positive SERS primer assays were investigated utilizing a synthetic model. The demonstration and evaluation of four separation free SERS assays for the specific detection of pathogen DNA have been carried out. These assays prove that SERS is a reliable and

competitive technique for direct target DNA detection with or without the use of PCR. Within the synthetic model assays, silver citrate and silver EDTA nanoparticles provided the best discrimination between singe- and double-stranded DNA. The use of partly self-complementary uni-molecular oligonucleotide sequences for the SERS primer significantly increased the contrast between positive and negative samples. The results have shown that a SERS primer or probe to target ratio of 0.5 could be detected, and when increasing the target to probe ratio significantly, higher SERS signals were obtained for all SERS probe models. By increasing the concentration of nanoparticles, the assay was fully quantitative up to a DNA concentration of 50 nM. Finally, SERS primer overhangs had no significant effect on the performance of the synthetic SERS primer assay. For the detection of PCR products, it was best to use the new internal SERS probe digestion assay because with this assay no false negative results were obtained. A significant cost reduction was achieved when using bi-molecular SERS primers and probes coupled to the PCR without any compromises toward sensitivity or selectivity. This is a significant improvement for new approaches using SERS.

■ ASSOCIATED CONTENT

Supporting Information

Experimental details, characterizations, Figure S1−S7, and Tables S1−S3. This material is available free of charge via the Internet at http://pubs.acs.org.

■ AUTHOR INFORMATION

Corresponding Author

*E-mail: Duncan.Graham@strath.ac.uk.

Notes

The authors declare no competing financial interest.

■ ACKNOWLEDGMENTS

The authors thank Renishaw Diagnostics Ltd. and the Scottish Funding Council for funding to D.vL. through a SPIRIT award and the Royal Society for a Wolfson Research Merit award to D.G.

■ REFERENCES

(1) Gill, P.; Ghaemi, A. *Nucleosides, Nucleotides Nucleic Acids* **2008**, *27*, 224−243.

(2) Huletsky, A.; Lebel, P.; Ficard, F. J.; Bernier, M.; Gagnon, M.; Boucher, N.; Bergeron, M. G. *Clin. Infect. Dis.* **2005**, *40*, 976−981.

(3) Zuo, X.; Xia, F.; Xiao, Y.; Plaxco, K. W. *J. Am. Chem. Soc.* **2010**, *132*, 1816−1818.

(4) Park, H.-Y.; Driskell, J.; Kwarta, K.; Lipert, R; Porter, M.; Schoen, C.; Neill, J.; Ridpath, J. In *Surface-Enhanced Raman Scattering: Physics and Application*; Kneipp, K., Moskovits, M., Kneipp, H., Eds.; Topics in Applied Physics 103; Springer-Verlag: Berlin/Heidelberg, 2006; pp 427−446.

(5) Larmour, I. A.; Graham, D. *Analyst* **2011**, *136*, 3831−3853.

(6) Faulds, K.; McKenzie, F.; Smith, W. E.; Graham, D. *Angew. Chem., Int. Ed.* **2007**, *46*, 1829−1831.

(7) Sun, L.; Yu, C. X.; Irudayaraj, J. *Anal. Chem.* **2007**, *79*, 3981−3988.

(8) Faulds, K.; Jarvis, R.; Smith, W. E.; Graham, D.; Goodacre, R. *Analyst* **2008**, *133*, 1505−1512.

(9) Dou, X.; Takama, T.; Yamaguchi, Y.; Hirai, K.; Yamamoto, H.; Doi, S.; Ozaki, Y. *Appl. Opt.* **1998**, *37*, 759−763.

(10) Cao, Y. W. C.; Jin, R. C.; Mirkin, C. A. *Science* **2002**, *297*, 1536−1540.

(11) Monaghan, P. B.; McCarney, K. M.; Ricketts, A.; Littleford, R. E.; Docherty, F.; Smith, W. E.; Graham, D.; Cooper, J. M. *Anal. Chem.* **2007**, *79*, 2844−2849.

(12) Graham, D.; Mallinder, B. J.; Whitcombe, D.; Watson, N. D.; Smith, W. E. *Anal. Chem.* **2002**, *74*, 1069−1074.

(13) MacAskill, A.; Crawford, D.; Graham, D.; Faulds, K. *Anal. Chem.* **2009**, *81*, 8134−8140.

(14) Wabuyele, M. B.; Ve-Dinh, T. *Anal. Chem.* **2005**, *77*, 7810−7815.

(15) Faulds, K.; Fruk, L.; Robson, D. C.; Thompson, D. G.; Enright, A.; Smith, W. E.; Graham, D. *Faraday Discuss.* **2006**, *132*, 261−268.

(16) Graham, D.; Thompson, D. G.; Smith, W. E.; Faulds, K. *Nat. Nanotechnol.* **2008**, *3*, 548−551.

(17) van Lierop, D.; Faulds, K.; Graham, D. *Anal. Chem.* **2011**, *83*, 5817−5821.

(18) Hildebrandt, P.; Stockburger, M. *J. Raman Spectrosc.* **1986**, *17*, 55−58.

(19) Wang, L.; Roitberg, A.; Meuse, C.; Gaigalas, A. K. *Spectrochim. Acta, Part A* **2001**, *57*, 1781−1791.

(20) Whitcombe, D.; Theaker, J.; Guy, S. P.; Brown, T.; Little, S. *Nat. Biotechnol.* **1999**, *17*, 804−807.

(21) Thelwell, N.; Millington, S.; Solinas, A.; Booth, J.; Brown, T. *Nucleic Acids Res.* **2000**, *28*, 3752−3761.

(22) Li, H. X.; Rothberg, L. J. *J. Am. Chem. Soc.* **2004**, *126*, 10958−10961.

(23) Meyer, M. W.; Smith, E. A. *Analyst* **2011**, *136*, 3542−3549.

(24) Le Ru, E. C.; Etchegoin, P. G. *Principles of Surface-Enhanced Raman Spectroscopy*; Elsevier: Amsterdam, 2009.

ChemComm

Dynamic Article Links

Cite this: *Chem. Commun.*, 2012, **48**, 8192–8194

www.rsc.org/chemcomm

COMMUNICATION

Positively charged silver nanoparticles and their effect on surface-enhanced Raman scattering of dye-labelled oligonucleotides†

Danny van Lierop,‡ Željka Krpetić,‡ Luca Guerrini, Iain A. Larmour, Jennifer A. Dougan, Karen Faulds* and Duncan Graham*

Received 8th March 2012, Accepted 10th April 2012
DOI: 10.1039/c2cc31731a

Improved positively charged nanoparticles are described to provide a simplified SERS substrate for DNA detection. Complete flocculation of the nanoparticles is prevented due to the controlled analyte induced aggregation. This provides a stable aggregation state which significantly extends the analysis window simplifying DNA detection by SERS.

Silver nanoparticles have become widely utilised in diagnostics in recent years.[1–3] In particular owing to their intrinsic properties, silver nanoparticles have been extensively used in SERS due to their higher enhancement factors over other metallic nanoparticles, *e.g.* gold and copper.[4,5] Metallic silver is highly sensitive to light and air, and the resulting nanoparticles can be easily oxidised compromising overall particle stability in solution rendering their preparation and handling more difficult, when compared to gold.

For the analysis of DNA by SERS, negatively charged silver nanoparticles have mainly been used in aqueous solution.[6,7] In the method of Bell *et al.*, DNA strands were adsorbed onto metal surfaces with direct interaction of nucleotide chains with the metal surface and the addition of magnesium sulphate facilitated aggregation of the nanoparticle to improve the SERS detection.[7] Graham *et al.* further enhanced the SERS detection by addition of small molecules with positively charged functional groups as aggregating agents to overcome the electrostatic repulsion between the negatively charged DNA phosphate groups and the metal surface.[8,9]

Amongst reported aggregating agents, the polyamine spermine offered high SERS sensitivity when used in combination with negatively charged particles acting as a sandwich molecule bringing dye-labelled DNA molecules close to the particle surface and further aggregating the nanoparticles.[10] However, spermine itself can interact with free DNA in solution inducing its agglomeration.[11] On one hand this detection approach offered high sensitivity, however the bi-functional nature of spermine in this system might lead to over aggregation compromising the stability of the system rendering stable SERS more difficult over time. As such, controlling the aggregation of the nanoparticles[12,13] and the interparticle distance have become important considerations for SERS analysis.[14]

An alternative approach for detection of DNA is to use positively charged nanoparticles ensuring electrostatic attraction between the analyte and the enhancing substrate. Gill *et al.* recently employed hexadecyltrimethylammonium bromide (CTAB) capped silver nanoparticles in SERS-based detection of dye-labelled DNA.[15] Although this method brings effective adsorption of the negatively charged analytes, the CTAB double layer surrounding the nanoparticles hampers, on the one hand, the SERS sensitivity due to its intrinsic shell thickness and, on the other hand, limits the nanoparticle stability to the presence of a significant concentration of unbound surfactant in solution.[16] As an alternative, positively charged polymers such as poly-L-Lysine (PLL) and polyethyleneimine (PEI) have been employed in the preparation of gold nanoparticles.[17–19] Although polymer coated particles may improve overall stability of the particle ligand shell, large interparticle gaps are created during the formation of particle clusters substantially limiting the SERS sensing performance. Polymer coated particles can also present high background signals which compromises both the multiplexing potential of SERS and decreases the distinction of the analyte signals from the particle background.

Here we report for the first time the preparation of extremely stable positively charged silver nanoparticles using spermine, a homo-bi-functional amine molecule as the stabilising ligand, which prevents interparticle aggregation *via* electrostatic repulsion producing a stable colloid in aqueous solution. This allows the creation of a ligand shell with an overall positive surface charge that is particularly suitable for DNA detection.

These particles bring several advantages. Firstly, by anchoring spermine ligands onto the particle surface, the negatively charged analyte adsorbs onto the nanoparticle surface *via* controlled electrostatic interaction through charged secondary amine moieties readily available on the particle surface with either the phosphate backbone and/or DNA bases.[20,21] Secondly, the addition of aggregation agents is no longer needed in order to obtain SERS signals. The DNA induces nanoparticle aggregation allowing

Centre for Molecular Nanometrology, WestCHEM, Department of Pure and Applied Chemistry, University of Strathclyde, 295 Cathedral St., Glasgow, G1 1XL, UK. E-mail: Duncan.Graham@strath.ac.uk, Karen.Faulds@strath.ac.uk; Tel: +44 141 548 2507

† Electronic supplementary information (ESI) available Experimental procedures, nanoparticle characterisation data, ligand structures and surface plasmon shifts of the nanoparticles after addition of DNA. See DOI: 10.1039/c2cc31731a

‡ DvL and ŽK have contributed equally to this work.

straightforward DNA detection by SERS. In this way reducing the number of variables and aggregation dynamics are more controlled, rendering these particles very attractive for quantitative DNA analysis by SERS. Thirdly, as DNA sequences are positioned in the interparticle hot spots and close to the nanoparticle surface, high SERS sensing performance in terms of sensitivty, is efficiently provided. This system is suitable for the analysis of both single and double stranded DNA molecules.

To support our findings, this study compares the SERS based detection of dye labelled DNA with positively charged particles previously reported in the literature. We believe that the results of this study will be of particular use to the scientific community aiming to improve simplicity, and stability of both single and double stranded DNA detection strategies. Detailed experimental procedures are reported in the Supplementary information.† Silver nanoparticles with a diameter of 26.8 ± 6.0 nm (n = 225) were prepared *via* a sodium borohydride reduction in aqueous solution using spermine hydrochloride as a stabilising ligand molecule. Importantly, nanoparticle synthesis was performed in glass vials that were pre-coated with a positively charged polymer to prevent binding of the positive nanoparticles to the negatively charged glass walls. No leakage of the coating polymer was observed (ESI†). The molar ratio of the ligand to Ag(I) was carefully tuned to prevent uncontrolled aggregation of the particles. The obtained nanoparticles were kept in the dark at room temperature (10–20 °C) and were stable for several months.

The SERS sensing performance of spermine stabilised nanoparticles was compared to other silver nanoparticles stabilised with poly-L-lysine, CTAB, citrate and branched PEI.

Each of the different types of nanoparticles had similar core sizes (ESI†), and were adjusted to similar concentrations by adjusting the optical density (OD), providing nanoparticle concentrations of ~190 pM.[1] As a Raman reporter, 5-carboxyfluorescein covalently attached to a 25-mer DNA sequence was utilised (ESI†). The negative charge of the dye (FAM) showed to have limited contribution to the DNA adsorption, because DNA labelled with a positive dye (Cy5) could easily be detected (ESI†).[15,22,23]

Firstly aggregation caused by adsorption of dye-labelled ssDNA onto the silver nanoparticles was analysed colourimetrically. Different concentrations of ssDNA were added (ranging from 0.05 to 10 nM) to 33 pM silver colloidal dispersions.[4] Addition of ssDNA caused aggregation of the nanoparticles evidenced by colour change and a decrease in absorbance at 395 nm and an increase in absorbance at 550 nm (ESI†). Following these findings, DNA in a concentration range from 1–10 nM was chosen for the subsequent SERS analyses. The spermine stabilised nanoparticles offered highest performance, in terms of SERS sensitivity (Fig. 1). For CTAB coated nanoparticles, signal could only be obtained when the nanoparticles were diluted. This indicates that the SERS signal appearance was a result of the CTAB molecules displacement from the particle surface leading to a high degree of uncontrolled particle aggregation.[16] Otherwise when the CTAB layer was intact, a surface enhanced fluorescence (SEF) background was obtained with an approximate factor of 350 times (ESI†).

Detection of dye labelled DNA at 10 nM was not achieved with PLL-coated nanoparticles, while PEI functionalised

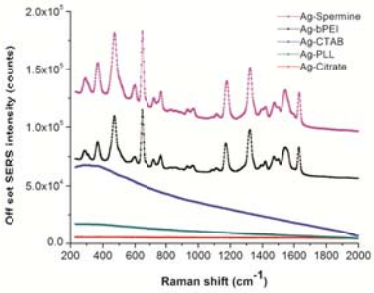

Fig. 1 SERS spectra obtained from 10 nM FAM labelled DNA. Spectra are off set. Silver nanoparticles with spermine (blue), PLL (cyan), CTAB (purple), negative citrate particles (black), and branched PEI (red). A 532 nm laser excitation of approximately 24 mW at the sample was used (three accumulations of 1 s).

surfaces allowed the detection of the target analyte, although with SERS signal approximately three times less intense after 30 min than those reported for the spermine functionalised nanoparticles (Fig. 2). We suggest that the use of branched polyamines and surfactants as nanoparticle coatings induces larger distances between the adsorbed analyte and the metal surface, leading to significantly lower enhancements of the dye signal. The lowest observable concentration of dye labelled DNA in the case of spermine-stabilised nanoparticles was 1 nM. In addition spermine stabilised nanoparticles produced a lower background signal when compared to branched PEI-stabilised nanoparticles (ESI†). The stability of the samples was measured over a time period of 120 min (Fig. 2) confirming the higher stability of spermine stabilised Ag nanoparticles over longer periods of time. This makes spermine stabilised particles attractive for analysis within an automated system.

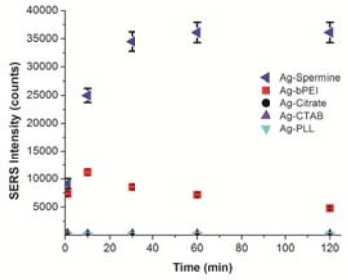

Fig. 2 SERS signal stability over a time period of 120 min. Silver nanoparticles with branched PEI (red squares), negative citrate particles (black circles), CTAB (purple upwards pointed triangle), PLL (cyan downwards pointed triangle), and spermine (blue leftwards pointed triangle). Error bars represent ± one standard deviation of three separate samples. A 532 nm laser excitation of approximately 24 mW at the sample was used (three accumulations of 1 s).

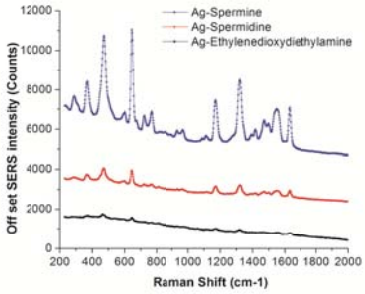

Fig. 3 Off set SERS signal intensity of 1 nM FAM labelled DNA, using silver nanoparticles with spermine (blue), spermidine (red), or ethylenedioxydiethylamine (black), ligands. A 532 nm laser excitation of approximately 24 mW at the sample was used (three accumulations of 1 s).

Additionally, we have investigated the effect of the ligand charge on the SERS peak intensity using three similar length ligands; spermine (+4), spermidine (+3), and ethylenedioxydiethylamine (+2) (ESI†). These ligands vary with respect to their internal chemistry and overall charge, however the λ_{max} of the functionalised nanoparticles determined by UV-Vis and the size of these nanoparticles as determined by DLS was found to be very similar (ESI†). Ligand charge was found to be directly proportional to the observed SERS peak intensity of the dye labelled DNA, with more positive charge on the ligand providing more intense SERS signals (Fig. 3). The affinity of the spermine for the interaction with single stranded DNA resulted in highly effective SERS active silver nanoparticles. This data is in agreement with previous studies reporting the greatest SERS enhancements of dye labelled DNA using spermine.[8,24] The focus of future work is label free detection of DNA *via* the specific Raman bands of the individual bases.

In conclusion, we have shown how spermine stabilised silver particles with positive surface charge are particularly suitable as platforms for detection of dye labelled DNA with surface enhanced Raman spectroscopy. Herein we have used these particles for the direct detection of negatively charged 5-carboxyfluorescein labelled DNA, and compared them to other positively charged nanoparticles found in the literature. Introduction of the analyte to the Ag-spermine nanoparticles resulted in their aggregation giving rise to intense and stable SERS spectra for up to 120 min. Addition of aggregating agents or diluents were not required, significantly simplifying quantitative SERS analysis. In addition the spermine stabilised Ag nanoparticles showed a limited background signal, which is of particular importance for sensitive analysis of multiple analytes in solution. The affinity of the spermine functionalised particles for ssDNA was found to be greater than ligands of similar length with lower charge. These particles may even be useful for detection of unlabelled DNA obtaining the Raman specific bands of the DNA bases.

Due to their ease of preparation and herein described advantages, we anticipate these particles finding widespread use in the detection of other negatively charged analytes, improving sensitivity and allowing direct SERS analysis, circumventing the need for additional aggregating agents, and this providing extended sample stability over the conventional SERS methods.

The authors thank Renishaw Diagnostics Ltd. and the Scottish Funding Council for funding to DvL through a SPIRIT award, the EU FP7 Project SMD for funding IAL, the EPSRC (EP/F005407/1) for funding KF and JAD, and the Royal Society for a Wolfson Research Merit award to DG.

References

1 N. L. Rosi and C. A. Mirkin, *Chem. Rev.*, 2005, **105**, 1547–1562.
2 M. D. Porter, R. J. Lipert, L. M. Siperko, G. Wang and R. Narayanana, *Chem. Soc. Rev.*, 2008, **37**, 1001–1011.
3 I. A. Larmour, K. Faulds and D. Graham, *Chem. Sci.*, 2010, **1**, 151–160.
4 J. Yguerabide and E. E. Yguerabide, *Anal. Biochem.*, 1998, **262**, 137–156.
5 E. C. Le Ru and P. G. Etchegoin, *Principles of Surface-Enhanced Raman Spectroscopy*, Elsevier, Amsterdam, 2009.
6 K. Faulds, W. E. Smith and D. Graham, *Anal. Chem.*, 2004, **76**, 412–417.
7 S. E. J. Bell and N. M. S. Sirimuthu, *J. Am. Chem. Soc.*, 2006, **128**, 15580–15581.
8 D. Graham, W. E. Smith, A. M. T. Linacre, C. H. Munro, N. D. Watson and P. C. White, *Anal. Chem.*, 1997, **69**, 4703–4707.
9 S. E. J. Bell and N. M. S. Sirimuthu, *Chem. Soc. Rev.*, 2008, **37**, 1012–1024.
10 D. Graham and K. Faulds, *Chem. Soc. Rev.*, 2008, **37**, 1042–1051.
11 B. C. Hoopes and W. R. McClure, *Nucleic Acids Res.*, 1981, **9**, 5493–5504.
12 I. A. Larmour, K. Faulds and D. Graham, *J. Phys. Chem. C*, 2010, **114**, 13249–13254.
13 Ž. Krpetić, L. Guerrini, I. A. Larmour, J. Reglinski, K. Faulds and D. Graham, *Small*, 2012, **8**, 707–714.
14 F. McKenzie and D. Graham, *Chem. Commun.*, 2009, 5757–5759.
15 R. Gill and G. W. Lucassen, *Anal. Methods*, 2010, **2**, 445–447.
16 A. McLintock, N. Hunt and A. W. Wark, *Chem. Commun.*, 2011, **47**, 3757–3759.
17 M. Thomas and A. M. Klibanov, *Proc. Natl. Acad. Sci. U. S. A.*, 2003, **100**, 9138–9143.
18 Y. Ma, Y. Guo, J. Li, J. Guan, L. Xu and W. Yang, *Chem.–Eur. J.*, 2009, **15**, 13135–13140.
19 B. L. Frey and R. M. Corn, *Anal. Chem.*, 1996, **68**, 3187–3193.
20 B. G. Feuerstein, N. Pattabiraman and L. J. Marton, *Nucleic Acids Res.*, 1990, **18**, 1271–1282.
21 H. Deng, V. A. Bloomfield, J. M. Benevides and G. J. T. Jr, *Nucleic Acids Res.*, 2000, **28**, 3379–3385.
22 V. Zanker and W. Peter, *Chem. Ber.*, 1958, **91**, 572–580.
23 M. M. Harper, J. A. Dougan, N. C. Shand, D. Graham and K. Faulds, *Analyst*, 2012, **137**, 2063–2068.
24 R. J. Stokes, A. Macaskill, P. J. Lundahl, W. E. Smith, K. Faulds and D. Graham, *Small*, 2007, **3**, 1593–1601.